ACOUSTIC EMISSION CHARACTERIZATION OF SIX WIND TURBINES: A DIAGNOSTIC TOOL TO ISOLATE, IDENTIFY, AND QUANTIFY POINT SOURCE CONTRIBUTORS TO A WIND TURBINE'S NOISE

A Thesis
by
JON CHRISTOPHER KIRCHNER

Submitted to the Graduate School
Appalachian State University
in partial fulfillment of the requirements for the degree of
MASTER OF SCIENCE

MAY 2012
Department of Technology

ACOUSTIC EMISSION CHARACTERIZATION OF SIX WIND TURBINES: A DIAGNOSTIC TOOL TO ISOLATE, IDENTIFY, AND QUANTIFY POINT SOURCE CONTRIBUTORS TO A WIND TURBINE'S NOISE

A Thesis
by
JON CHRISTOPHER KIRCHNER
May 2012

APPROVED BY:

_____
Marie Hoepfl
Chairperson, Thesis Committee

_____
Brian W. Raichle
Member, Thesis Committee

_____
Dennis M. Scanlin
Member, Thesis Committee

_____
Jeffrey S. Tiller
Chairperson, Department of Technology and Environmental Design

_____
Edelma D. Huntley, PhD
Dean, Graduate School and Research & Sponsored Programs

ABSTRACT

ACOUSTIC EMISSION CHARACTERIZATION OF SIX WIND TURBINES:
A DIAGNOSTIC TOOL TO ISOLATE, IDENTIFY, AND QUANTIFY POINT SOURCE CONTRIBUTORS TO A WIND TURBINE'S NOISE. (May 2012)

Jon Christopher Kirchner, B.A., University of Virginia

M.S., Appalachian State University

Chairperson: Dr. Marie Hoepfl

The diagnostic tool developed in this study was designed to perform acoustic analyses to enhance the International Electrotechnical Commission's (IEC) 61400-11, edition 2.1 Standard. The IEC Standard, which is the current international standard for collecting wind turbine acoustic data, describes a methodology for measuring, characterizing, and reporting wind turbine acoustic emissions. However, the IEC results only provide non-specific, total acoustic emissions data that may include sound pressure levels from contributors unrelated to a wind turbine's components or operation. The developed diagnostic tool uses enhanced tonal analysis to allow for identification of peak frequencies and a more detailed characterization of a turbine's acoustic emissions.

In this study, the IEC Standard 61400-11 methodology was followed for acoustic and meteorological data acquisition. Acoustic analysis software was then used to identify the various sound pressure levels contained within 10 Hz frequency bins to reveal the specific peaks that comprised a wind turbine's overall sound. Band pass filters were used to isolate the distinguished peaks into successive audio tracks. The goal of this enhanced analysis was to isolate, identify, and quantify individual point source contributors to better characterize a

wind turbine's acoustic emissions. Through mathematical conversion from the logarithmically-scaled decibel unit into a linearly-scaled Pascal unit, a comparison and quantification of sound pressure levels was performed. Each identified sound pressure percentage was then associated with a point source contributor through application of a decision tree developed for this study.

The diagnostic tool provides a process that allows individual peak contributors of a wind turbine's total acoustic emissions to be acoustically isolated, identified, and quantified. The diagnostic tool has shown to illustrate a process that presents concise acoustic information that may be useful to wind turbine manufacturers to target specific major component contributors for mitigation and subsequent reduction of their wind turbines' acoustic emissions. When applied to the six turbines analyzed in this study, major contributors to the acoustic emissions of small-scale wind turbines were identified to be vortex shedding and the generator. On larger scale wind turbines, cooling fans, blade impulsive noise, and inflow turbulence were the dominant point source contributors.

DEDICATION

I owe an eternal debt of gratitude to my soul mate, April Leigh Walters. She has provided an essential guiding hand, not only throughout my academic career, but also in my life choices that have brought me to the place I am today.

ACKNOWLEDGEMENTS

I would like to express my thanks to Dr. Marie Hoepfl for her support and guidance throughout my graduate career here at Appalachian State University. She has been more than generous with her time commitment and devotion to making sure that I am able to produce the most in-depth, succinct thesis possible. Her stick-to-itiveness that she has passed on to me through this process will serve throughout my entire lifetime.

For his knowledge and understanding of the physical world around us, Dr. Brian Raichle has played a major role in helping me progress through issues that I have encountered in executing this study's acoustic testing.

Also, I am very grateful to Dr. Dennis Scanlin for his passionate love for wind power and never giving into the naysayers who stand in way of its development and eventual acceptance into our culture.

I would also like to recognize my parents who have given me nothing but love and support throughout my life's bumpy road, with all of the ups and downs. My mother, Jean Kirchner, is the first person I have called in times of joy as well as hurt, and her love for me is unsurpassable. My father, Fred Kirchner, has set a high standard for me through his life endeavors. I know he is honored by my accomplishments and I hope this thesis makes him proud by showing him the depth of knowledge that he has provided the basis for through his mentoring as my father.

Finally, I would like to acknowledge Pilot Walters-Kirchner for being *this* man's best friend.

TABLE OF CONTENTS

LIST OF TABLES

LIST OF EQUATIONS

LIST OF FIGURES

Chapter 1: INTRODUCTION

Power production by means of wind turbines is still an emerging technology. According to Pichert and Katsikopoulos (2008), because of unfamiliarity with this technology and the general population's tendency to accept the "default" (p. 65), people have been reluctant to adopt alternative forms of energy production. Wind energy is an environmentally friendly energy production method, yet it has not been universally accepted. Some major reasons for this denial include particular public perceptions that electrical production by means of wind turbines is visually obtrusive, that they impose a relatively higher cost of energy than conventional fossil fuels, and that they have a low reliability of electrical production as a result of the wind's natural intermittence. One additional major reason for the delayed acceptance by the public is the sound of the acoustic emissions created by the fundamental moving parts of a wind turbine.

Hansen (2008) describes the natural problem with noise associated with wind turbines, noting that "wind turbines create a certain amount of noise when they produce electricity" (p. 3). However, manufacturers of modern wind turbines have focused attention on reducing much of the mechanical noise produced by the turbines, and now seek to minimize the aerodynamic noise created by the moving turbine blades. In fact, noise reduction can give manufacturers a relative competitive advantage, since developers will seek to reduce noise, particularly in populated areas (Hansen, 2008, p. 3). If the wind turbine is quiet, people are more likely to choose it over a louder wind turbine.

Research on acoustic emissions from wind turbines has already had a large impact on the overall wind turbine design process. In the past, the main goal of a wind turbine designer was to make a wind turbine that produced the highest ratio of power to wind (i.e., the most energy efficient). This focus has now shifted to limit particular site installations due to public annoyance with wind turbines' acoustic emissions. Migliore, van Dam and Huskey (2004) state that "there have been occasions when acoustic emissions proved so vexing they overshadowed performance and reliability issues" (p. 1). This again reinforces the importance of an acoustically quiet wind turbine, which has recently consumed many manufacturers' design criteria.

This study includes six subject wind turbines ranging in size from 160 watts with a 1.17 meter rotor diameter to 2.3 megawatts with a 93 meter rotor diameter. The *61400-11 edition 2.1 Standard* for testing wind turbine generator systems set forth by the International Electrotechnical Commission, or IEC, is the most widely adopted methodological standard (International Electrotechnical Commission, 2006). This standard has been internationally used for data collection procedures.

The diagnostic tool described in this study adds supplementary acoustic characterization to the international Standard by isolating individual acoustic frequencies contained within a wind turbine's sound to enable a determination of an identity to each physical point source of noise that contributes to the total sound of the wind turbine. These individual acoustic values can be placed in comparison to the total wind turbine sound to associate a percentage contribution from each identified component to the overall wind turbine sound emitted. Use of this diagnostic tool to analyze a wind turbine may describe significant acoustic factors that would otherwise be difficult to isolate, identify, and quantify

for eventual mitigation. These findings could contribute to future turbine design decisions and help manufacturers reach their goals for lower levels of acoustic emissions.

Statement of the Problem

The current IEC Standard for acoustic emission testing on wind turbines is designed to provide a standardized set of particular parameters to describe the characteristics of the acoustic emissions produced by a wind turbine. The necessary characteristic parameters required by the Standard may be insufficient for some manufacturers in their ability to describe the quality and uniqueness of each wind turbine's noise emissions. The Standard provides a solid methodology for data collection, although the reporting stage may lack the ability to satisfy specific needs set forth by particular manufacturers to isolate and identify individual contributors to the total wind turbine sound.

The presented diagnostic tool's methodology unites two disjointed disciplines: the wind energy industry and science of acoustics. The current Standard for acoustic testing on wind turbines may lose some credibility among acousticians due to the lack of particular tonal acoustic specificity that is lost as a result of the standardizing process which the Standard has adopted in order to accommodate all test subjects. On the same note, few acousticians devote their expertise to such a specialized industry as wind power, resulting in a diminutive level of requested tonal acoustic description included in the Standard. By connecting these dissimilar disciplines, we can expand upon previous wind turbine acoustic emission characterizations, achieving an isolation, identification, and quantification of individual point source contributors that add together to compose the total sound the particular wind turbine under investigation emits. By contrast, the current Standard limits the overall tonal description to a one-third-octave analysis.

Purpose of the Study

This diagnostic tool is designed to obtain measurements that are not recognized by the IEC Standard but that may contain valuable information useful to wind turbine manufacturers. The Standard currently only asks for a one-third-octave analysis to characterize the tonal analysis of the wind turbine. This one-third-octave analysis equalizes peak sound pressures with adjacent frequencies occurring within the same one-third-octave. If these adjacent frequencies do not contain individual point source acoustic contributors, the overall sound pressure level for that one-third-octave disseminates the physically evident peak produced from the contributing acoustic point source. This diagnostic tool builds upon the IEC Standard by using acoustic methods to isolate particular point source producers emitting noise from each wind turbine. It is designed to better assist a human ear receiver in the interpretation and understanding of each wind turbine's individual point sources that simultaneously create the whole sound.

The IEC Standard is based around a declaration of the sound pressure level of a wind turbine's acoustic emissions at each integer wind speed. This correlation provides a way to determine how loud a wind turbine may be and is used for planning an installation; however, it does not provide much useful information that a manufacturer may be interested in for research and development purposes. A manufacturer may utilize the diagnostic tool's results to assist in efficiently targeting major acoustic components supplying individual contributions to the total acoustic emissions of their wind turbine. This information would result in a more effective noise mitigation process. This study will attempt to provide a diagnostic tool to obtain this information through a more detailed analysis of acoustic

emission contributors contained within a wind turbine's total noise than is currently requested by the IEC Standard.

The rationale behind the diagnostic tool's deviation from the Standard is that there is no individuality to the analysis procedure dependent on the unique frequencies emitted by a wind turbine. The Standard specifies that one-third-octave analyses are performed to characterize the tonality of a wind turbine. The problem with this procedure is that it groups adjacent frequencies based upon the octave scale. This presents the possibility that point source contributor frequencies are effectively dulled down by adjacent frequencies that do not contain sound pressure created by any wind turbine component. This dulling down greatly reduces the effectiveness of the IEC's acoustic characterization.

An understanding of acoustics has been applied in this study to increase the utility of the IEC Standard's methodology results to better represent the individual characteristics of the acoustic emissions of the wind turbine, thus providing results that supplement those typically reported when applying the Standard.

Research Questions

This research is guided by four questions:

Q1: Does the diagnostic tool described in this paper allow the total sound of a wind turbine to be separated into individual acoustic tracks of specific point source contributors?

Q2: Does the diagnostic tool described in this paper provide a method to quantify the comparison of individual point source contributor's sound pressure levels to a wind turbine's total acoustic emissions?

Q3: Does the greatest sound pressure contributor percentage of the total sound pressure emitted from all subject wind turbines tested occur as a result of the blade impulsive noise?

Q4: Do small scale wind turbines of the same rotor diameter emit relatively similar sound signatures (FFT analyses) due to the tendency for a natural frequency of acoustic resonance related to that rotor diameter's dimension?

Definition of Terms

Acoustic Resonance – the tendency of an object to oscillate at its natural frequency based upon the object's dimensional length.

A-weighted – a filter applied at all frequencies to provide a close approximation of the frequency response of a normal human ear.

Amplitude – the proportional relationship that is represented on a scale of -1 to 1 between localized air pressure difference and the ambient atmospheric air pressure.

Audacity – an audio editing program used to amplify the recording enough to be easily audible during analysis.

Background Noise – the level of sound pressure emitted by the surrounding environment.

Background Noise Corrected ($Leq_{(A),C}$) – the calculated sound pressure level of a wind turbine after the measured background noise sound pressure level has been logarithmically subtracted, leaving the prospective sound pressure level of the wind turbine as if it were operating on its own, in dB.

Blade Impulsive Noise – short, periodic acoustic impulses or thumping sounds that vary in amplitude and time. It is caused by the interaction of wind turbine blades with disturbed air flow around the tower of a downwind machine.

Broadband Noise – a noise that is composed of peak frequencies that occur in more than one-third-octave bandwidth.

Clip – a section of recording selected for analysis in noiseLAB 3.0.

Decibel (dB) - a unit used to express the intensity of a sound wave, equal to 20 times the common logarithm of the ratio of the pressure produced by the sound wave to a reference pressure, 0.0002 Pascals.

Equalized Sound Pressure Level (L_{eq}) – the root-mean-square value of acoustic energy contained within a given segment measured while the wind turbine is operational and the background noise level has not been subtracted, in dB.

Fast Fourier Transform (FFT) – an algorithm for computing the Fourier transform of a set of discrete data values. This is the analysis used to obtain the sound pressure levels at various frequencies that contribute to the total sound over the analyzed segment.

Hertz (Hz) – the SI unit of frequency, equal to one cycle per second.

Hub Height – the distance (meters) from the base of the wind turbine to the center of the wind turbine rotor.

Inverse Square Law – this acoustic property states that a source sound's intensity is equal to the reciprocal of the square of the distance.

Low Frequency Sound – any sound with a frequency of 10 Hz – 200 Hz, the low frequency range of human hearing.

Meteorological Mast – a ten-meter tower used to mount the anemometer and wind vane.

Narrowband Noise – a noise that is composed of one or more peak frequencies that all occur within the same one-third-octave bandwidth.

noiseLAB 3.0 – software used to record information produced by the microphone and create clips of desired temporal segments of the recording for further analysis.

noiseLAB Batch Processor 3.1 – software that uses recordings made in noiseLAB 3.0, necessary to perform sound level, one-third-octave and Fast Fourier Transform (FFT) analyses.

One-Third-Octave Bandwidth Analysis – an acoustic analysis of a sample that determines the sound pressure level within each progressive one-third-octave.

Pascal – a reference pressure value equal to 1 $Newton\ /\ meter^2$.

Peaks / Bandwidth – sound pressure concentrations of frequencies (in Hz) emitted by a wind turbine that can also be defined as its tonal signature.

Shadow Effect – a disturbance of the air flow as a result of the wind passing around a tower.

Signal-to-Noise Ratio – the sound pressure relationship between a chosen signal's information and the sound pressure of any undesired noise contained within the same recorded segment.

Sound Power Level – the calculated acoustic pressure emitted at an acoustic source location.

Sound Pressure Level (SPL) – the amount of acoustic pressure experience by a receiver at a specified distance from the acoustic source.

Wind Turbine Noise – a single point source contributor's acoustic emission resulting from an individual component of the wind turbine.

Wind Turbine Sound – the total sound pressure emitted from a wind turbine ranging in frequencies from 20 Hz – 20000 Hz.

Limitations of the Study

The principal limiting factor in this study is the low number of active wind turbines subjects available for testing. Six turbines have been included in this study, four of which are passive (non-electronically controlled) and are considered to be categorized as small scale. The remaining two subject wind turbines are active (electronically controlled); one is categorized as small scale (50kw) and one as utility scale (2.3MW). Additional active wind turbines may have presented a more complex variety of test subjects to fully examine the adaptability of the diagnostic tool to varying rotor sizes as well as to an increased number of wind turbine mechanical components.

Proximate busy populations and roads are other factors that restrict the ability to collect valid data. Cars driving on nearby roads and activity within the populated area can render a recording invalid throughout the duration of any segment in which people or operating cars can be heard on the recording. This is also true if anyone's voice is received by the microphone. Activity at the Pinnacle Inn Resort as well as the nearby connecting roads are noted sources of acoustic interruptions to testing performed at the Appalachian State University Beech Mountain Wind Test Facility (Figure 1). Although this site is considered semi-rural in nature, the amount of activity observed from these acoustic interruption sources is relatively steady. The proximity of the Resort and Elderberry Ridge Road posed a large number of interruptions to the acoustic recording. Any recoding interruption makes the surrounding 10 seconds invalid for analysis.

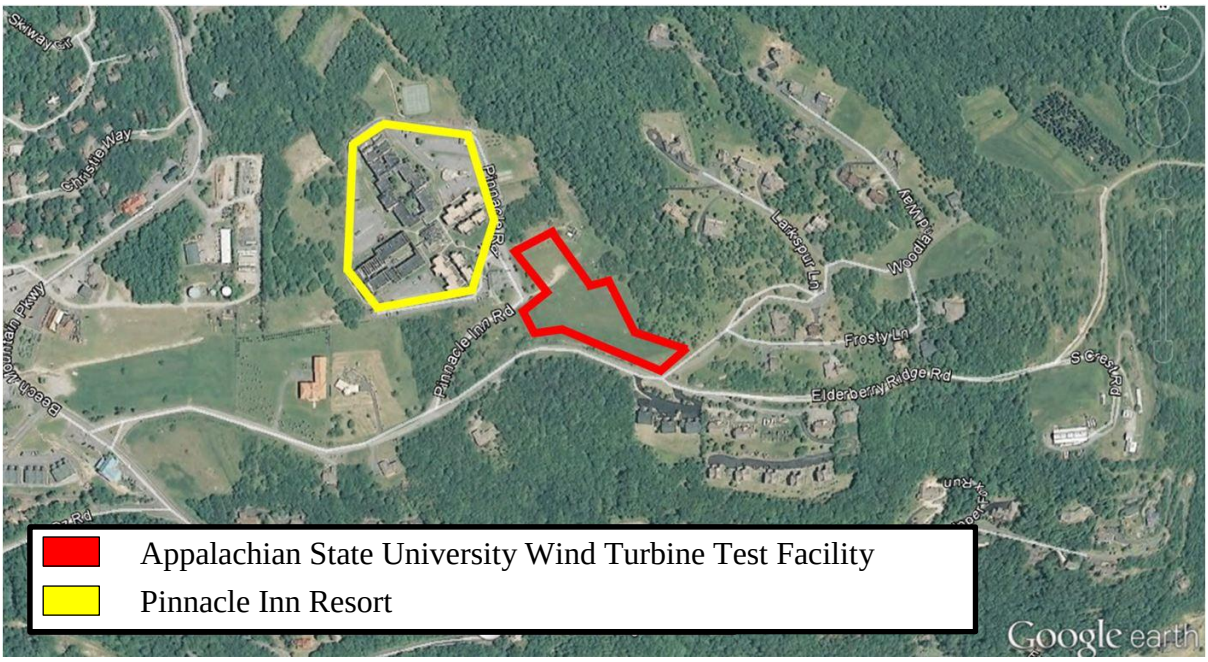

Figure 1. A satellite image of the Appalachian State University Wind Turbine Test Facility at Beech Mountain, North Carolina. This figure shows a map of the test bed and proximate roads with associated centers of population. From "Beech Mountain, NC" (Google Earth, 2011).

Other interruptions resulted from aircraft in the sky. The aircraft spends a relatively long time in the visible sky, disqualifying those extended periods of recording, which further reduces the number of samples. The Appalachian State University Beech Mountain Wind Test Facility has a low horizon because it is located on top of Beech Mountain at 5130' in elevation. This increases the number of airplane noises that can interrupt the recording of usable wind turbine segments. Any acoustic interruptions previously mentioned effectively reduce the total number of segments that can be considered valid for data analysis and force the tester to record the acoustic emissions of the wind turbine subjects for an extended period of time to accommodate the eventual reduction of data later in the analysis process.

Significance of the Study

In the past, the main goal of the designer was to make a wind turbine that produced the highest ratio of power to wind (most efficient). Research on acoustic emissions from

wind turbines has increasingly come into play during the overall wind turbine design process. Within the wind energy industry, failure to address acoustic emissions can overshadow performance in power output and reliability of a turbine, since noise issues can effectively derail a wind project (Migliore, van Dam, & Huskey, 2004, p. 1).

The diagnostic tool presented in this paper is an expanded tonality study of the acoustic emissions produced by wind turbines that is supplementary to the IEC Standard. The diagnostic tool is designed to provide a more complete acoustic emission description than requested by the Standard's report. All wind turbines designed for manufacture and installation must be shown to adhere to a certification performed using the standards outlined by the IEC.

With the supplementary detailed information gained by using the diagnostic tool developed in this study, turbine manufacturers could increase the effectiveness of their research and development procedures on their products and achieve a quieter design that operates more smoothly and more efficiently. The quieter a wind turbine operates, the better the wind turbine will perform on the Standard's test. It will therefore be more universally accepted, rendering a more sought-after product, which is in any manufacturer's best interest.

Chapter 2: REVIEW OF LITERATURE

Acoustic Fundamentals

Energy Wave Form

Acoustics can be described as "the science of sound waves" (Ramen, 2010, p. 11). Ramen goes on to say that the difference between acoustic waves (Figure 2) and other types of mechanical waves (Figure 3) is that acoustic waves are longitudinal. The two factors that define the wave type are the medium's particles' direction of propagation and direction of the particles' displacement. Acoustic waves displace the medium through compressions and rarefactions in parallel to the wave's direction of travel (Ramen, 2010, p. 11).

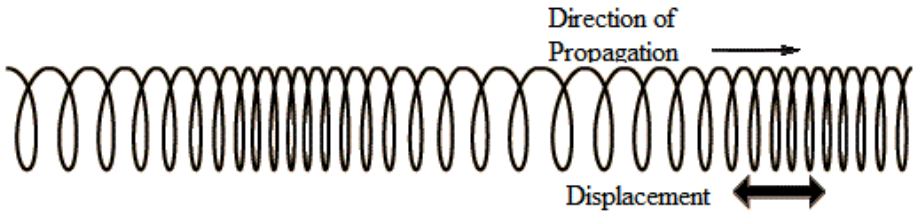

Figure 2. An illustration of a longitudinal wave. From "Longitudinal Waves" (Nave, 2012b).

Figure 3. An illustration of a transverse wave. From "Transverse Waves" (Nave, 2012e).

The medium for acoustic propagation relevant to this discussion is air within the atmosphere. The air at a particular location in the atmosphere is constantly under pressure created by the weight of the column of air directly above that air space. This can be described

as the ambient atmospheric air pressure. When a sound source's wave propagates through this location, the pressure alternately increases and decreases within particular regions. This causes the air density to compress and rarefy in relation to the ambient air pressure, increasing and decreasing the relative air pressure respectively.

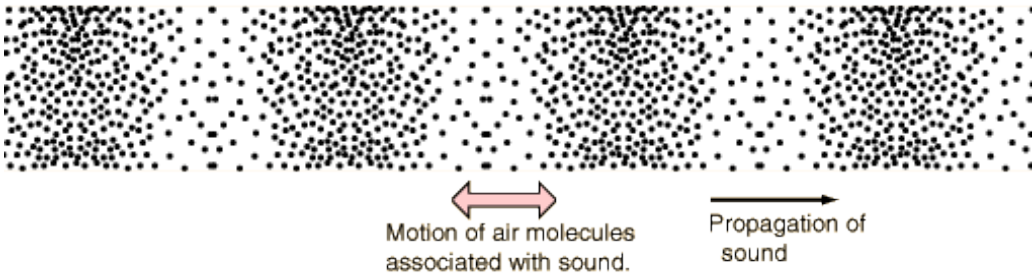

Figure 4. An illustration of an acoustic longitudinal wave propagating through air. From "Sound Waves in Air" (Nave, 2012d).

The black dots in Figure 4 represent individual air molecules in a given space. The areas that contain relatively more closely spaced dots represent regional compressions of the air molecules, resulting in a higher air density than the ambient atmospheric air pressure at that location. The regions that contain dots spaced further apart are rarefications of air molecules within the space containing a number of air molecules, resulting in a relatively lower air density than the ambient atmospheric air pressure. These quantities can be measured and the resulting information displayed in graphical form using a value called the sound's *amplitud*e.

Amplitude

Amplitude is defined as the proportional change in air pressure in relation to the localized ambient atmospheric air pressure. A time-domain graph (Figure 5) represents the oscillating amplitude's value as a result of an acoustic energy wave propagating through air. The regions of compression and rarefication in the air's density are represented by graphing a line that changes its Y (amplitude) axis value over the X (time) axis. The Y axis' amplitude

value is determined by measuring the relative percentage difference in air pressure at a particular moment in time to the ambient atmospheric air pressure.

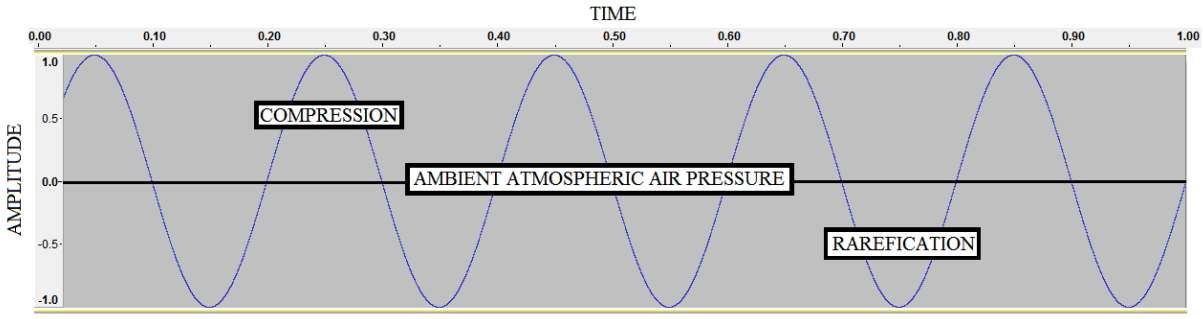

Figure 5. A time-domain graphical depiction of a longitudinal wave propagating through air.

Amplitude values are represented using a percentage proportion on a scale of 1 to -1 in relation to the ambient atmospheric air pressure. These changing relative air pressure values can be reproduced by a sound source such as a loudspeaker. The amplitude's value is translated into the relative position of a speaker at a particular time. The distance the loudspeaker travels is a result of the amplitude's value multiplied by the selected volume (amount of electrical power) of the amplifier. An amplitude value of zero means the loudspeaker is not being provided any electrical power, allowing it to stay in a resting position. This effectively leaves the localized air in front of the loudspeaker at the ambient atmospheric air pressure. A positive increase in the Y axis amplitude value on the graph represents the relative amount of compression over time the sound source produced, creating the respective forward movement of the loudspeaker to replicate the same change in air density measured from the sound source. An amplitude value of 1 represents the maximum compression of the localized air density created by the loudspeaker at the selected amplifier's volume.

Correspondingly, a negative decrease in the Y axis amplitude value represents a relative inward movement of the loudspeaker. This inward movement of the loudspeaker

rarefies the localized air molecules adjacent to the loudspeaker, relatively decreasing the localized air density. The amplitude value of -1 represents the maximum rarefication of the localized air density created by the loudspeaker at the selected amplifier's volume.

Sound Pressure Level

This physical pressure, when exerted, on a certain area can be measured using the Pascal unit. One Pascal, or Pa, is equal to one newton per square meter ($^{\mathrm{N}}/_{\mathrm{m}^2}$). The human ear has a comfort zone for these air pressure differences from .00002 Pa (20 µPa) up to 100 Pa. To account for this vast range of difference in air pressures, a unit called the decibel, or dB, has been utilized to describe the difference in air pressure in relation to the ambient atmospheric air pressure that creates audible sound. The dB unit is logarithmically scaled as opposed to the linearly-scaled Pascal unit. Epsilon Associates, Inc. (2006) describes the decibel scale as logarithmic in order "to accommodate the wide range of sound intensities found in the environment" (p. 1). The decibel can be defined as "20 times the $\log_{10}$ of the ratio of the mean-square sound pressure to the square of the reference sound pressure of 20 µpa" (International Electrotechnical Commission, 2006, p. 8). This can be described in the form of a formula (Equation 1). P_{rms} is equal to the root-mean-square of the measured sound pressure, in Pascals, and P_{ref} is a reference pressure of 2×10^{-5} Pascals (Rogers, Manwell, & Wright, 2006, p. 5).

$$decibel = 20 \log_{10}(^{P_{rms}}/_{P_{ref}})$$

Equation 1. A formula describing the decibel unit of sound pressure measurement.

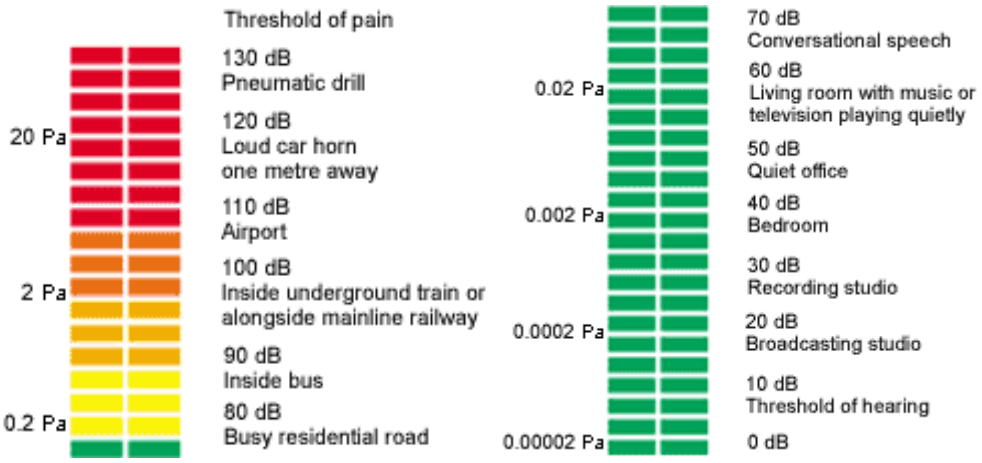

Figure 6. Sound pressure levels commonly found in the environment. This figure shows the dB scale, which provides examples of that sound pressure level compared to noises that we may encounter on in everyday situations. It also correlates the difference of air pressure from the ambient air pressure in Pascals, to the comparative dB value. From "Appendix I:A-3. Sound Propagation: Sound Pressure Level" (Occupational Safety & Health Administration, 2012).

As described in Figure 6, the threshold of the human ear's audibility is the reference sound pressure of .00002 Pa, which is defined as 0 dB. Similarly, the threshold for the ear's comfort level occurs when a tickling or painful sensation occurs in the ear at around 100 Pa, or 120 dB. In accordance with the decibel unit's scale (Equation 1), a doubling in the physical pressure exerted on the ambient atmosphere air pressure from a sound source does not represent a doubling of decibel level. Instead, for each doubling of sound pressure (in Pa), six decibels are added to the total sound pressure level (Occupational Safety & Health Administration, 2012). It is also worth noting that the human ear is unable to detect a sound pressure change of less than three dB and most people perceive a volume increase of 10 dB to be twice as loud as before the increase (Alberts, 2006, p. 6).

We may declare a sound source to have a certain *equalized sound pressure level*, or L_{eq}, even though there may be pressure fluctuations above or below that period's declared L_{eq} sound pressure level in dB. This is an equivalent dB value to a constant sound pressure level

that contains the same amount of energy as the total energy of the fluctuations above and below this level contained in the same amount of time (Figure 7). The greatest fluctuations are called the *peak* values. This reveals that a noise source can still be damaging to the ear, depending on the peak value, even if it has a L_{eq} value below 120dB.

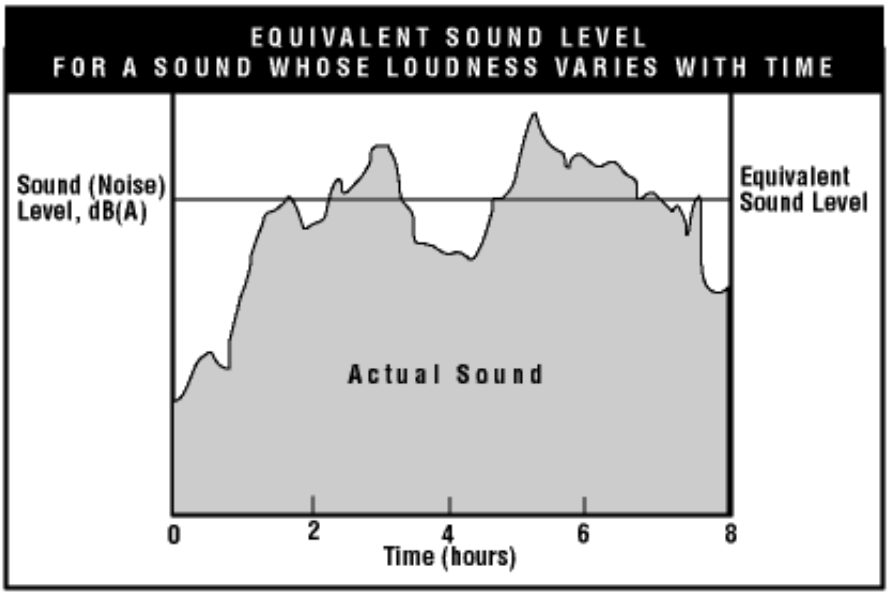

Figure 7. An example of a noise source with varying sound pressure levels over time. This figure shows a noise source whose sound pressure changes over time. The shaded area under the "curve" represents the actual measured sound pressure level over time where the rectangular area represents the calculated equalized sound pressure level value that remains constant over time and is equal to the shaded area. From "Figure 1. Equivalent Sound Level for a Sound Whose Loudness Varies with Time" (Canadian Centre for Occupational Health and Safety Administration, 2004).

Frequency

Frequency is a characteristic of sound that is defined as the number of oscillations between the compressions and rarefications occurring within one second. The frequency of a sound is interpreted by the ear as tone or pitch. Frequency can be calculated as the reciprocal of the period, or $f = {}^{1}/_{T}$ where f is frequency and T is the period (Ramen, 2010, p. 12). The faster a sound source oscillates between the compressions or rarefactions, the higher the frequency or pitch. We express this measurement using the term *Hertz*. Hertz, or Hz, is a unit

of measurement describing how many oscillations occur within one second. The typical human ear is able to hear frequencies that it can translate to the brain ranging from 20 Hz to 20 kHz, although this can slightly vary depending on the individual.

The simplest form of a sound maintains a consistent frequency and would be considered a pure sine wave. However, this is a not the typical situation when considering the types of sound sources we normally encounter in nature. Most sound sources emit a variety of frequencies at the same time, creating a complex acoustic wave form. Even sources that seem to sometimes sound like a pure sine wave contain harmonics, or integer multiples of the pure sine wave's fundamental frequency. For instance, a trumpet may play the same middle C note (which is equal to 261.6 Hz) as a trombone, but they have quite different tonal sounds because these two instruments each have a unique set of natural harmonic tones, or acoustic resonances associated with their physical structure. The sound wave's path in a trumpet is physically shorter, producing a higher set of fundamental frequency harmonics while the trombone creates a longer path for the sound, producing a lower set of fundamental frequency harmonics. Simultaneous fundamental frequencies can be mathematically added to produce a complex acoustic wave. This can be graphically displayed by in the time-domain (Figure 8), again using time as the X axis and amplitude as the Y axis.

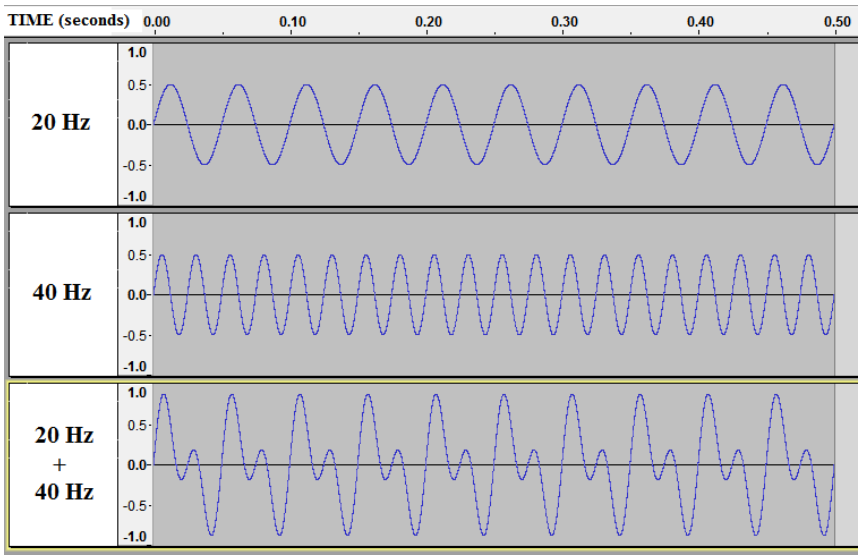

Figure 8. A time-domain graphical representation of the mathematical addition of two pure tones. This graphically shows how individual frequency tones add up to create a more complex acoustic wave form that exhibits the result of the sum of simultaneous frequencies created by an original sound source. A low frequency range has been used for this example for simplicity because the wavelength is longer and is more visible on the graph.

The same complex acoustic wave information can be described in the frequency-domain (Figure 9) using a Fast Fourier Transform, or FFT. This frequency-domain based analysis represents the acoustic wave form's *sound signature*. As previously defined, an FFT analysis is an algorithm used to obtain the sound pressure levels at various frequencies that contribute to the total sound over the analyzed segment.

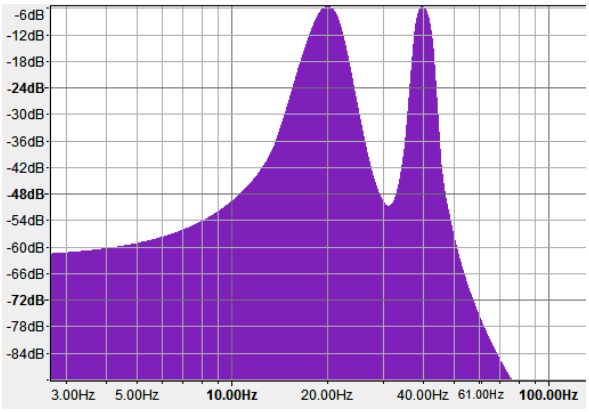

Figure 9. An FFT analysis showing the frequency-domain graph of the sound signature produced by the previous 20 Hz + 40 Hz complex acoustic wave form example. This graph represents the same acoustic data used to produce the time-domain graph shown in Figure 8. It can be noticed that there are distinguished peaks located at 20 Hz and 40 Hz, respectively.

The Human Perception of Sound

The ear perceives these previously discussed small perturbations in the localized air density as sound. The volume, or loudness, perceived by the ear is a sensation resulting from the relative amount of pressure difference, small or large, between the ambient air pressure in relation to these compressions and rarefactions. These relative differences in the localized air pressure emitted from a sound source existing within the human ear's comfort zone are often less than a difference of one billionth of the total ambient air pressure at that location (Nave, 2012c).

The human ear consists of intricate components to translate minute differences in air pressure into electrical impulses that we perceive as sound (Figure 10). The outer ear catches the sound and directs it to the ear drum, which reacts directly to the sound source itself. The ear drum's vibrations are transmitted by three tiny bones located in the middle ear, behind the ear drum, to the cochlea, which is located in the inner ear and considered the main sensory organ for hearing acoustic waves.

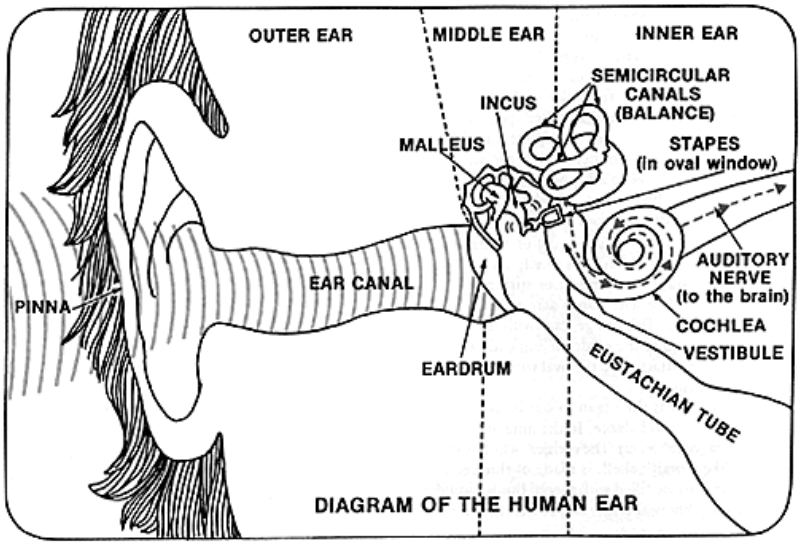

Figure 10. A diagram of the human ear. This figure describes the path through which the ear captures a sound and transforms it into electrical signals which can be perceived by the brain. From "Understanding the Ear" (Clerc, 2011).

The cochlea contains microscopic, inner ear hair cells that protrude in numerous clusters called “stereocilia” (Figure 11). The stereocilia serve the purpose of performing a process called *mechanotransduction*, translating acoustic energy information into electrical impulses so it can be sent along the auditory nerve for interpretation by the brain. The actual electrical production occurs at the tip links which are located at the end of the stereocilia. “As the stereocilia are deflected, pore-like channels on the surface of the stereocilia open up, allowing potassium to rush in, and generating an electrical signal” (Wenger, 2006).

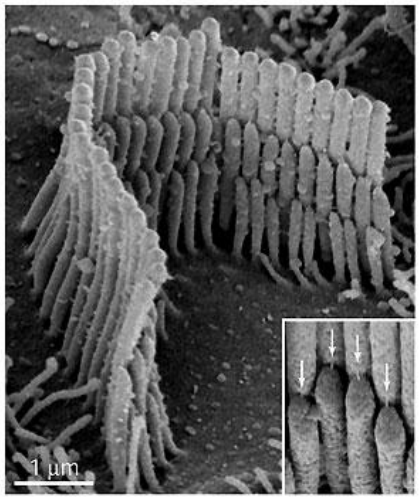

*Figure 11.*A close-up picture of a three-tierd cluster of stereocilia atop a hair cell. The picture contains an insert of the tip links connecting shorter stereocilia to their taller neighbors. A µm (micro meter) scale has also been provided to gain a sense of the scale of these cellular clusters. From “Protein Tied to Usher Syndrome May Be Hearing’s ‘Missing Link’” (Wenger, 2006).

The stereocilia have evolved over time to be more sensitive to a particular range of frequencies. The sensitivity of particular frequencies changes in relation to the sound pressure level. An increase in audible sensitivity can be noticed between 2 kHz and 5 kHz, as illustrated in Figure 12, and thus this range of frequencies requires less sound pressure to be heard. This range encompasses the average frequency (Hz) for human speech, although humans can produce frequencies both lower and higher than this range.

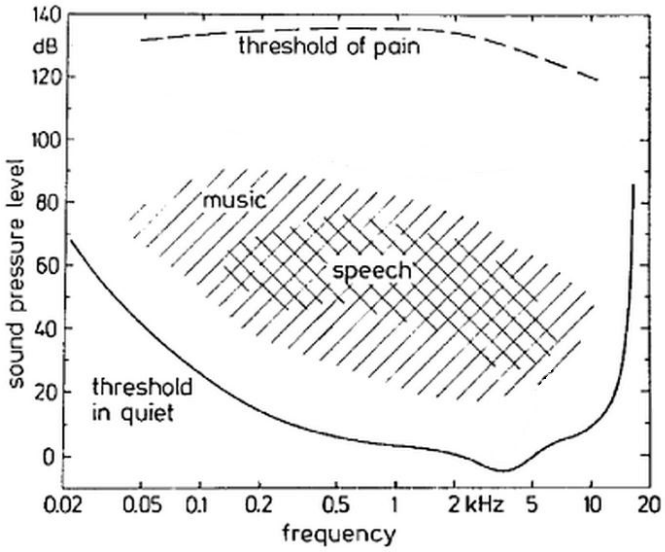

Figure 12. The thresholds of human hearing in relation to a sound's frequency and sound pressure level. This graph encompasses the typical range of frequencies (Hz) and comfort levels (dB) for hearing discussed earlier. Also shown are the typical ranges for music and human speech. Adapted from "Psychoacoustics: Facts and Models" (Fastl & Zwicker, 2007, p. 19).

With sound sources closer to the human threshold of pain (loud), we perceive the loudness of varying frequencies more equally, which is quite different from how we perceive varying frequencies close to the threshold of audibility (quiet). With low sound pressure level sounds, the human ear is most sensitive to the middle range of frequencies, less sensitive to higher frequencies, and least sensitive to low frequencies. This can be noticed through listening to music. If the volume of the stereo is turned all the way up, we hear all frequencies of the sound at equal amplitudes; however, with the same sound's volume turned down, the bass (low frequencies) is lost and we are only left with the middle and less so the high frequency ranges.

The amount of time that the human ear is exposed to a particular sound pressure level is also important in relation to causing hearing damage. "Hearing loss is related to the total sound energy to which a person is exposed" (Alberts, 2006, p. 10). Multiple agencies, charged with monitoring human health and safety, have determined what they believe to be

acceptable limits to a human's time period of exposure to particular sound pressure levels (Figure 13).

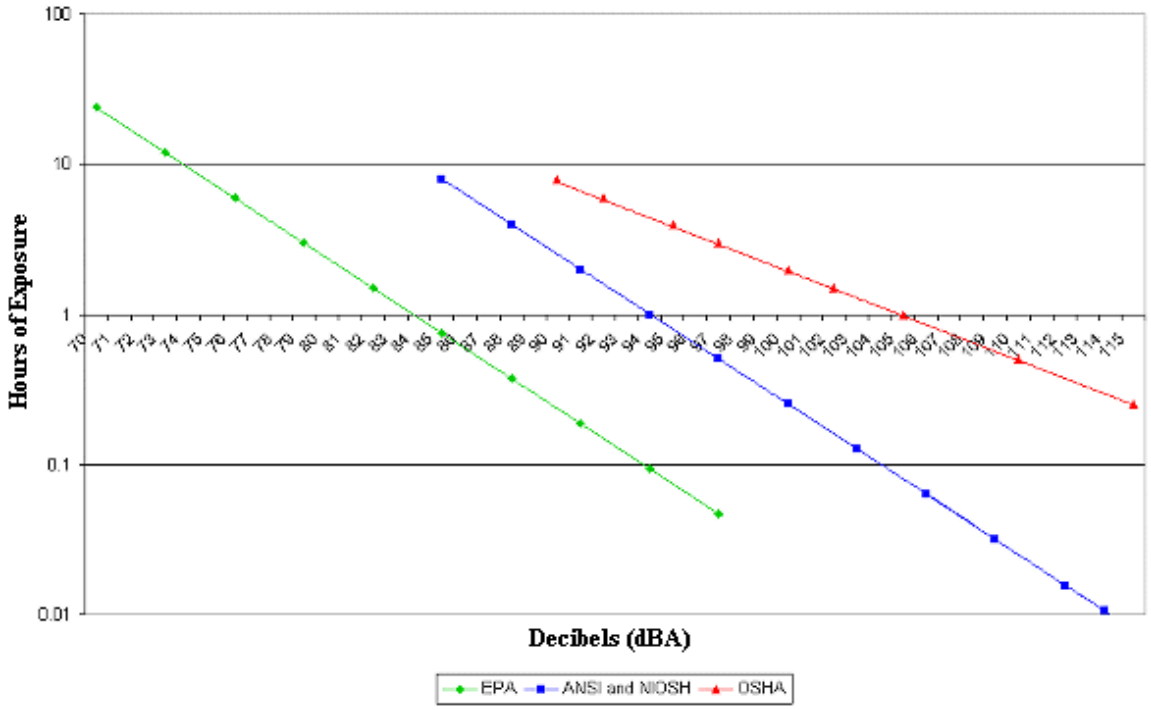

Figure 13. Comparison of noise exposure standards set forth by various organizations. This figure shows the sliding scales that the EPA, ANSI, NIOSH, and OSHA have determined to be the maximum exposure time periods that a human can withstand to avoid hearing loss. From "Comparing Standards for Safe Noise-Exposure" (Noise Pollution Clearinghouse, 2012).

Wind Turbine Acoustics

The system through which wind turbine noise is perceived can be simplified into three discrete modules: noise sources, propagation pathways, and acoustic receivers (Hubbard & Shepherd, 1994). This is graphically shown in Figure 14.

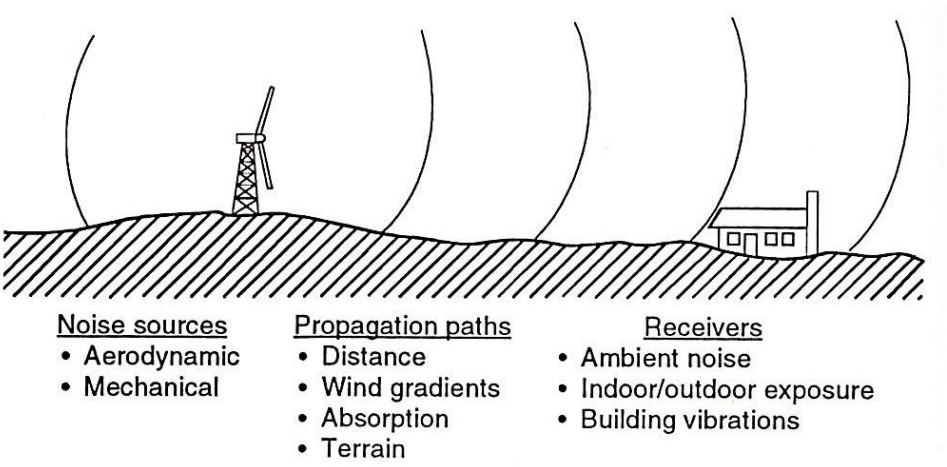

Figure 14. Factors that affect wind turbine noise. This figure divides the system through which wind turbine noise is affected into three discrete categories. From "Figure 7-1. Wind Turbine Acoustics," (Hubbard & Shepherd, 1994, p. 324).

The sound of a wind turbine is the result of a variety of independent acoustic point sources emitted from the various components that compose the wind turbine's total structure. This extensive variety of components is separated into two fundamental contributing acoustic source categories, aerodynamic and mechanical. The acoustic sound waves leave the wind turbine and propagate through an atmospheric medium, where the sound pressure level diminishes as its energy is lost. Finally, the sound is received at a particular location where it can be measured. The reception of the wind turbine sound is dependent on the location's background noise level.

Acoustic Emission Point Sources

Wind turbines can produce a wide variety of sound levels and frequencies depending on chosen blade design, tower type, and the specific complexity (number and type) of mechanical parts. The blade design and mechanical configuration are determined by the manufacturer during the design process of the wind turbine, whereas the tower type is typically chosen by the end user. As previously stated, it has been well documented that the two main categories of wind turbine noise sources are either mechanical or aerodynamic.

Component contributors that are labeled as being mechanical sound sources are produced as a result of the variety of moving parts located within the nacelle of the wind turbine. Component contributors that are categorized as aerodynamic result from the air flow disturbances from the air encountering the blade, creating varying localized air pressure difference zones. The air encountering the tower after being disturbed by the moving blade is also considered to be aerodynamic.

Mechanical component contributors. The mechanical noises that add to a wind turbine's sound are produced by moving components within the wind turbine nacelle (Figure 15). The mechanical point source contributors may include, but are not limited to, rotor bearings, drive train, gears within a gearbox, generator, brakes, yaw drive, cooling fans, or other auxiliary accessories depending on the individual wind turbine model (Hubbard & Shepherd, 1994, p. 325). "Mechanical noise is normally perceived within the emitted noise from wind turbines as an audible [narrowband] tone which is subjectively more intrusive than a broadband noise of the same sound pressure level" (ETSU Working Group on Wind Turbine Noise, 1996, p. 13). This results in the specific point source emissions produced by mechanical component contributors to contain their sound pressure in discrete frequencies, producing less harmonics and in effect, becoming more noticeable to the human ear. Because these narrowband sounds are more intrusive to the human ear, they are of a higher importance for acoustic emission point source mitigation.

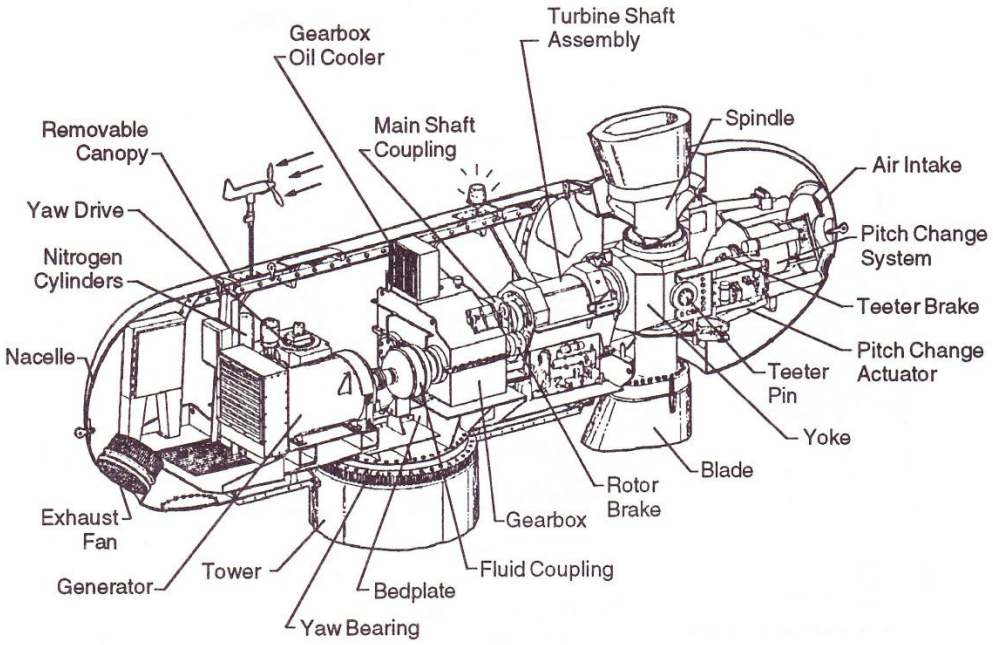

Figure 15. A diagram of mechanical components within the nacelle of a medium scale wind turbine. From "Figure 4-12. Power trains in representative medium-scale HAWTs" (Lynette & Gipe, 1994, p. 168).

Bearings: These are small metal spherical objects. They reduce the resistance of the rotating turbine shaft assembly on its mount which is located at the wind turbine's hub. These will resonate if they are improperly lubricated, creating a relatively high pitched acoustic emission. The yaw bearings are used less frequently and therefore are usually less of an acoustic contributor to the operating turbine's sound.

Brake: There are varying types of brakes used on a wind turbine depending on the manufacturer's design. One form of brake is a disc brake which can be applied mechanically, electrically, or hydraulically to stop the rotor in emergencies. If the brake is out of alignment it can rub, producing periodic amplitude modulated squeaks that occur within a relatively high frequency range during the wind turbine's normal operation.

Exhaust Fans: A cooling system is sometimes used to avoid possible overheating within the nacelle. These fans remove the heat radiating from the internal machinery of the

nacelle by pulling cold air over the components and expelling the hot air from the nacelle through the fans. In utility scale wind turbines, they run continuously while electricity is being produced. The acoustic emission produced by this component of the wind turbine is non-amplitude modulated and does not change in sound pressure level in relation to wind speed. They are considered a mechanical contributor because they are a component of the nacelle even though they produce aerodynamic noise as a result of the blades moving through air (similar to the rotor of a wind turbine passing through air). For this reason, the exhaust fans are observed as broadband noise.

Gear box: Gears are used on many larger wind turbines to connect the low-speed rotor shaft to the high-speed generator as required by most generators. Vibrations produced by interaction of the gears' teeth are emitted as noise as they pass through "direct mechanical linkage… and may be re-radiated as sound at any position where the structure is exposed to atmosphere" (ETSU Working Group on Wind Turbine Noise, 1996, p. 13). To reduce the acoustic contribution of the gear box, manufacturers have isolated the gear box vibrations from the supporting structure by adding dampening materials to break any hard linkage that may allow the vibrational energy to transition to the supporting structure. Some manufacturers have chosen to use a *direct-drive* configuration. The direct drive option removes the gears entirely, totally eliminating the gearbox as an acoustic contributor to the wind turbine noise emissions. Northern Power Systems is one wind turbine manufacturer in particular that offers a direct drive configuration. They claim:

> Our gearless, direct drive train is at the heart of Northern Power's leading edge 'less is more' wind turbine design focus. Our turbine's generator and rotor are directly coupled and move together at the same speed. By

> eliminating the gearbox feature, we have simplified the drivetrain design by radically reducing the number of moving parts and wear items. (Northern Power Systems, 2012)

Generator: This component converts the mechanical energy obtained from the wind by the rotor blades into electricity. It may produce a buzzing or humming sound which is typical for electrical devices as a result of the alternating electrical fields within the generator.

Turbine Shaft Assembly: This component transfers mechanical energy from the rotor assembly to the gear box and then to the generator. This part of the wind turbine should only produce sound if the bearings holding it in place are not properly lubricated.

Yaw Drive: The yaw drive consists of a small electric motor that produces acoustic emissions when it changes the position of the nacelle and rotor blade. Upwind turbines utilize this component but downwind turbines do not require a yaw drive as a result of the fundamental design that relies on the wind blowing into the downwind position. The acoustic emissions produced by the yaw drive are similar to the sound of a generator because the yaw drive is effectively composed of the same components, only in reverse order; in this case, it transforms electrical energy into kinetic energy for physical movement.

The totality of the listed components is the basis for the mechanical identifiers within the *point source contributor identification* section described in Chapter 4 of this study.

Aerodynamic component contributors. Aerodynamic contributors to the total wind turbine acoustic emissions are the result of the blade design and the type of tower used. Wind turbines acquire kinetic energy from the wind as a result of the fundamental airfoil (or aerofoil) shape of the rotor blades. This shape creates a differential in the rate of speed that

air moves over the upper and lower surfaces of the foil, creating a lower air pressure (faster-moving air) beneath the blade in comparison to the air pressure above the blade (slower-moving air). This causes movement of the rotor blades as the air pressure seeks to equalize itself by, in effect, pulling the blade towards the lower pressure side. The air flow disturbances caused by the aerodynamics of the moving blades through the surrounding air as well as other possible flow disturbances produce acoustic emissions.

The airfoil shape interacts with the wind to produce acoustic emissions that can be categorized into multiple individual point sources. The aerodynamic sounds are produced "when the rotating blade encounters localized flow deficiencies due to the flow around the tower, wind speed changes, or wakes shed from other blades" (Rogers, Manwell, & Wright, 2006, p. 11).

The aerodynamic contributors (Figure 16) to a wind turbine's acoustic emissions as a result of the airfoil shape of the blade can be categorized into four discrete point source contributors: inflow turbulence, turbulent boundary-layer flow (laminar transition flow), trailing edge bluntness vortex shedding, and tip vortex shedding.

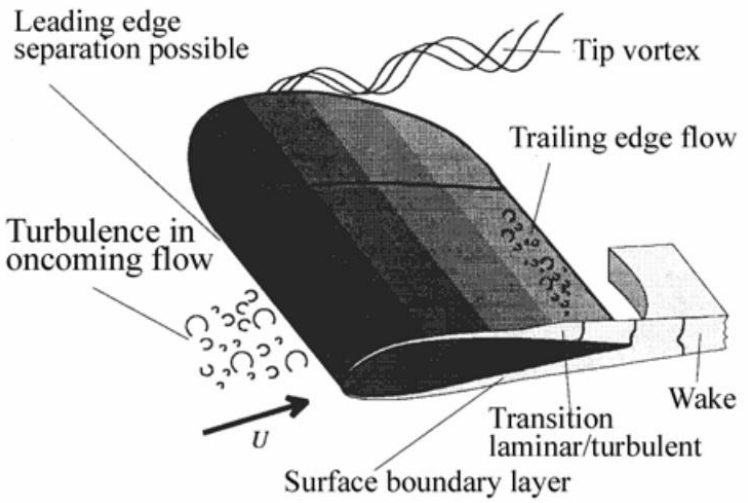

Figure 16. A diagram of the aerodynamic point source contributors to a wind turbine blade's acoustic emissions. From "Figure 7: Schematic of Flow around a Rotor Blade" [Wagner, 1996] (Rogers, Manwell, & Wright, 2006, p. 12).

The inflow turbulence is caused by the leading edge of the rotating wind turbine blade's interaction with "atmospheric turbulence that causes variations in the local angle of attack, which in turn causes fluctuations in the lift and drag forces" (Hubbard & Shepherd, 1994, p. 336). As the incoming air flow encounters the blade, the air is split above and below the blade. This acoustic emission is also non-amplitude modulated because the blade is constantly encountering new air flows that are unrelated to the rotation of the blade. The resulting noise is observed as broadband in nature, creating multiple peak frequencies that vary in range greater than one-third of an octave.

The turbulent boundary-layer flow, also termed the laminar transition flow, is the result of the air flowing over the upper and lower surfaces of the blade. This point source contributor is also non-amplitude modulated and contains multiple peaks outside of one-third of an octave in relation to each other, rendering it a broadband noise contributor.

The trailing edge bluntness vortex shedding is the result of the two turbulent boundary-layer flows' interaction as they congregate on the trailing edge of the airfoil. This is a pronounced contributor in small scale wind turbines because they are sometimes purposefully designed to use this principle to their advantage for passive stall protection against over-speed rotations. This design feature adds to their acoustic noise emission levels. Migliore, van Dam, and Huskey (2004) suggest that "some wind turbines suffer an unfavorable reputation for noise problems associated with high tip speeds, furling, or blade flutter" (p. 1).

Utility scale wind turbines are typically more complex in their design to minimize aerodynamic acoustic emissions. Some manufactures integrate *vortex generators* (Figure 17).

Vortex generators are small serration-like shapes that are installed on the trailing edge of the blade.

Figure 17. An example of vortex generators located on a wind turbine blade developed by LM Wind Power. From "Aerodynamics – a balance between performance and load" (LM Wind Power, 2012).

Tip vortex shedding is another point source contributor to a wind turbine's aerodynamic noise production. Specific peak frequencies are produced depending on the designed geometry (shape) of the blade tip. One manufacturer of small scale wind turbines, for example, is Southwest Wind Power. The company has chosen to utilize a sharply pointed blade tip design (Figure 18) that disturbs less air; however, in return it emits a higher pitched, narrowband acoustic emission that contains a more discrete set of frequencies, rendering it more noticeable to the human ear. Another small scale wind turbine manufacturer, Bergey Wind Power, has chosen to use a simple squared-off blade tip design (Figure 19) with only a small angled notch to cut the air more easily. This design emits more of a broadband noise emission than the sharper tip design, but as a drawback, produces a larger contribution to total sound pressure level.

Figure 18. Skystream 3.7 blade tip design. From "Skystream 3.7™ Compact Wind Turbine and Wind Energy System" (Solar Direct, 2012).

Figure 19. Bergey XL.1 blade tip design. From "Bergey 1kW Battery Charging Wind Turbine" (Connexa Energy, 2012).

Blade impulsive noise is produced as a result of the interaction of the disturbed air created by the blade with the tower that mounts the wind turbine for upwind wind turbines. Because this noise depends on the wind turbine's blade design and tower type, the shape of the blade creating the air disturbances as well as the tower (monopole or lattice) both have an impact on the acoustic emissions.

Blade impulsive noise has a greater influence on the total wind turbine acoustic emissions for downwind wind turbines (Figure 20). The disturbance of the air flow by the tower prior to the blade's interaction with the air adds complexity to the air flow, resulting in a louder sound. For this reason, downwind turbine configurations are not used on the utility scale.

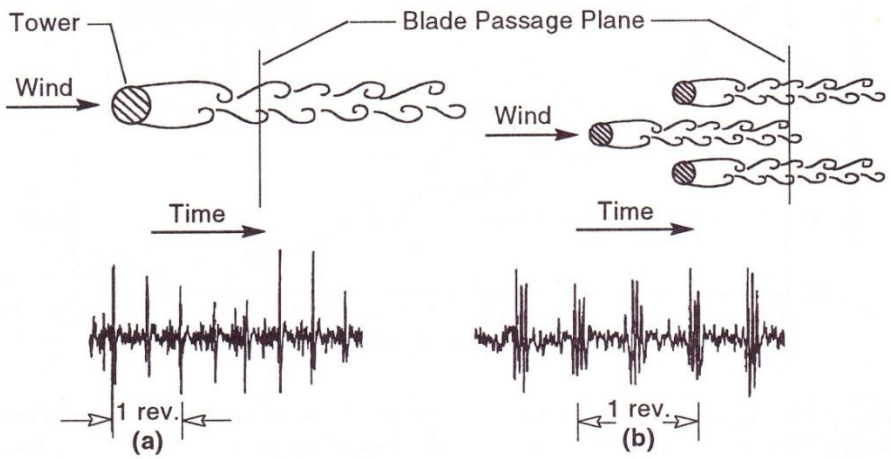

Figure 20. Sound pressure time histories from two downwind-rotor HAWTS. This figure shows the impact of using a lattice tower versus a monopole configuration. The lattice tower effectively causes three blade impulses for each blade rotation instead of just one. The lattice tower's blade impulsive noise can be recognized to contain broadband acoustic emission features than the monopole's. From "Figure 7-3. Sound pressure time histories from two downwind-rotor HAWTS" (Hubbard & Shepherd, 1994, p. 326).

The totality of these aerodynamic point source contributors is the basis for the aerodynamic identifiers within the "acoustic point source identification" section found in Chapter 4.

These concepts of blade design and presented information about mechanical componentry are taken into account by manufacturers who have utilized these principles when designing their wind turbines to make the overall wind turbine as quiet as possible. Manufacturers are currently using fewer components and making them as simple as possible.

Pathways of Wind Turbine Noise

Simultaneous acoustic measurements to measure the direction in which the sound propagates have been taken. The results are graphically shown by a *wind turbine sound rose* (Figure 21) in respect to the wind turbine as a single point source (dimensionally the hub of the wind turbine). Hubbard and Shepherd (1994) state that "acoustic radiations upwind and downwind are about equal and are greater than that in the crosswind direction" (p. 328). In

other words, the acoustic point source radiation appears as an acoustic dipole; this is directly related to the fact a sound will emit most easily in the perpendicular direction from its source.

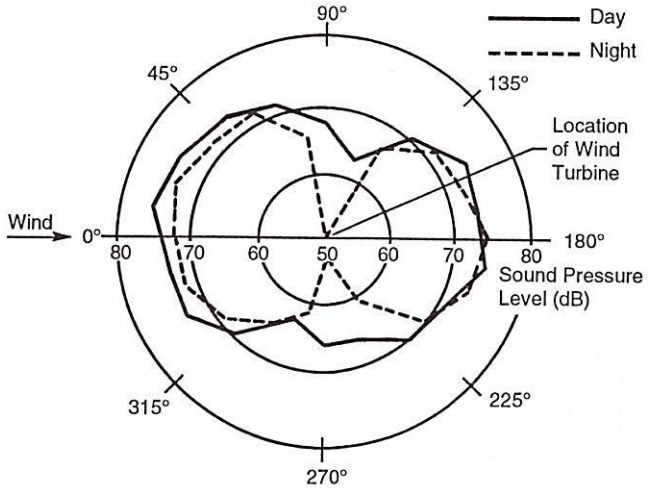

Figure 21. A wind turbine sound rose. This figure describes the direction of sound propagation from a wind turbine in terms of the sound pressure during both day and night time. From "Figure 7-16. Example radiation patterns for low-frequency rotational noise 200 m from a large-scale HAWT" (Hubbard & Shepherd, 1994, p. 328).

After the sound departs the wind turbine, the distance from the emitter to the receiver is the single largest impacting factor on a sound's pressure level. Integrating the atmosphere as a propagation medium attenuates the sound pressure, as shown in Figure 22.

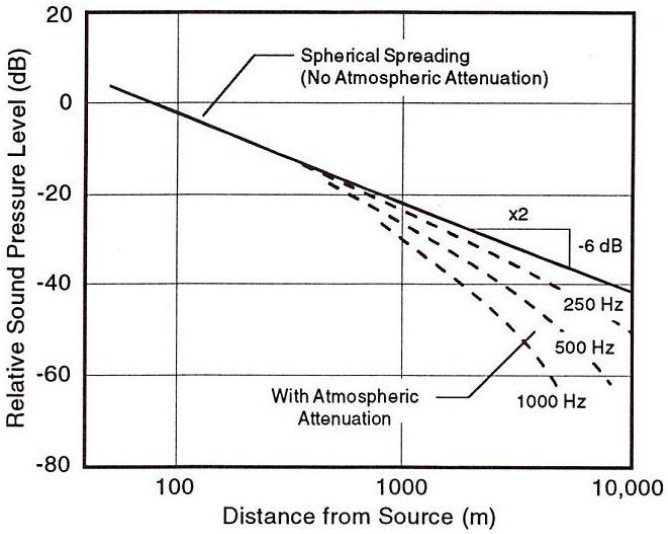

Figure 22. Atmospheric attenuation to sound pressure level in relation to the distance from a sound source. From "Figure 7-18. Decrease in the sound pressure levels of pure tones as a function of distance from a sound source" [ANSI 1978] (Hubbard & Shepherd, 1994, p. 342).

"As sound propagates through the atmosphere, its energy is gradually converted to heat by a number of molecular processes such as shear viscosity, thermal conductivity, and molecular relaxation, and thus atmospheric absorption occurs" (Hubbard & Shepherd, 1994, p. 342). Sound decreases with distance at a rate of approximately $1/_{r^2}$ which is derived from a geometrical ratio of a sphere's surface area over a distance in space. It is most commonly called the *inverse square law* (Figure 23). Sound being logarithmic means that "sound pressure levels decay at the rate of -6 dB per doubling of distance, in the absence of atmospheric effects" (Hubbard & Shepherd, 1994, p. 341).

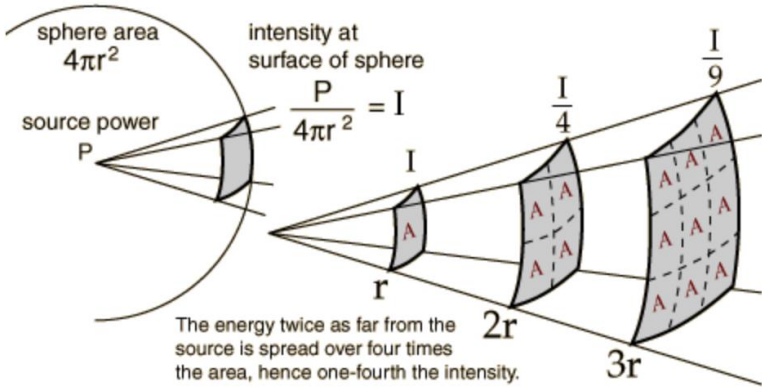

Figure 23. A three-dimensional illustration representing sound pressure diffusion over a doubling of successive distances. This figure exhibits the effect that distance has on the sound pressure as the sound radiates from a source in a three dimensional space. From "Inverse Square Law, Sound" (Nave, 2012a).

The roughness of the terrain can have an absorption effect on the sound waves when the two encounter each other. Locations such as flat farms that are spread out with a fairly even terrain have a small absorption effect on the sound propagation; therefore, the sound follows the inverse square law more closely and fewer measurements "at any specific location on the site under virtually any wind condition" (Hessler & Hessler, 2006, p. 11) are necessary to obtain accurate readings that contain little uncertainty. In accordance with this

idea, Prospathopoulos and Voutsinas (2005) argue that "in complex terrain cases, the wind velocity and the relief of the topography can significantly affect noise propagation, suggesting the necessity for using sophisticated propagation models" (p. 234). Therefore, in these complex terrain locations, the sound has a harder time propagating and a larger quantity of samples must be obtained at various locations to map out sound pressure levels at various locations.

These variations in the site conditions between multiple tests at varying locations are accounted for through the application of formulae provided by the IEC that standardize the varying conditions to a standard test condition. The result should yield a measured unit that is comparable between multiple tests by adjusting the recorded measurements to the predefined standardized reference testing conditions.

Background Noise Measurement

As previously stated, wind turbines only spin and produce electricity when the wind is blowing. The wind creates sound on its own. This plays a particularly important role because the wind effectively masks a portion of the wind turbine noise. If the turbine is quieter than existing background noise levels, the turbine's acoustic emissions will be masked and therefore become unnoticeable to proximate inhabitants.

Hubbard and Shepherd (1994) discuss the importance of background noise:

> Sources of background noise are the wind itself; its interaction with structures, trees, and vegetation; human activities; and, to a lesser extent, birds and animals. Natural wind noises are particularly important because they can mask wind turbine noise, as a result of the fact that their broadband spectra are similar to those of wind turbines. (p. 358)

Epsilon Associates, Inc. (2006) states that to be able to accurately determine if a sound is a result of the wind turbine, we must examine the "ambient noise level in order to characterize the existing 'baseline' acoustical environment in the vicinity of the proposed wind turbine project" (p. 3).

A pre-installation noise survey is integral in the planning stage of a wind turbine project. Hessler and Hessler (2006) describe the importance of this measurement:

> A noise impact assessment for any proposed wind turbine project requires a survey of existing environmental sound levels at the site to establish what minimum level of natural masking noise is consistently present to obscure noise from the [wind turbine] project. (p. 12)

This is a critical measurement due to the fact that "the turbines only produce noise under windy conditions when the background sound levels are also elevated" (Hessler & Hessler, 2006, p. 10).

Noise Ordinances

Noise ordinances have been developed to encourage thoughtful wind turbine installation siting. They serve to acoustically protect civilian comfort. These ordinances are based upon the sound pressure levels and tonal frequencies observed by an acoustic receiver at a particular location. Some municipal ordinances specify the maximum allowable acoustic emissions that may be heard outside of the turbine's installation property line.

The ordinance's levels are typically set in relation to the measured background noise levels observed at the particular region where the noise ordinance is to be enforced as well as the number of people that may be affected (determined by population density). Residential environments present relatively higher background noise levels but contain a greater

population density. Rural or agricultural areas, on the other hand, exhibit relatively lower background noise levels but present a less dense population. Stankovic, Campbell, and Harries (2009) discuss the noise impact on urban locations:

> In contrast [to residential locations], in urban locations, the ordinary background noise levels can reach 70dB$_{(A)}$. The lack of precedents for the siting of wind turbines in urban/residential locations will usually mean that planning conditions are set on a case-by-case basis based on the existing noise regulation relative to the urban environment. (p. 89)

One example noise ordinance (Table 1) from the township of Mundy, Michigan has been provided for this discussion. This example has been chosen in particular because Michigan has pursued wind turbine farm development and a great deal of effort has gone into examining the quality and accuracy of their noise ordinances. This can be observed in the ordinance itself because it has the specificity of sound pressure levels at particular frequencies, which is much greater detail than most current noise ordinances in place globally. This supports examining acoustic principles in greater depth, as discussed in this paper, instead of simply stating a single decibel level threshold.

Table 1. *An Example Noise Ordinance from Mundy, Michigan*

		Frequency at center of octave band					Total Noise Limit
District Type		31.5 Hz	63 Hz	125 Hz	250 Hz	500 Hz	
Residential	Day	72 dB	71 dB	65 dB	57 dB	51 dB	55 dB(A)
	Night	67 dB	66 dB	60 dB	52 dB	46 dB	50 dB(A)
Agricultural	Day	82 dB	81 dB	75 dB	67 dB	61 dB	65 dB(A)
	Night	72 dB	71 dB	65 dB	57 dB	51 dB	55 dB(A)

Note. The table specifying the sound pressure level limits has been divided into residential and agricultural regions as a result of residential areas containing a greater population density. From "Table 10. Mundy Township Octave Band Noise Limits" (Alberts, 2006, p. 18).

The International Standard for Acoustic Emission Measurement on Wind Turbines

The IEC Standard 61400-11 (edition 2.1) is the current global standard for wind turbine acoustic emission measurement, characterization, and reporting of results. "The purpose of this part of IEC 61400-11 is to provide a uniform methodology that will ensure consistency and accuracy in the measurement and analysis of acoustical emissions by wind turbine generator systems" (International Electrotechnical Commission, 2006, p. 6). The IEC Standard dictates the placement of the microphone used to measure the sound pressure level of the wind turbine as well as the placement of a meteorological tower to measure wind speeds and wind directions. It also describes the weighting scale used to report the measured sound pressure level values.

Placement of Microphone

The IEC Standard prescribes the placement of the microphone in relation to the wind turbine (Figure 24). This is referred to by the IEC Standard as the "tip-height." Equation 2, which is described as R_0, calculates the horizontal distance between the base of the wind turbine's tower and the location of the microphone.

$$R_0 = H + \frac{D}{2}$$

Equation 2. IEC formula to calculate horizontal distance for microphone placement from wind turbine. From "Formula (1)", (International Electrotechnical Commission, 2006, p. 14).

The microphone is placed on a circular piece of wood placed on the ground, downwind of the turbine at the tip-height and within plus or minus fifteen degrees of the wind direction at the time of the recording. The wind turbine sound rose (Figure 21) dictates the reason that the IEC Standard positions the microphone for acoustic measurement directly

downwind from the wind turbine. This is designed capture all point sources of acoustic emissions produced by a wind turbine.

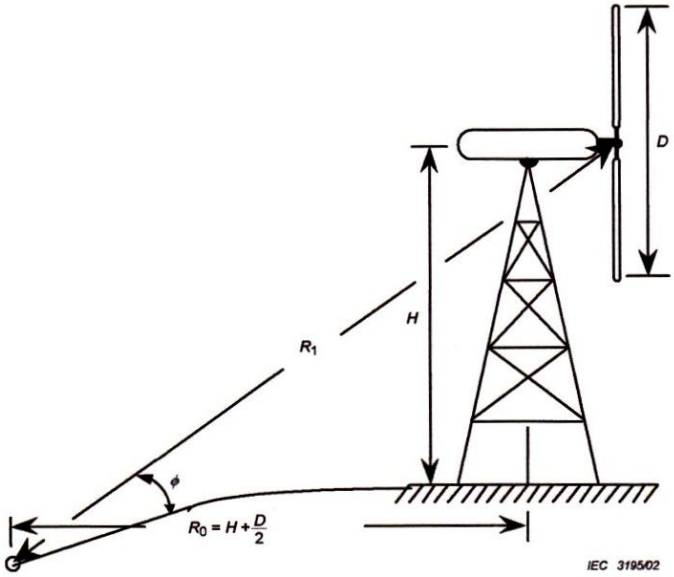

Figure 24. Illustration of the placement of the microphone for acoustic testing on horizontal axis wind turbines. This figure shows the horizontal distance, R_0, from the base of the wind turbine to the microphone position. From "Figure 4a – Horizontal axis turbine" (International Electrotechnical Commission, 2006, p. 32).

The IEC Standard also specifies that the R_0 is a reference distance for the ideal location for the microphone. However, the tester may place the microphone ± 20% in relation to R_0 and still be within the allowable region for recording (International Electrotechnical Commission, 2006, p. 14). This formula is only to be used on horizontal axis wind turbines. A different formula is specified for testing on vertical axis wind turbines, although it is not relevant to this study.

Placement of Meteorological Tower

The IEC Standard specifies the placement of the meteorological mast that holds the anemometer and wind vane (Figure 25). The meteorological measurements should be at a height between ten meters and hub height upwind of the turbine and installed within a horizontal distance of two to four rotor diameters.

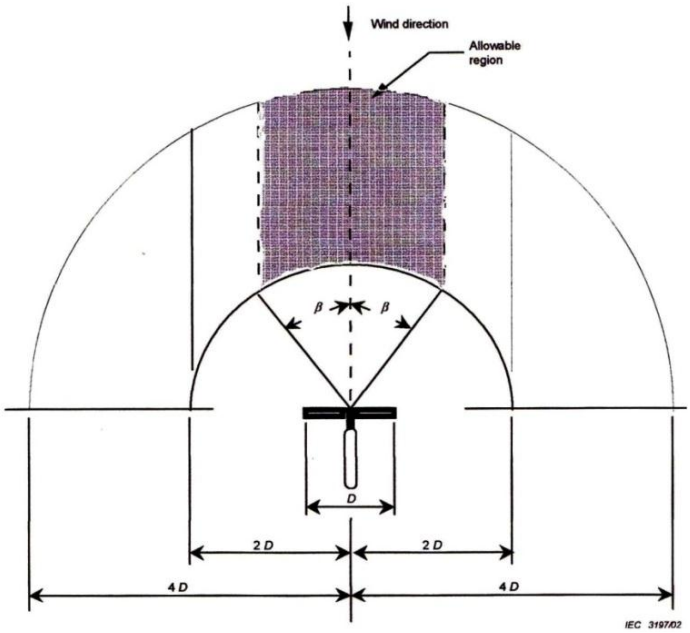

Figure 25. IEC placement of the meteorological tower. This figure shows the region in which the meteorological mast may be placed while remaining in the allowable region specified by the IEC. From "Figure 5 – Allowable region for meteorological mast position as a function of β – plan view" (International Electrotechnical Commission, 2006, p. 33).

The allowable region's angle (β) adjusts depending on the meteorological tower's height for placement of the anemometer. β is calculated using Equation 3.

$$\beta = \frac{Z - Zref}{H - Zref}(\beta max - \beta min) + \beta min$$

Equation 3. IEC formula to determine the allowable degree range for placement of the meteorological tower. From "Formula (3)" (International Electrotechnical Commission, 2006, p. 15).

This equation is mathematically stating that the closer the anemometer is installed to the reference height of ten meters, the smaller the acceptable angle is for a valid installation location for the meteorological tower to be installed (down to ±30°). As the anemometer becomes closer to the hub height of the wind turbine, the β angle can increase up to ±90° while still remaining in accordance with the IEC 61400-11 Standard (i.e., if $Z=Zref$, then $\beta=\pm30°$, or if $Z=H$, then $\beta=\pm90°$).

Weighting Scales

To account for the non-linear sensitivity (discussed earlier) that the human ear experiences in relation to frequency, a widely used method of weighted scaling is used to adjust the sound pressure levels to louder or quieter depending on their frequency, in order to more accurately relate a non-human instrument receiver's (such as a microphone) measurement of the sound pressure level to what a human ear may experience.

Measuring sound using a device will not represent how the human ear would perceive a sound since the device is mechanical in nature and does not contain the same intricacies that the human ear has developed over its evolution. As a result, the measuring device will report the sound pressure levels for all frequencies equally. As mentioned earlier, two sounds at varying frequencies with the same amount of sound pressure level may be perceived as different amplitudes to the human ear. This is not true of man-made mechanical devices for measuring sound. The device has no consideration for what the frequency is; it just records the sound pressure level received by the device. From a weighting perspective, we would consider this to be linear weighted. To compensate for this difference, we usually put the received levels by the microphone through a filter to make the levels more closely relate to what the human ear would have heard from the same sound source.

The IEC has produced a weighting curve (Figure 26) that takes the linearly measured values by the microphone and skews them proportionally to how a particular acoustic receiver would perceive the sound pressure levels in terms of the frequency they are measured in. A-weighting most resembles a normal human ear's perception of the sound pressures.

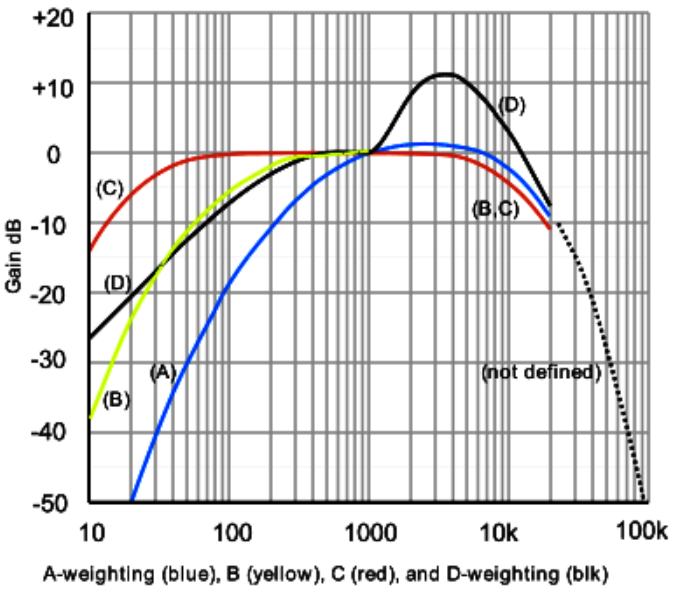

Figure 26. A, B, C, and D weighting curves from 10 Hz to 100 kHz. The IEC 61672-1 ed.1.0 Standard provides this graph for multiple weighting distributions. It shows multiple accepted weighting scales. From "IEC 61672-1 First edition Electroacoustic – Sound level meters, Part 1: Specifications" (International Electrotechnical Commission, 2002).

A-weighting remains the most widely used weighted curve when describing environmental noise and industrial noise because human acoustic receivers are the primary concern when reporting the results of the measurements. When the use of the A-weighting scale has been applied to a measurement, the transformation is denoted by adding a subscripted "(A)" after the dB value, *i.e.* $45dB_{(A)}$.

Chapter 3: METHODOLOGY, PART I:

ACQUISITION AND ANALYSIS OF IEC 61400-11 DATA

General Overview of the Research Design

This was a two-part study. The design of Part I, which involved collecting acoustic data from six wind turbines and performing IEC Standard analyses, is reported in this chapter. Part II of this study (Chapter 4) addresses the developed diagnostic tool that provides additional tonal analyses of the acquired acoustic data to create a more detailed description than requested by the Standard of noise emitted by the six wind turbine subjects.

Part I of this study's methodology used the data acquisition methodology of the IEC 61400-11 Standard for acoustic measurement of wind generator systems in order to allow the proposed diagnostic tool to build upon information gathered through any previous standard testing. The IEC Standard is primarily concerned with defining the A-weighted decibel levels emitted by a wind turbine in relation to the average wind speed observed during an analyzed segment, although this study was primarily concerned with the tonal data acquisition that can be retrieved at any given wind speed. Part II is where this study deviated from the IEC Standard.

Test Subjects

A total of six horizontal axis wind turbines were used for acoustic testing (Table 2). The test subjects ranged from a wind turbine with a rotor diameter of 1.17 meters and rated at 160 watts to a wind turbine with a rotor diameter of 93 meters rated at 2.3 megawatts. The

four smallest wind turbines included in the study were located at Appalachian State University's Wind Turbine Testing Facility at Beech Mountain. This was advantageous because of their proximity and accessibility for acoustic testing. The two largest rotor diameter wind turbines included in this study were made available through external contract work for a third-party product certifying corporation. These two particular wind turbines' models and test locations were requested to be presented as anonymous for use in this paper.

Table 2. *Wind Turbine Test Subject Specifications*

Test Subject	Hub Height (m)	Rotor Diameter (m)	Tip Height (R_0)	Swept Area (m^2)	Rated Power (Watts)	Tower Type
AIR Breeze	13.72	1.17	14.30	1.08	160	Guyed Tilt-up
AIR X	13.72	1.17	14.30	1.08	400	Guyed Tilt-up
Sunforce 600	13.72	1.31	14.37	1.35	600	Guyed Tilt-up
Skystream 3.7	21.34	3.72	23.20	10.87	2,400	Guyed Monopole
Anonymous 50kW	48.78	16.50	57.03	213.82	50,000	Lattice
Anonymous 2.3MW	80.00	93.00	126.50	6792.91	2,300,000	Tubular Steel Monopole

Note. This table shows the wind turbine specifications required by the IEC 61400-11. The two largest wind turbines have been named 'Anonymous' to preserve manufacturer confidentiality. It can be noticed in that a large gap in rotor diameter and rated power exists for the larger scale wind turbine test subjects as was previously mentioned in the 'limitations of the study' section of this paper.

Each wind turbine was recorded while operating in its natural environment. This ensured a realistic setting that included all natural variables such as wind speed, atmospheric temperature, atmospheric pressure, humidity, and background noise created by the surrounding vegetation. This allowed for the most accurate representation of how a wind

turbine acts in normal operation. The IEC 61400-11 Standard requires these "site conditions" to be noted during testing (International Electrotechnical Commission, 2006, p. 27).

For this study, the four smallest wind turbines were tested at Appalachian State University's Wind Turbine Test Facility at Beech Mountain, North Carolina. This is a complex terrain site with grass that is around .5 meters tall (mowed shorter around wind turbines). The 50kW wind turbine test site was on flat farmland with a bare-dirt ground containing areas of sprouting corn stalks approximately 50 meters downwind from the microphone. The 2.3MW wind turbine was located on hilly farmland with sprouting soybeans around the wind turbine and fully developed corn fields in a distance greater than 100 meters from the microphone.

Sampling

Acoustic emissions were recorded for continuous periods on each individual wind turbine. Long (greater than four hours) recording periods were used for each wind turbine to present enough data so that after the reduction process at least 30 valid measurements on each subject remained for within-subject verification. Analyses were performed on 10 continuous-second segments for the small scale wind turbines, whereas the utility scale wind turbines required one-minute segments for valid measurement due to the lower rotational speed of large rotor diameter wind turbines, as required by the IEC 61400-11 Standard. The slower rotational speed means a longer analysis is needed to capture the infrasound created from the blade passing the tower in order to fully add its sound pressure into the FFT analysis.

The sampling rate of the data logger was set to record the average wind speed for each second of acoustic measurement. It also documented a sample of the wind direction for the same second of time. The reason the data logger was set to record each parameter once per second in particular was to ensure a reasonably high time resolution of data to yield the greatest ability to choose segments of data that were uninterrupted by man-made outside influences.

Instrumentation

Acoustic instrumentation for this study included a free-field microphone, circular microphone mounting baseboard made of plywood, microphone wind screen, pre-amplifier, USB Carrier, sound level calibrator, sound level analyzer, and noiseLAB 3.0 acoustic recording software. Non-acoustic instrumentation included a meteorological mast, anemometer, wind vane, data logger, surveyor's measuring tape, and a Dell Studio 1555 Laptop with LoggerNet 4.0 software.

The microphone, sound level analyzer, sound level calibrator, pre-amplifier, laptop computer, and anemometer devices were all calibrated and certified by a National Institute of Standards and Technology (NIST) traceable verifier within one year of performing the acoustic test (in accordance with the IEC 61400-11 Standard). This ensured that the instruments were providing accurate and reliable results that coincided with other instruments that have been similarly calibrated to this same NIST standard. This creates comparable results with pronounced confidence in instrumentation consistency.

Acoustic

The free-field microphone used for acoustic recording was the model MP201 (Figure 27), manufactured by BSWA TECH. This "Class 1" microphone meets the IEC 61400-11 Standard.

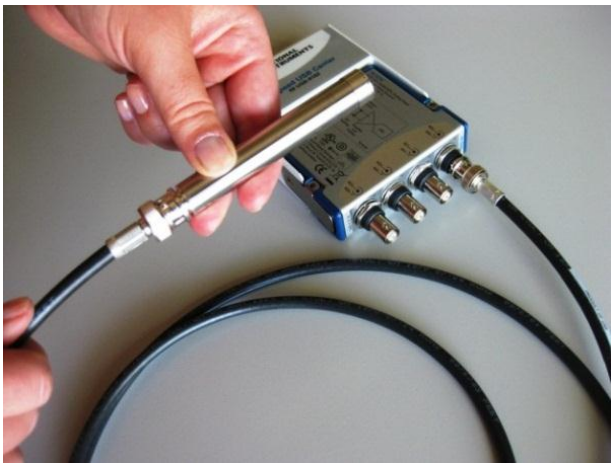

Figure 27. A picture of the MP201 free-field microphone used for acoustic measurement.

The microphone software (noiseLAB 3.0 and noiseLAB Batch Processor 3.1) served as a sound level meter, Fast Fourier Transform (FFT) analyzer, as well as a one-third-octave analyzer while used in conjunction with the MP201 microphone. The purpose of the sound level meter was to determine the decibel output of the wind turbine.

The circular piece of plywood used as the microphone mounting baseboard was 1 meter in diameter and 1.27 cm thick for compliance with the Standard. The purpose of this plywood disc is "to reduce the wind noise generated at the microphone and to minimise [sic] the influence of different ground types" (International Electrotechnical Commission, 2006, p. 11). The microphone wind screen was 90 mm in diameter, which also meets the stipulations of the IEC 61400-11 Standard. This wind screen eliminated unwanted noise created by the wind.

The pre-amplifier model used was National Instruments' NI 9233 (Figure 28). This component amplified the analog input of the microphone transmitted to the USB carrier to acquire a high signal-to-noise ratio. The USB carrier was the USB-9162 Hi-Speed USB Carrier manufactured by National Instruments. This component of the microphone system converted the analog signal received from the pre-amplifier into a formatted language that could be understood by the computer's USB port.

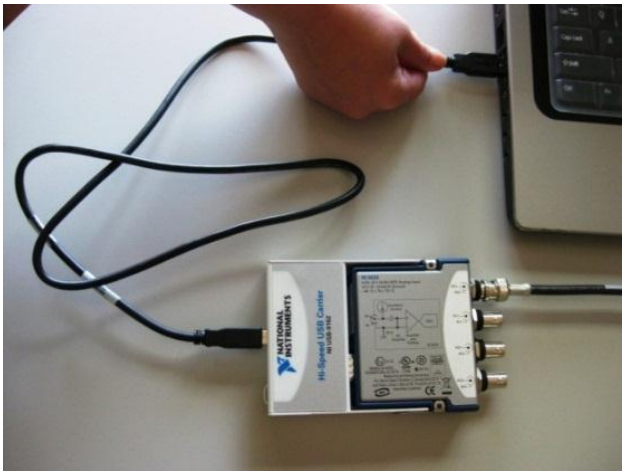

Figure 28. A picture of the NI 9233 pre-amplifier's connection with the USB-9162 Hi-Speed USB Carrier.

The sound pressure level was measured through the coupling of the free-field microphone sending an electrical signal to computer software called noiseLAB 3.0 and noiseLAB Batch Processor 3.1 through the Dell Studio 1555 laptop. These programs were used to perform all acoustic recording and analyses, respectively. The sound level calibrator was the model CA111 (Figure 29), also manufactured by BSWA TECH. It complies with the IEC 60942:2003 Standard as "Class 1." The sound level calibrator was used on-site before and after each recording period.

Figure 29. A picture of the CA111 sound level calibrator with inserted microphone.

Non-Acoustic

The meteorological mast being used was the CM375 (Figure 30), a 10 meter portable mast manufactured by Campbell Scientific. It extends 10 meters vertically into the air in order to meet the requirements of the IEC 61400-11 Standard for the reference height wind speed. The anemometer used was the Thies CLIMA Wind Transmitter "First Class" Advanced 4.3351.10.000. The wind direction was measured using the NRG #200P wind direction vane.

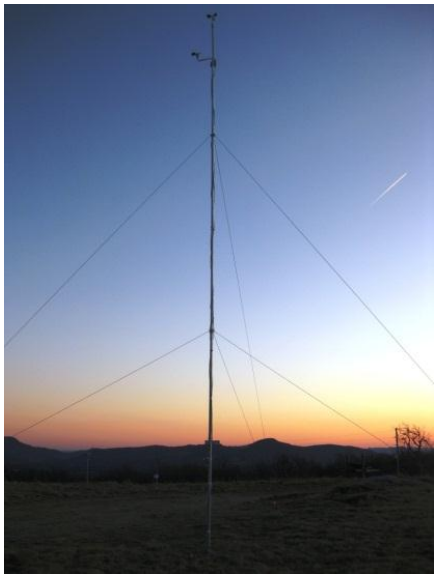

Figure 30. A picture of the CM375, 10 meter portable meteorological mast.

The surveyor's measuring tape served to locate the correct "tip-height" distance from the turbine's base to place the microphone and the circular piece of plywood. The data logger used was the CR1000 manufactured by Campbell Scientific. This communicated with the Studio 1555 Dell laptop using the program called LoggerNet 4.0.

Methodological Procedures, Part I

As mentioned earlier, the study was split into two discrete methodological sections. The purpose of this strategy was to distinguish between the IEC 61400-11 Standard acoustic characterization procedures that are current industry practice and the diagnostic tool that was developed through this study to build upon the IEC results for further characterization of a wind turbine's acoustic emissions. Part I, methodological procedures of the data acquisition, are reported here.

A flow chart describing the on-site methodology for data acquisition (Figure 31) as well as a flow chart describing the post-site methodology for data analysis (Figure 32) has been provided to assist the reader in the multi-step process designed to obtain the necessary results requested by the IEC 61400-11 Standard.

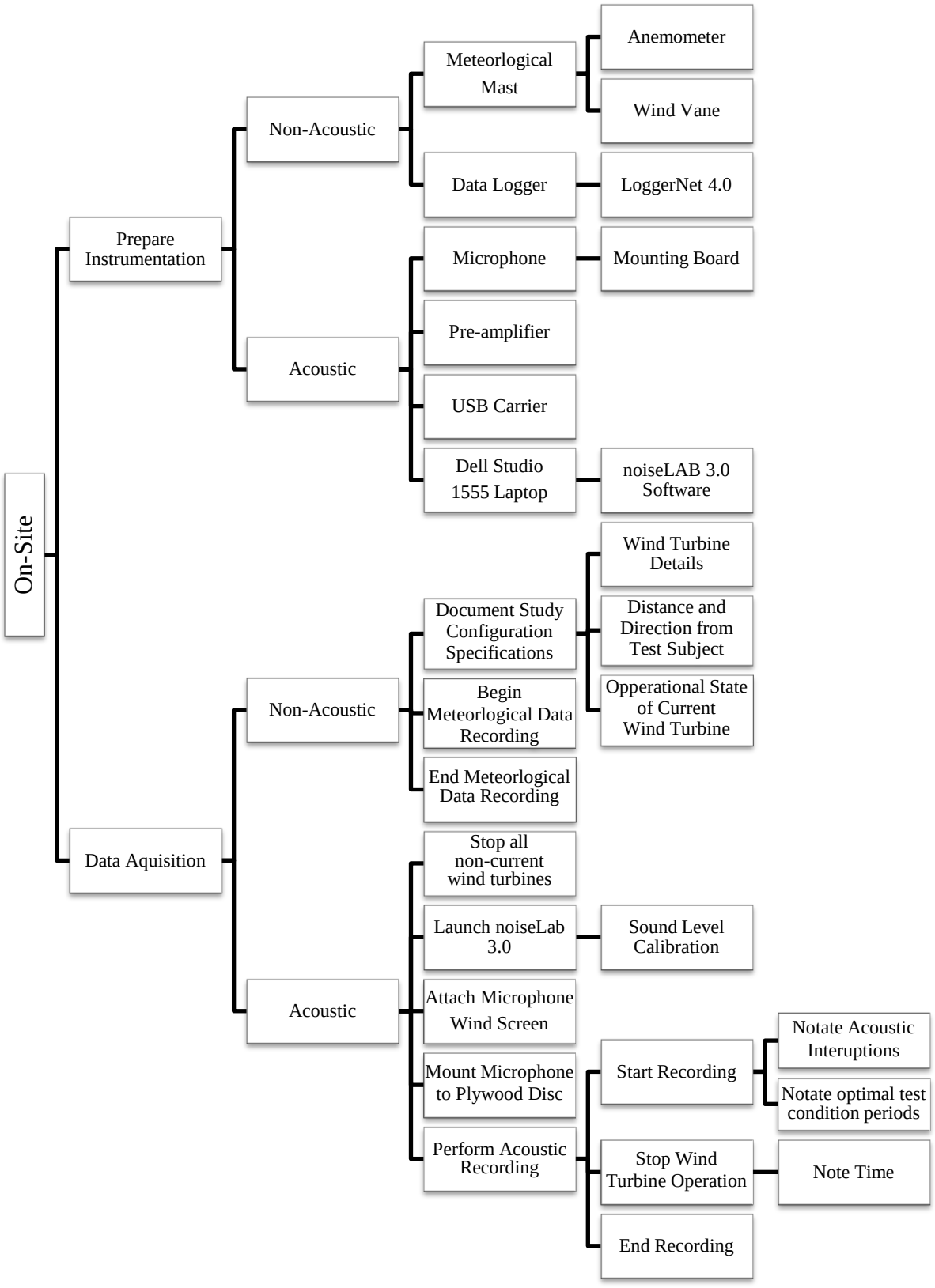

Figure 31. Flow chart for the on-site IEC 61400-11 data acquisition of Part I methodology.

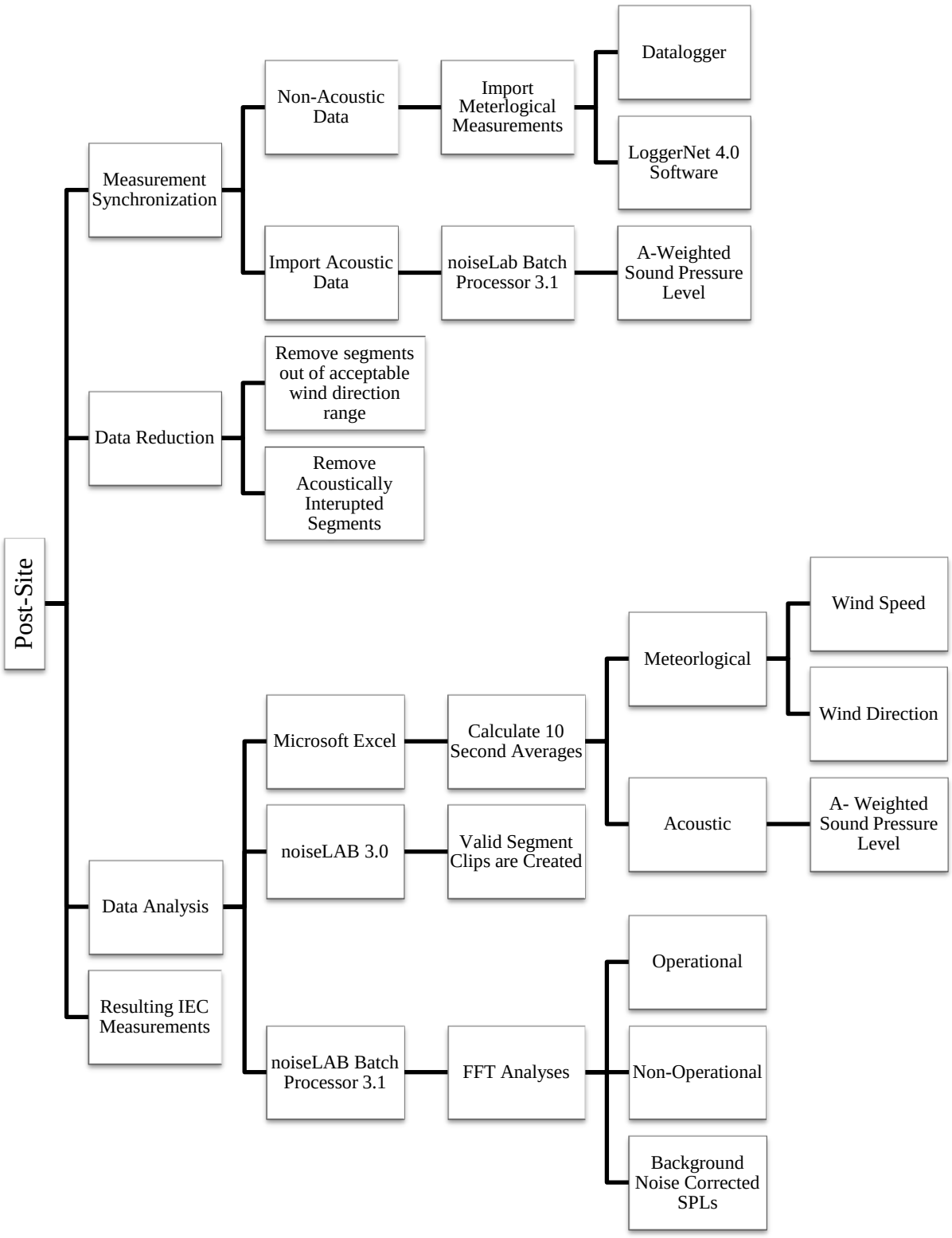

Figure 32. Flow chart for the post-site IEC 61400-11 data analysis of Part I methodology.

Prepare Instrumentation

Non-acoustic. The 10 meter meteorological mast was installed in a central location (Figure 33) at Appalachian State University's Wind Turbine Test Facility to obtain the necessary meteorological data measurements. Provided is a plot plan of the positions of the tested wind turbine subjects at the Appalachian State University Wind Turbine Test Facility. The diagram describes the location of the stationary meteorological tower, each tested wind turbine, and each subject's associated placement of the microphone. Also noted are the Pinnacle Inn Resort, bordering tree line, and the topography of the site elevation.

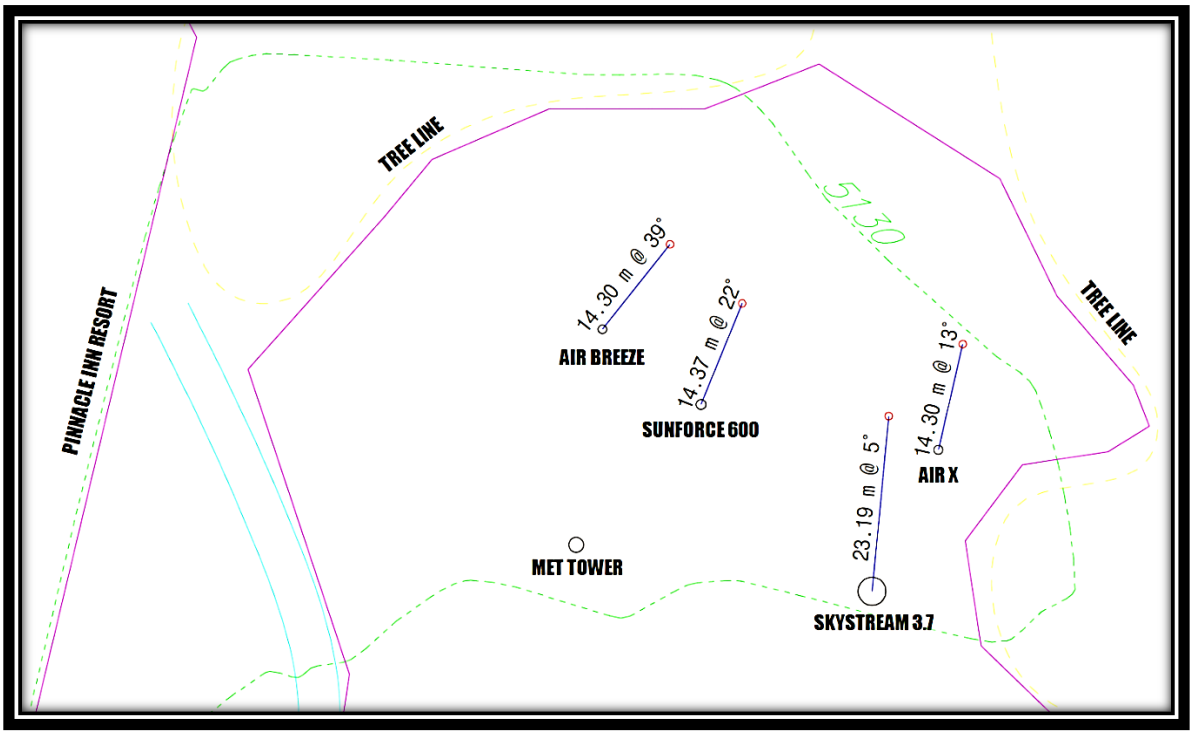

Figure 33. Plot plan of all test subjects' locations at the Appalachian State University Wind Turbine Test Facility. This figure shows the placement of the stationary meteorological tower as well as each test subject wind turbine's with their associated microphone placement.

The anemometer was located atop the 10 meter meteorological mast to procure the wind speed. The reason for mounting the anemometer above the top of the tower was to avoid any air flow disturbance created by the meteorological tower itself. This is also

specified as the correct methodology by the IEC requirement for sensor locations set forth by the IEC 61400-11 Standard.

The wind vane was placed on the same metrological mast to acquire the wind direction. It was placed on a boom, located 1.5 meters below the anemometer in accordance with the IEC 61400-11 Standard. The boom projected the wind vane far enough away from the tower to avoid the possibility of receiving any shadow effect created downwind by the mast. The main goal of using the wind vane was to ensure that the acoustic noise emitted from the wind turbine was being produced from the same wind creating the data observed at the location of the meteorological mast.

A data acquisition program (Figure 34) was written using "short-cut," a supplementary program in LoggerNet 4.0. It was then installed onto the data logger to allow the meteorological sensors to communicate with LoggerNet 4.0. The program was set to record the average wind speed and a sample of the wind direction once per second.

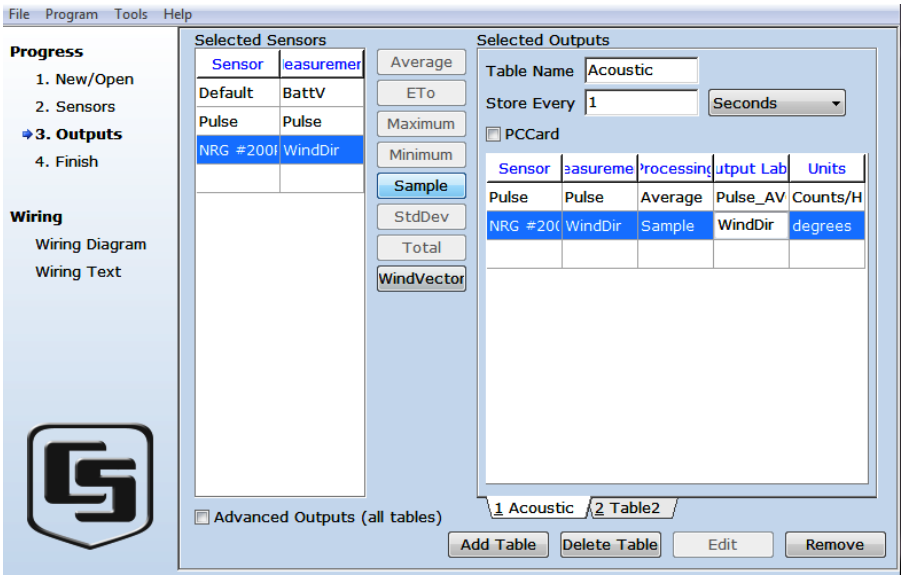

Figure 34. Screenshot of the short-cut program written to allow the data logger to communicate with the meteorological sensors.

For each second of logging, a timestamp with the date and time of measurement was associated with the observed meteorological measurements to allow for later synchronization with acoustic measurements in the analysis process.

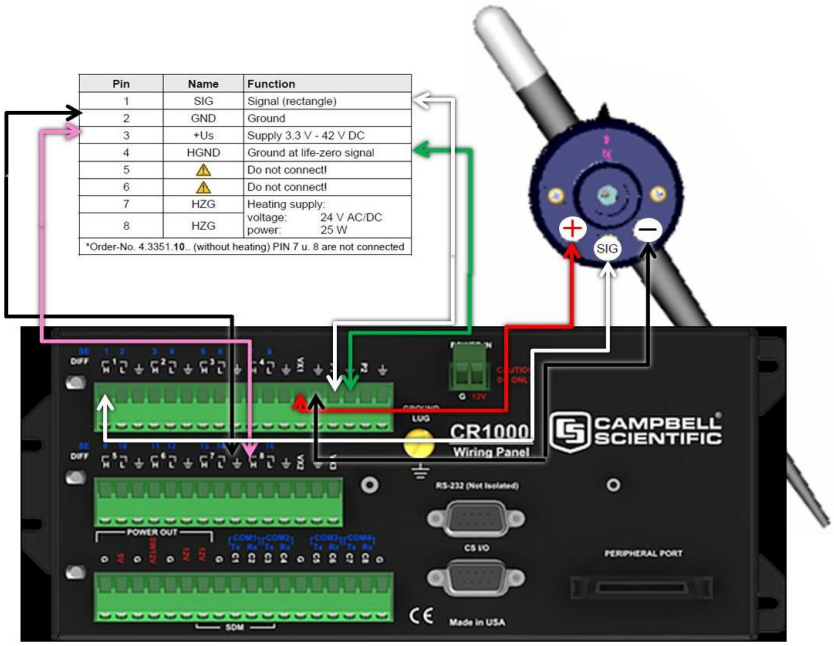

Figure 35. A diagram of the anemometer and wind vane wire connections to the data logger.

Sensor wires connected the anemometer and wind vane to the data logger (Figure 35 and Figure 36). The meteorological tower was raised into the upright position for correct placement of the reference height of 10 meters for the non-acoustic measuring devices.

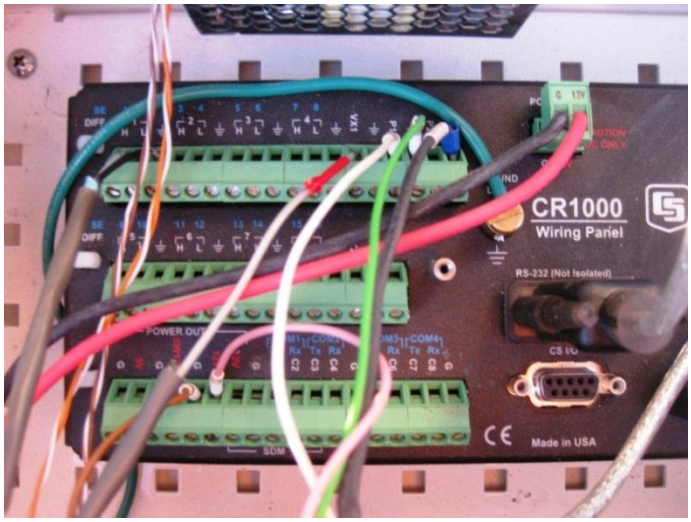

Figure 36. A picture of the actual data logger's wired connections used for testing.

Acoustic. Acoustic measurements were obtained using the free-field, directional microphone, which was placed at the tip-height for each respective wind turbine test subject. After the optimal distance was calculated, the surveyor's measuring tape was used to physically locate this distance, directly downwind of the wind turbine depending on the current prevailing wind direction during testing. The microphone mounting board plywood disc was placed flat on the ground at this distance.

The microphone sent an electrical signal (in analog form) to the preamplifier, which amplified the signal to increase the signal-to-noise ratio. This signal was then sent through a USB carrier which digitized the signal for interpretation by the Dell Studio 1555 laptop computer.

Data Acquisition

Non-acoustic. The CR1000 data logger was turned on to begin obtaining the necessary non-acoustic data. This allowed for recording of the measured meteorological conditions observed during the testing period. The data logger immediately began logging the meteorological conditions, once per second, as previously programmed in the instrument preparation stage. This data was used for synchronization with the acoustic measurements later in the procedure.

In accordance with the IEC 61400-11, the test subject wind turbine specifications were recorded. These specifications included the manufacturer, model, tower height, and rotor diameter. These parameters were noted in a notebook for later use in the data analysis procedure.

At the end of each recording session, the data logger was turned off to end the logging of observed meteorological measurements. Although this step is shown at this

particular location of the flow chart and narrative explanation, it was actually not carried out until after all acoustic data acquisition (described in the following section) was accomplished.

Acoustic. To ensure that the only wind turbine acoustic emissions entering the microphone were coming from the current test subject, all other wind turbines in the vicinity were short circuited to discontinue their operational state. The program noiseLAB 3.0 was launched on the Dell Studio 1555 laptop computer.

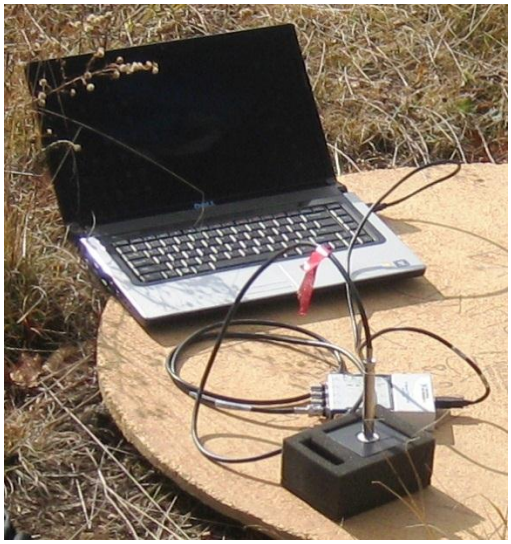

Figure 37. Microphone calibration set-up before performing acoustic recording.

The microphone was inserted into the acoustic calibrator (Figure 37) to adjust the measured sound pressure levels under a controlled condition in order to conform to the NIST calibrated source. This calibration ensured that the microphone was calibrated to accommodate the atmospheric conditions during the recording session (Appendix B). After noiseLAB 3.0 verified that it was receiving the correct parameters entered (noiseLAB 3.0's default calibration setting of 94 dB at 1000Hz), acoustic measurements were taken. The microphone wind screen was attached and the microphone was placed flat in the center of the

plywood mounting disc (Figure 38), facing directly towards the subject wind turbine (Figure 39).

Figure 38. Picture of microphone mounted to circular plywood disc.

Figure 39. Picture of the methodological set up on the AIR X wind turbine.

The "Record Now" icon was pressed in noiseLAB 3.0 to begin recording. During the recording, anomalous background noises were noted in a journal (Figure 40) for assisting later data validation. This included, but was not limited to, airplanes, insects around the microphone, and passing cars. "Insect noise [in particular] during summertime surveys

frequently causes a dramatic increase in recorded A-weighted sound levels" (Hessler & Hessler, 2006, p. 10). Thus, when these instances occurred, the time was noted to assist later in data reduction. This ensured that portion of the recording would not be used in the analysis of the acoustic emissions of the wind turbine.

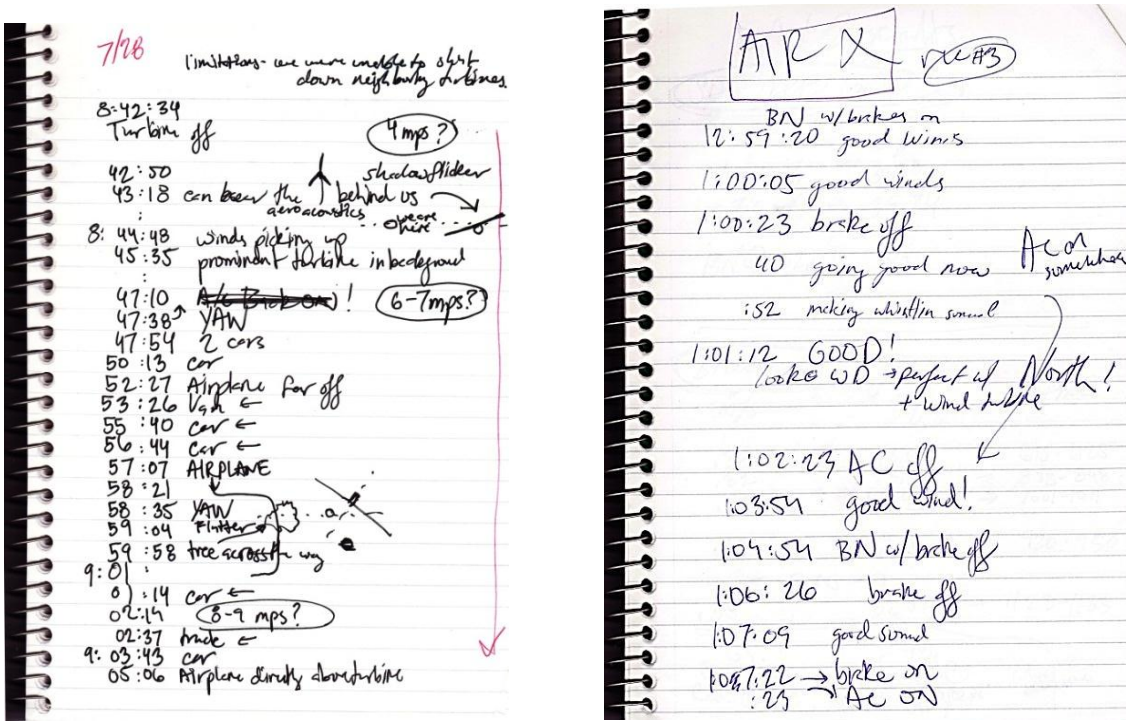

Figure 40. Example notes taken during on-site acoustic emissions tests.

Optimal recording conditions were also noted which occurred when there were no audible obstructions added to the natural environment such as airplanes or cars, the prevailing wind direction was within 15° (allowed by the Standard) of the line created between the wind turbine and the microphone, and the wind speed was fairly steady for at least 10 seconds. This provides periods of the most accurate acoustic measurement of the subject wind turbine in the operational state (as long as the wind is blowing and the turbine is producing power).

In addition to recording the acoustic output of the turbine in its operating state, a background (baseline) recording was taken. This measurement was used later in the background noise subtraction, which helped to differentiate which frequencies were being produced by the test wind turbine itself and which occurred as a result of natural processes. Hessler and Hessler (2006) state that "the background sound level must be determined as a function of wind speed" (p. 10). This was accounted for by subtracting a background noise level that was measured at the same wind speed as the operating wind turbine's sound pressure level. As the wind encounters any vegetation, such as a corn plant in the field, it moves the object, emitting the natural acoustic resonant frequency of that object. One particular seasonal factor indicated by Hessler and Hessler (2006) that may directly affect the sound level of the recording is "an increase of 8 to 10 $dB_{(A)}$ in ambient sound level from leafed out trees as a breeze or wind gust occurs" (p. 12).

To obtain the background noise level, the current test subject wind turbine was stopped by intentionally short-circuiting it so that no wind turbine noise was being received by the microphone to obtain the background noise level recording. The current time and operational state of the wind turbine (non-operational) were noted to assist in later acoustic analysis.

After the desired recording time length was reached, "Stop Recording" was pressed in the recording tab of noiseLAB 3.0 to end the recording segment. Each segment was saved and noiseLAB 3.0 could be closed.

Measurement Synchronization

Acoustic and meteorological data were synchronized using Microsoft Excel. The measured meteorological conditions, along with their associated time stamps, were collected

from the data logger. The Studio 1555 laptop was connected to the CR1000 data logger via the LoggerNet 4.0 software and the "Collect Now" button was pressed. This data was imported into a blank Excel spreadsheet. This provided the main Excel spread sheet used to compile all acoustic and meteorological measurements produced by noiseLAB Batch Processor 3.1 and LoggerNet 4.0, respectively.

To synchronize the meteorological data with the acoustic data, the A-weighted, sound pressure level for each second of recording was exported using noiseLAB Batch Processor 3.1 into another Excel spreadsheet. This acoustic data did not contain individual timestamps; however, noiseLAB Batch Processor 3.1 does present the start time (down to the second) and recording duration to the user. This allowed the individual second sound pressure level measurements to be copied and pasted into the Excel spreadsheet along with each respective second timestamp and meteorological measurement captured by the data logger. As a result, each second of recording was aligned with an associated wind speed and wind direction. This information was used later in the data analysis section of the study.

Data Reduction

In order to determine which segments of the recording were valid, the entire acoustic recording was exported as a ".wav" formatted file from noiseLAB 3.0. This .wav file was opened using the program Audacity to acoustically examine the recording in addition to using the notes made in the notebook that contained information stating which time segments were valid. To physically be able to hear the recording, the entire recording was amplified using Audacity to a comfortable listening level. This amplification increased the signal to noise ratio, allowing the listener to more easily detect any interruptions that may have occurred to the acoustic emissions of the wind turbine but that were not noted during testing.

This was a product of the incredible sensitivity of the directional microphone that was able to measure sound pressure levels much lower than the human ear can detect unaided (and thus were not noted during the recording).

When a time segment was reached that contained a notation made during the on-site recording, the Excel file was updated with information to reflect the particular characteristics of that period of recording. The information inserted into the respective cells denoted whether the acoustic segment was determined to be valid after listening to the segment in Audacity to make a final judgment on that period's measurement validation. The operational state of the wind turbine during this particular segment was also noted in the Excel file along with any other anomalies that were either written down during the testing procedure and then confirmed after listening back to the recording or that had been detected after amplification in Audacity. As noted earlier, this amplification sometimes revealed interruptions not originally heard or noted during the acoustic data recording. If the period of recording did contain unnatural interruptions to the acoustic emissions of the wind turbine, the measurements in the cells containing the one-second timestamps rendered invalid by these interruptions were removed so they would not be utilized later in the analysis section of the study. Only valid recording segments that contained no interruptions to the acoustic emissions of the wind turbine remained at this point in the study.

Data Analysis

Ten-second wind speed, wind direction, and A-weighted sound pressure level averages were calculated using Excel. The calculated ten-second averages were inserted in a new column of the same Excel spreadsheet. These averages were used to characterize acoustic and meteorological conditions of the wind turbine or background noise for each

valid segment. A clip was then created using noiseLAB 3.0 for each valid contiguous ten-second segment. To keep all created clips organized, each clip name contained the average wind speed and total sound pressure level for that particular segment. These clips were used later for FFT analyses.

After the entire recording period was processed, noiseLAB Batch Processor 3.1 was used to perform FFT analyses on the valid segment clips. The FFT analysis was set to use a Hanning type window to determine the sound pressure level observed for each successive 10 Hz over a range of 10 Hz – 20,000 Hz. After noiseLAB Batch Processor 3.1 performed this calculation, the results were exported into a new Excel file. The results were displayed in two columns, the first of which was the frequency bin and the second of which was the respective, A-weighted sound pressure associated with that bin frequency. The two columns of data were copied and pasted into a new worksheet of the first Excel spreadsheet containing the meteorological and acoustic measurements.

This formed an X-Y relationship that correlated the sound pressure level contained created by noiseLAB Batch Processor 3.1 with each relative 10 Hz bin. The chart wizard in Excel was used to graphically represent this data set. This FFT analysis procedure was performed for all valid clips created in noiseLAB 3.0.

FFT analyses were performed for clips of the wind turbine in operation as well as in non-operational mode. This enabled me to calculate the sound pressure levels of the turbine alone, without the addition of natural background noise levels. The resulting background noise corrected sound pressure level is denoted by adding a ‘C’ after the A-weighting notation, appearing as $Leq_{(A),C}$. This calculation (Equation 4) was performed using Formula

(8) of the IEC 61400-11 Standard. The $Leq_{(A),C}$ is equivalent to the following calculated L_s value.

$$L_S = 10\log\left[10^{(.1L_{s+n})} - 10^{(.1L_n)}\right] = Leq_{(A),C}$$

Equation 4. IEC formula to calculate the background noise corrected sound pressure levels. From IEC 61400-11, "Formula (8)" (International Electrotechnical Commission, 2006, p. 21).

L_s is the calculated, background noise corrected sound pressure level, in dB, of the wind turbine operating alone after the background noise correction has been applied. L_{s+n} is the measured equivalent continuous sound pressure level, in dB, of the wind turbine with the natural background noise still as a contributing factor of the sound pressure level observed. L_n is the measured background noise equivalent continuous sound pressure level, in dB, obtained with the turbine shut down, in the non-operational state. (See Table 3 for an example of the results obtained through the background noise corrected calculation.)

The background subtraction was performed for each 10 Hz bin sound pressure level created by noiseLAB Batch Processor 3.1. The result was an FFT analysis of only the wind turbine, without the addition of the background noise levels. These values were plotted in their respective frequency bins, along with the operational and non-operational values.

At this point, all necessary data was accumulated and compiled to satisfy the IEC 61400-11 Standard. In other words, data collected up to this point represents the total data collection and analysis that would typically be done in accordance with the international Standards. Chapter 4 details the additional analytical protocol that was developed and used in this study.

Chapter 4: METHODOLOGY, PART II: DIAGNOSTIC TOOL

Part II of this study is a more in-depth analysis of the recorded wind turbine's acoustic emissions to gain a better understanding about specific wind turbine mechanical and aerodynamic noise contributors. To accomplish this, a novel diagnostic tool was developed. The diagnostic tool's methodology described in this chapter builds upon the current IEC 61400-11 Standard's requested source data to provide a more comprehensive characterization of a wind turbine's acoustic emissions. The diagnostic tool was designed to isolate precise frequency (Hz) ranges based upon the individual turbine's unique sound signature in order to identify individual point source contributors. This acoustic process was designed to break a total wind turbine's sound down into individual component noises to isolate the observed peak bandwidths.

Previously-developed engineering formulae use dimensional measurements to add modeled point source contributions (shown in Figure 41 by solid lines) to predict the wind turbine's total sound spectrum, or sound signature (shown in Figure 41 by a dotted line).

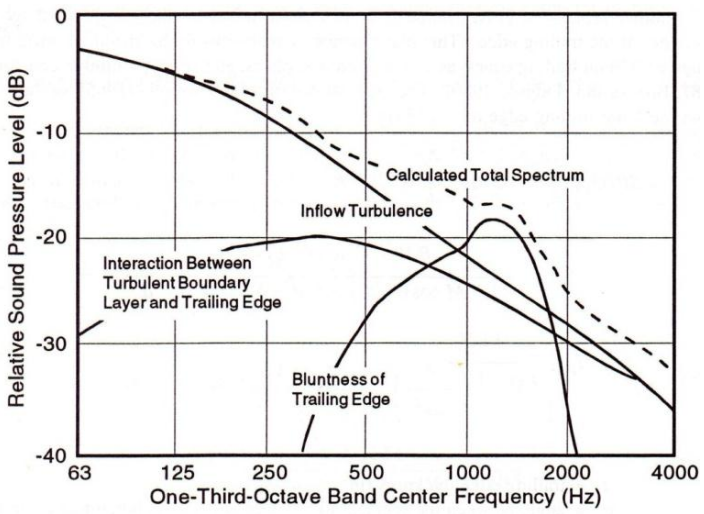

Figure 41. An example of the of point source contributor addition using engineering formulae to calculate a predicted total spectrum of a wind turbine's sound. From "Figure 7-16. Relative contributions of broadband noise sources to the total noise spectrum calculated for a large-scale HAWT." [Grosveld 1985] (Hubbard & Shepherd, 1994, p. 340).

The current study's diagnostic tool uses actual acoustic measurements to decompose a measured total spectrum to isolate individual point source contributors. The notable difference between the engineering formulae and the described diagnostic tool is that the diagnostic tool can account for changes in acoustic emissions after turbine installation and use. For instance, this procedure could pick up noises resulting from manufacturing defects during production or from particular maintenance problems, such as non-lubricated bearings, that may develop over time, effectively changing the way a component operates, divergent to the original manufacture's specifications.

A flow chart (Figure 42) is included to assist the reader in understanding the multi-step methodology used to apply the developed diagnostic tool.

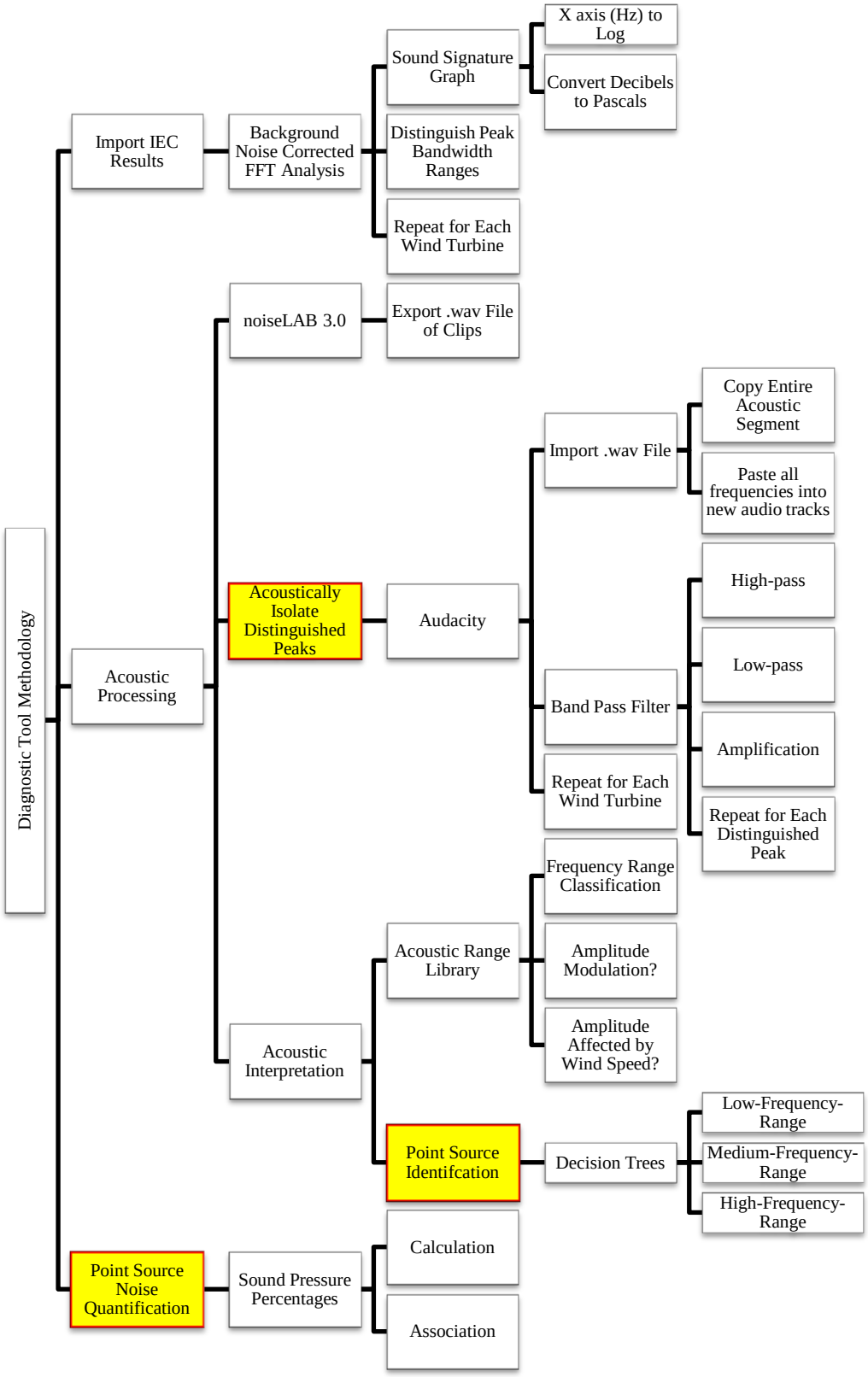

Figure 42. A flow chart of the methodology Part II, the diagnostic tool. The most important deliverables from the novel methodology have been highlighted in yellow.

Import IEC Data

This study's diagnostic tool was designed to be as universally applicable as possible by using the widely-accepted methodology prescribed in the IEC 61400-11 Standard (as described in Chapter 3 of this document). This should ensure that data collected from other projects in accordance with the IEC Standard could be used for the supplementary tonal analyses developed in this study.

Background Noise Corrected FFT Analyses

The background noise corrected, or $Leq_{(A),C}$, FFT analysis calculations served as the particular form of data used to create the sound signature graph which was necessary to perform the diagnostic tool. The results were displayed in Microsoft Excel as an X-Y correlation (Table 3). The X axis was frequency (Hz) and the Y axes were the equalized sound pressure levels of the total wind turbine's operating sound; the background noise with the wind turbine non-operational; and the calculated, background noise corrected, sound pressure level of what the wind turbine's acoustic emission sound pressures would be without the addition of the test environment's natural background noise for each associated frequency bin. Again, the IEC Standard's formula (8) was used to calculate these prospective background noise corrected sound pressure levels. This correlation formed a data set that contains the information describing each wind turbine's sound signature. This calculation was performed for all test subjects.

Table 3. *An Example FFT Analysis Correlation Data Formation*

Frequency Bin (Hz)	Leq $dB_{(A)}$	Background Noise $dB_{(A)}$	$Leq_{(A),C}$ SPL (dB)
10	19.59	2.85	9.07
20	25.68	8.75	19.66
…	…	…	…
19970	-14.42	-17.49	-17.37
19980	-15.08	-17.56	-18.69
19990	-15.08	-17.95	-18.23

Note. The middle section of the data set was replaced with '…' for simplicity of this example. Negative dB values are physically possible as a result of the conversion from the linearly-scaled Pascal unit to the logarithmically-scaled decibel unit. See Appendix C for a chart of mathematical equivalent conversions from decibels to Pascals.

Sound Signature Graph

The FFT analysis data sets (e.g. Table 3) that were used in accordance with the IEC 61400-11 Standard produced a graph (Figure 43) of each wind turbine's background noise corrected sound signature, which revealed multiple peaks. This sound signature graph contains all audible frequencies that can be attributed to the summation of all acoustic point source contributors that individually create distinct protruding peaks above the background noise.

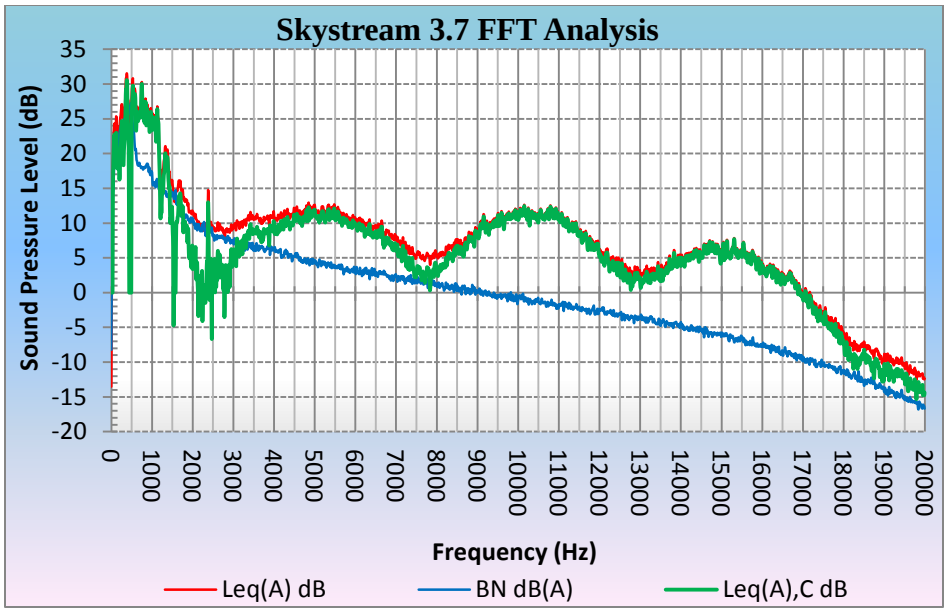

Figure 43. An example sound signature graph created using the FFT analysis calculations in Excel. The graph provides the FFT description of the total wind turbine noise (red line) along with background noise sound pressure (blue line) and the background noise corrected ($Leq_{(A),C}$) wind turbine noise (green line), which is the wind turbine's sound signature.

Modification of the X axis (Hz) to a logarithmic relationship. The X axis (frequency, Hz) of the sound signature graph used for peak detection was scaled logarithmically (Figure 44) to decompress the lower frequency sound pressure level values as well as to increase the accuracy of the each specific frequency's detection in Excel. Also, all other graphed lines ($Leq_{(A)}$ and BN $dB_{(A)}$) other than the background noise corrected, $Leq_{(A),C}$, line were deleted to avoid confusion.

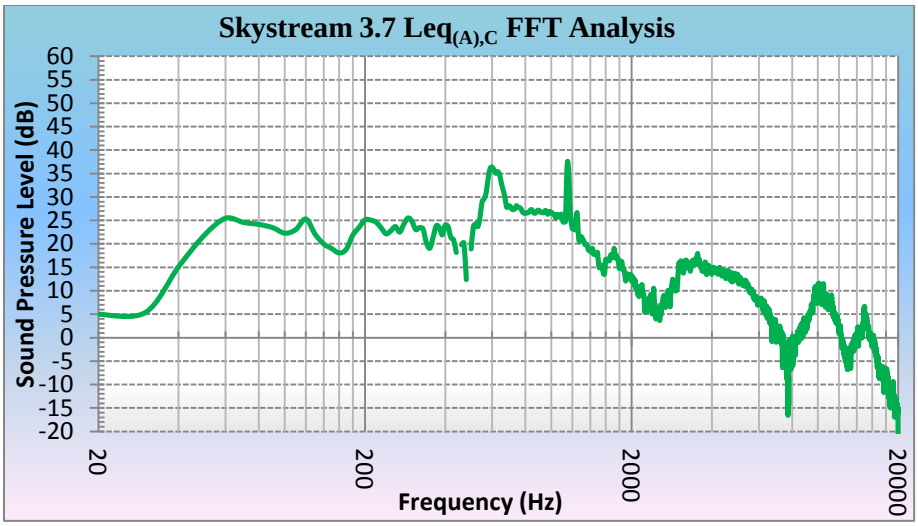

Figure 44. An example of the Skystream 3.7's FFT analysis with the X axis (Hz) scaled logarithmically to allow the tester to more specifically find the range of frequencies for use as the band pass filter parameters later in Audacity.

This was done for all subject wind turbines because many observed peaks were in the low and middle frequency ranges. The only wind turbine acoustic emission peaks observed above 10 kHz were found in the smallest wind turbines, and these peaks were an almost indistinguishable percentage of the total sound.

Convert decibels to Pascals. The measured sound pressure level values reported by noiseLAB 3.0 cannot be simply calculated as a percentage of the total Leq $dB_{(A)}$ value because the decibel scale is logarithmic. To overcome this obstacle, the Leq $dB_{(A)}$ FFT analyses values were converted into the Pascal scale (Figure 45), which greater accentuated the peaks by showing their linear relationship to the "noise." The Pascal values were calculated for each sound pressure level contained within the 10 Hz bins. Because the decibel unit is a function of pressure, which is included in its mathematical definition, the reversed function (Equation 5) was able to be calculated by mathematically solving for the Pascal unit. The resulting formula has been provided.

$$Pascal = (2 \times 10^{-5}) \times 10^{Decibel/20}$$

Equation 5. Formula to convert a measured decibel unit value into a Pascal unit.

The specific data points in Excel found on the logarithmically-scaled X axis (Hz) were used to most easily distinguish the exact minimum and maximum frequency values for later use as acoustic parameters in Audacity in the band pass filter applications. In other words, the Pascal scale essentially decompressed the sound signature graph to show its linear relationship of adjacent peaks, making the peaks proportionally taller.

The same data creating the sound signature graph for Figure 43 and Figure 44 were converted into Pascals and plotted (Figure 45) to show the linear relationship of sound pressure contained within the sound signature's profile.

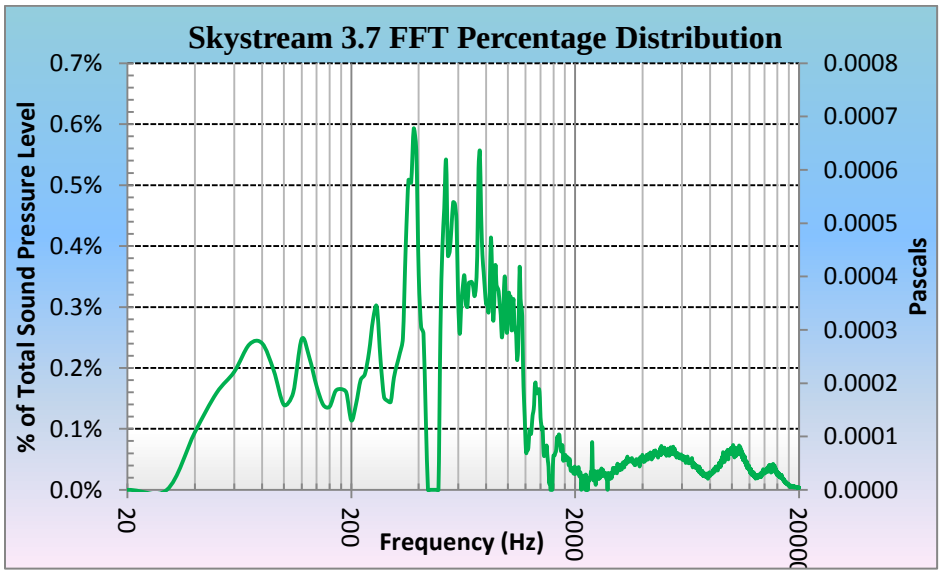

Figure 45. An example of the sound signature graph using the dB values converted into Pascals with the X axis graphed logarithmically.

Distinguish Peak Bandwidth Ranges

The Pascal unit-scaled previously created (Figure 45) signature graph was used to find exact frequency values that contained individual peaks. These distinguished peaks were marked using red letter boxes (Figure 46) to relate that particular peak to individual table

results. The minimum and maximum frequency values for each identified peak were noted for later use in the acoustic processing section of the diagnostic tool procedure.

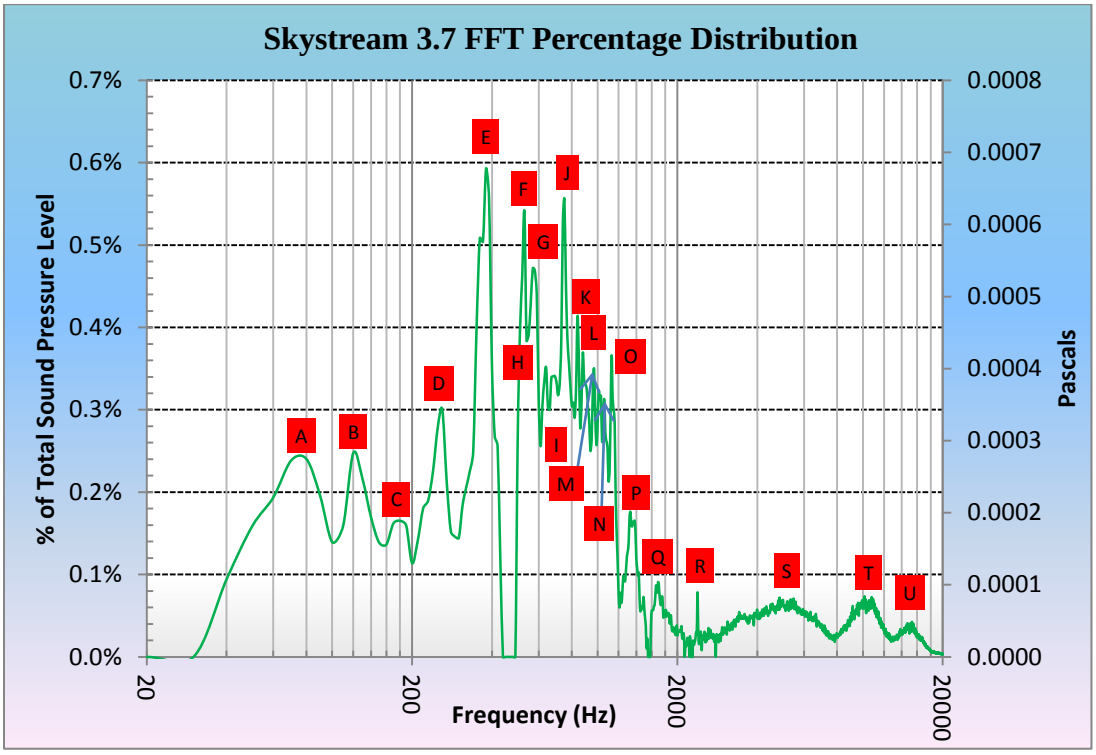

Figure 46. An example FFT Pascal distribution showing distinguished peaks, identified by red blocks with letters. These identified peaks will be referred to in later analyses.

Acoustic Processing

All clips used for FFT analyses were exported as .wav formatted files from noiseLAB 3.0. This produced an acoustic file of the segment recording that represented the identical wind turbine acoustic recording that was used to obtain the FFT analysis data for each individual wind turbine. The .wav file was created in particular because it is able to be imported into Audacity for the application of particular acoustic manipulation processes.

Acoustically Isolate Distinguished Peaks

The purpose of this step in the diagnostic tool's methodology was to create individual audio tracks contain noise from individual point source components of a wind turbine if that component was operating on its own, separate from all other components' acoustic

contributions to a wind turbine's total sound structure. Band pass filters were utilized to accomplish this acoustic isolation.

Import Audacity .wav file. The acoustic segment that was just exported from noiseLAB 3.0 was imported into Audacity. The entire acoustic segment of the recorded wind turbine's sound was copied and then pasted into a new audio track within the Audacity project. This ensured that the unfiltered original recording could be used repeatedly for each successive peak's filter analysis.

Band pass filter application. The identified peak's minimum and maximum frequency values were used as the acoustic constraints to subtract the sound pressure level present in all frequencies outside of the bandwidth range of the peak under investigation. This was accomplished using acoustic filters contained within the Audacity software. The particular filters used were the "High-pass Filter" and the "Low-pass Filter" under the "Effects" tab, in addition to the "Amplify" filter located within the same Effects tab in Audacity.

The concept of mathematically adding multiple frequencies that was described earlier within the "Acoustic Fundamentals" section of Chapter 2 is the basic concept upon which this diagnostic tool is based. The key difference is that instead of adding pure tones that have been intentionally generated, the entire process is reversed. A graphical representation of this process has been provided to show a simplified version of the resulting high-pass and low-pass frequency subtraction wave forms (Figure 47).

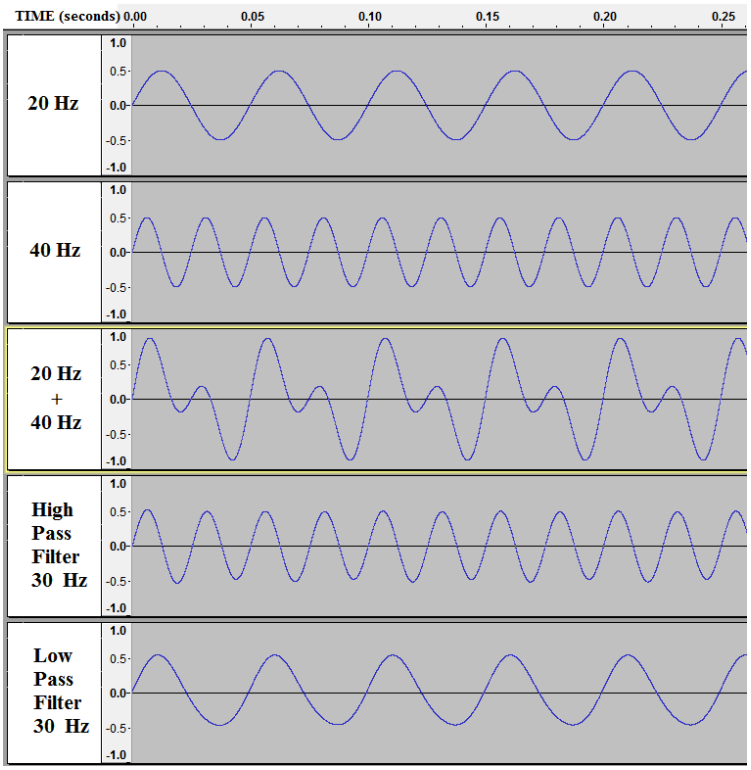

Figure 47. An example of the high-pass and low-pass filter applications on the same example acoustic wave forms that were used in the addition of pure tone frequencies described in Chapter 2 (Figure 8). This graph is presented in the time-domain.

High-pass filter. Each identified peak received the pass filters in order to create individual new audio tracks that only included the sound pressure levels under that peak. First, the low frequency threshold value for the current peak under investigation was utilized as the parameter value for the high-pass. This allowed any sound pressure contained in frequencies above the specific Hz frequency to remain. For instance, a peak may range from 200 Hz to 800 Hz. Therefore, a high-pass filter of 200 Hz would be applied. This essentially attenuated any sound pressures below 200 Hz.

Low-pass filter. The low-pass filter was then applied to the same, newly created audio track that had first received the high-pass filter. Similar to the high-pass filter, but in the opposite direction of frequency attenuation, the low-pass filter was applied to only allow sound pressure at frequencies below a designated frequency. In the described example case,

this low-pass filter's parameter setting would be set to a frequency of 800 Hz. As a result of the combination of the two filter applications, the resulting track only contained sound pressures within the frequency range chosen. For instance, in the described example, only sound pressures that existed within the frequency range of 200 – 800 Hz remained for acoustic identification of the point source component contributing to that particular peak.

Amplification. This new audio track was then amplified to an artificial level of six decibels below the maximum acoustic clipping sound pressure level limit. This was done to make the track audible to the tester because the majority of the wind turbine's total sound pressure was attenuated during the high-pass and low-pass filter applications. The amplification of the track for the peak under consideration also increased the signal (noise of the peak under investigation) to noise (sound pressures contained in frequencies outside of the peak under investigation) ratio. The end result of the described filtering and amplification processes was acoustic isolation of the peak under consideration. This was designed to assist the tester in concentrating on fewer simultaneous point sources within a given audio track for a more accurate identification process. The same acoustic processes were repeated for each additional distinguished peak. This procedure was carried out for all test wind turbine subjects.

Acoustic Interpretation

Each individual audio track resulting from the previously described processes was acoustically played back to try to identify possible point source(s) adding to the sound pressure of the peak under investigation. The set of acoustic characteristics that were used included the noise's frequency range classification (low-frequency-range, middle-frequency-

range, and high-frequency-range); amplitude modulation; and amplitude alterations in response to any change in wind speed (Figure 48, Figure 49, and Figure 50).

These acoustic characteristics were organized into three decision trees, which were designed to assist the tester in acoustic interpretation of the sound. The decision trees created a protocol to systematize the acoustic interpretation process as much as possible. Using this protocol made the process more efficient by narrowing down the possible parameters a listener should attempt to detect, which in effect made interpretation and identification of each point source contributor an overall less time-consuming and more accurate process. Also, this decision tree protocol may allow the point source identification process to be more easily replicated by other testers in the future.

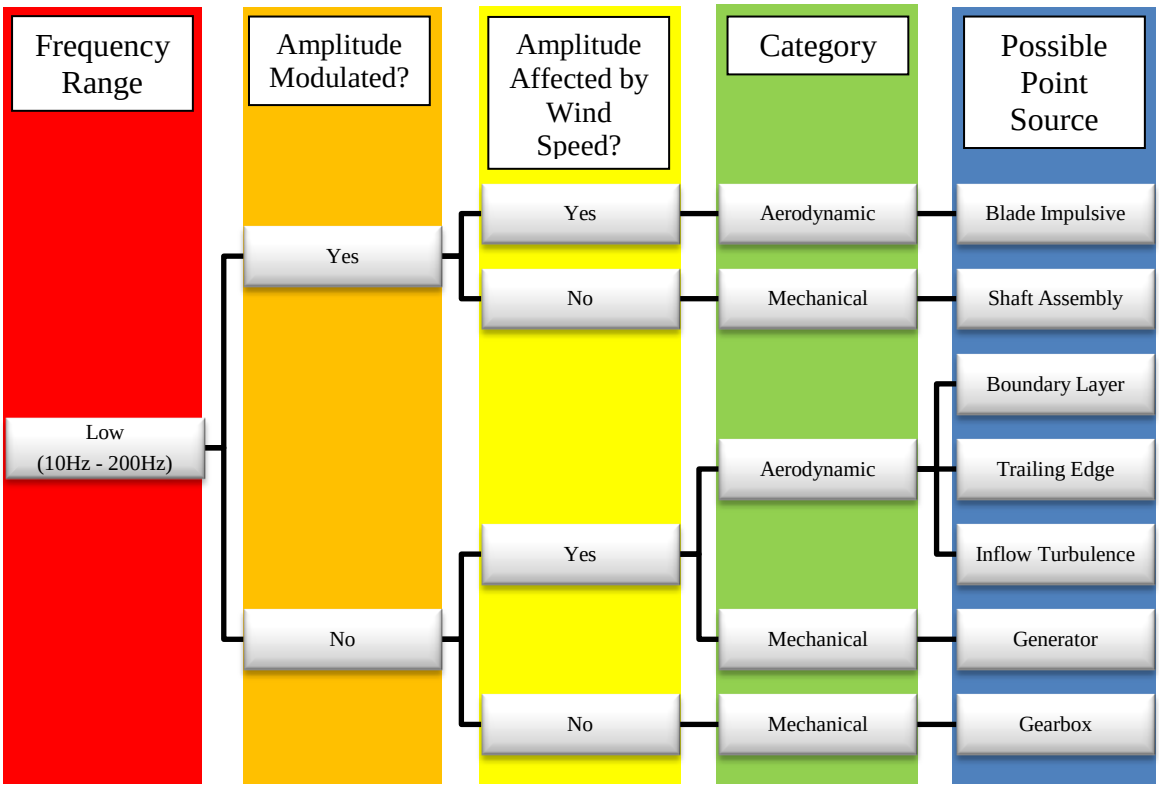

Figure 48. Decision tree for Low-Frequency-Range point source contributors.

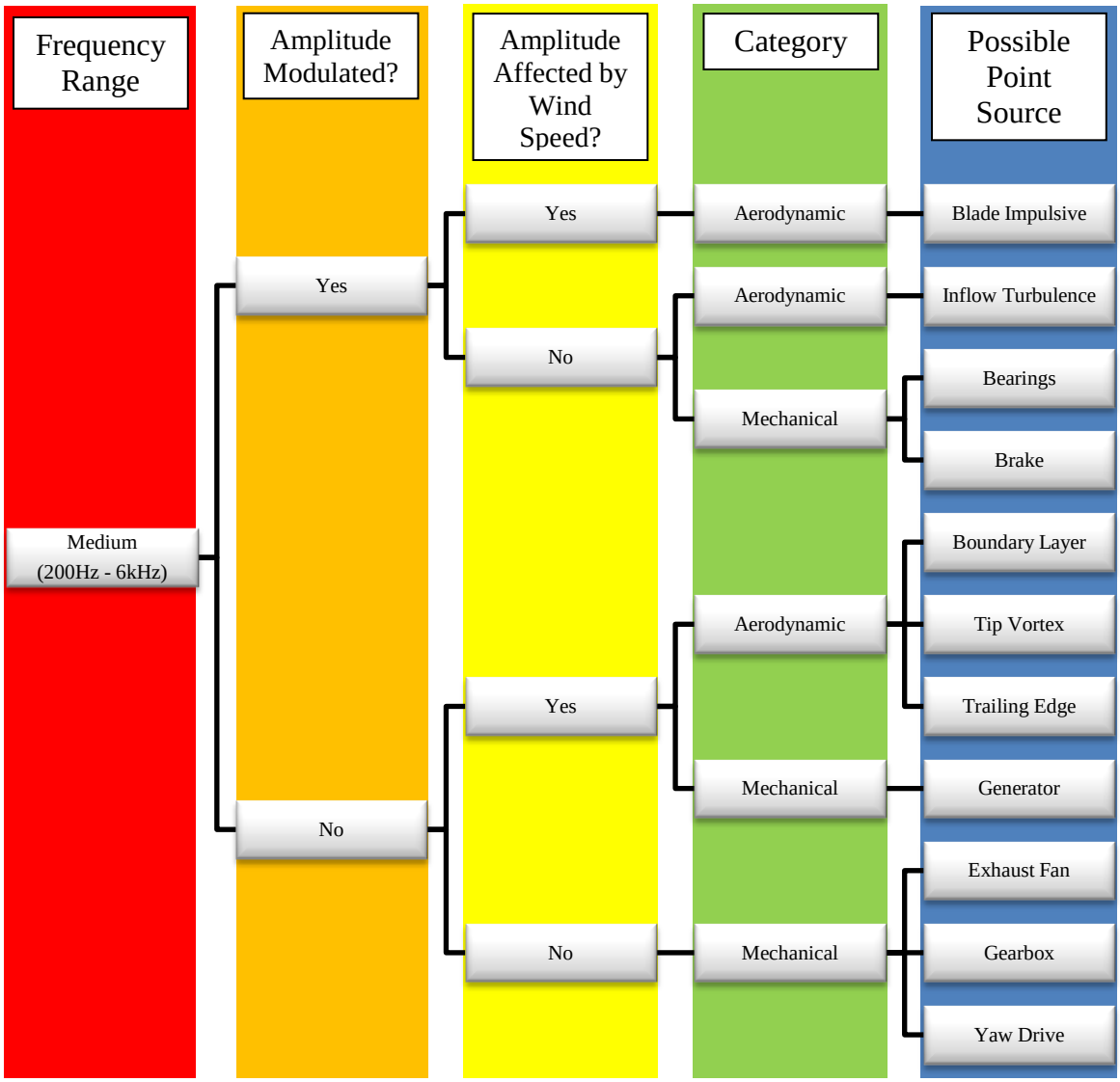

Figure 49. Decision tree for Medium-Frequency-Range point source contributors.

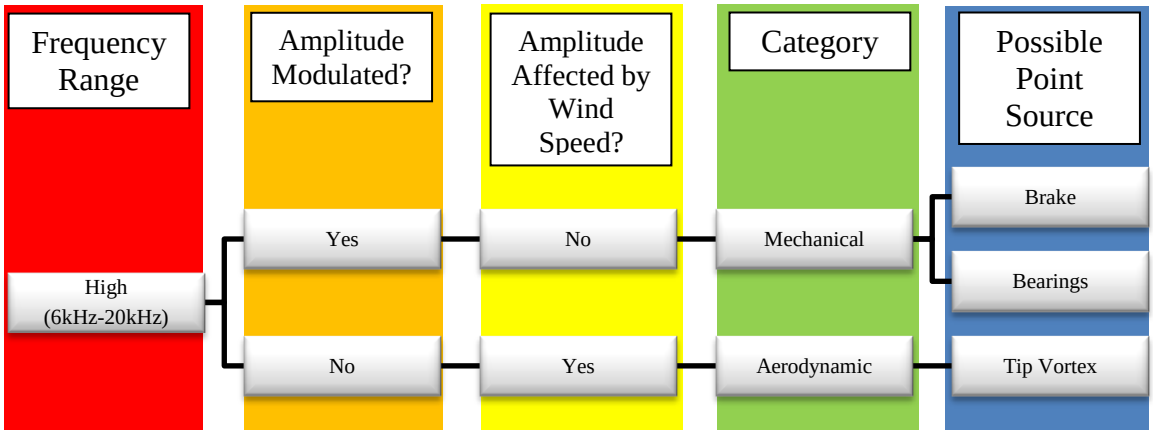

Figure 50. Decision tree for High-Frequency-Range point source contributors.

Acoustic Characteristics Library

Frequency range classification. Individual component contributors exhibited a tendency to create noise within particular classified frequency ranges. These classifications included a low frequency range, a middle frequency range, and a high frequency range.

Low-Frequency-Range sound is acoustic energy contained within the 10 – 200 Hz frequency range. The mechanical point source contributors that may present themselves within this range are the drive shaft assembly, generator, and gear box. The aerodynamic contributors within this range may be inflow turbulence, turbulence boundary layer flow, and the trailing edge components of the airfoil design.

Middle-Frequency-Range frequencies are contained with the 200 Hz to 6000 Hz range. This encompasses the majority of the mechanical contributors. The major mechanical contributors are the generator and gear assembly, with lesser contributors being the yaw drive and exhaust fan. Major aerodynamic contributors existing in this range were observed to be blade impulsive, inflow turbulence, and trailing edge with a lesser contributor being the tip vortex.

The High-Frequency-Range is considered to result from any contributor that produces acoustic energy above 6000 Hz. This range contained the fewest possible point source contributors. The aerodynamic contributor within this range was observed to be the tip vortex acoustic emitter. The mechanical contributors measured within the high frequency range were observed to be the rotor's bearings and brake.

Amplitude modulation. A noise is considered to be amplitude modulated if it has periodic repetition in amplitude that occurs in a consistent manner. In other words, amplitude modulated noises remain at a consistent Hz frequency but a lower Hz frequency is also

evident. This periodicity in amplitude levels may be most easily described using a graphical representation (Figure 51) of the difference between non-amplitude modulated acoustic waves and amplitude modulated acoustic waves.

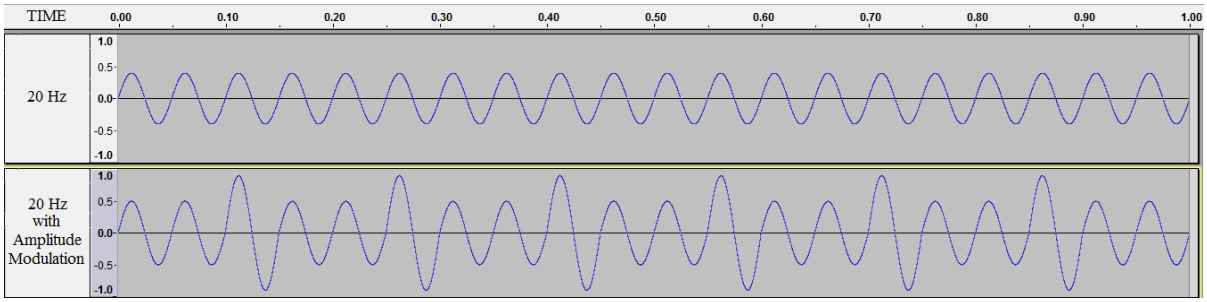

Figure 51. An example of a time-domain graph showing a 20 Hz acoustic wave with no amplitude modulation as well as the same 20 Hz acoustic wave with an added amplitude modulation. It can be noticed that the frequency (Hz) stays the same but the amplitude modulates between .5 and .9.

The observed aerodynamic component contributor that displayed amplitude modulation was the blade impulsive noise. This is directly related to rotational speed of the rotor (which is itself in a direct relationship to the particular wind turbine's response to wind speed). "This rhythmic swishing sound, dependent upon tip speed and blade profile, is normally centered around the 800-1000 Hz region" (ETSU Working Group on Wind Turbine Noise, 1996, p. 12). An example of an amplitude modulated mechanical noise may be the bearings or brake.

One of the utility scale test subject's point source contributors that exhibited non-amplitude modulation was the exhaust fan's mechanical acoustic contribution to the wind turbine's sound. Its frequency and sound pressure levels are independent of the wind speed because the cooling fans are turned on or off by the wind turbine's control center, which senses when the nacelle's internal machinery reaches a specific temperature set point. This set point is reached when the turbine is operational with the rotor spinning, which masks some of the cooling fan's acoustic output. However, in the utility scale wind turbine in this

study, the cooling fans tended to run for a short time after the rotor had stopped to continue to cool the nacelle's internal machinery until it registered a temperature below the control's set point. Intentionally shutting down the operation of the rotor (as part of the IEC background noise measurement) allowed the tester to acquire acoustic data from the cooling fans for comparison with the operating rotor state that, for a large percentage of the time, contained the acoustic contributor of the cooling fans.

Wind speed's effect on amplitude. Wind speed has an effect on the level of "noise due to inflow turbulence [which] becomes the dominant source at the higher wind speeds" (ETSU Working Group on Wind Turbine Noise, 1996, p. 11). The wind also has an indirect relationship to the operating state of the cooling fans through the operational state of the wind turbine's rotor. When the wind is blowing above the cut-in speed, the generator produces electricity, which emits heat, causing the cooling fans to turn on.

Point Source Contributor Identification

Associating peak noises with particular mechanical and aerodynamic point source contributors by applying the decision tree protocol described in Figure 48, Figure 49, and Figure 50 appeared to be quite effective. Some point sources were easier to identify than others. In particular, the noises that exhibited narrowband spectra indicated the most obvious acoustic resemblance to individual point sources. The broadband noise spectra proved to be a more difficult identification task for the diagnostic tool as a result of the narrowband pass filter application. To account for the existence of multiple point sources within a particular band pass filter's frequency range, weighted percentages were associated with each detected point source. This did not precisely quantify the sound pressure contributions as an experimental set up would have, but the results were closer than would be obtained without

the point source percentage weighting. Multiple peaks sometimes exhibited quite similar acoustic characteristics, which are clear markers that they are all coming from the same wind turbine component. The existence of multiple peaks resulting from the same point source contributor is well documented in published literature (Figure 52).

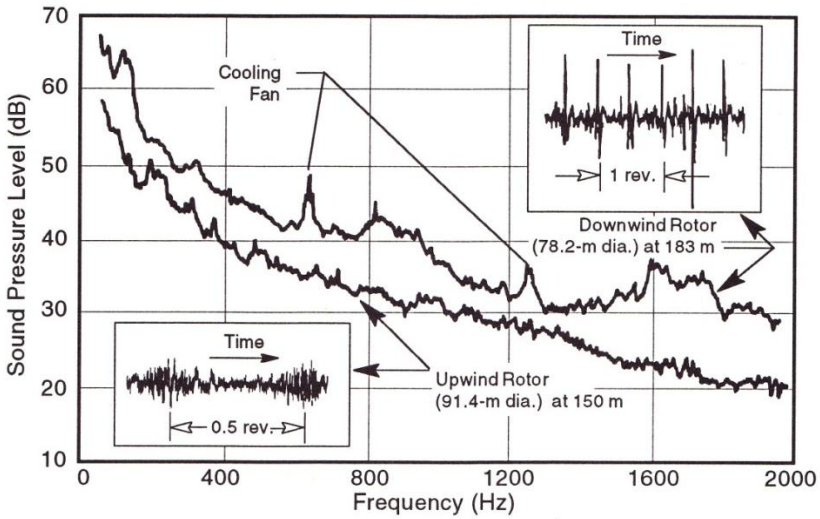

Figure 52. Narrow-band noise spectra from large-scale HAWTs with upwind and downwind rotors. The sheer magnitude difference between the sound pressure levels of acoustic emissions from a relatively smaller diameter upwind rotor versus the relatively larger diameter downwind rotor can be noticed in this graph as well. From Figure 7-4. Narrow-band noise spectra from large-scale HAWTs with upwind and downwind rotors. "Wind Turbine Acoustics" (Hubbard & Shepherd, 1994, p. 327).

Point Source Contributor Quantification

The purpose of the quantification for each distinguished peak was to associate a level of impact that each point source contributor had on the total sound pressure contained within the acoustic emissions of a wind turbine.

The sound level meter (microphone and noiseLAB 3.0) used to measure the acoustic emissions, by default, reports the acoustic energy it receives in terms of the decibel unit. The decibel unit must be effectively decompressed to remove the logarithmic relationship that is contained within the decibel scale to obtain a percentage comparison that relates each peak to the total sound pressure.

Sound Pressure Percentages

Calculation. All calculated Pascal values (see Appendix C) from the decibel to Pascal conversion were added to find a Pascal summation for each wind turbine that could be used to calculate a percentage of the total relationship that each distinguished peak's sound pressure contributed to the total sound pressure of the wind turbine's acoustic emission. Next, the Pascal value within each 10 Hz bin was divided by the total sum of Pascal values to determine the percentage of the total wind turbine's sound pressure contained within each bin. This resulted in a percentage of the total that each bin was contributing. Finally, the percentages contained within the bins of each distinguished peak's range were added to associate a percentage of the total sound pressure contained within each distinguished peak (noted using successive letters). An example of the resulting table (Table 4) using the same data in Figure 46 has been provided.

Table 4. *Individual Distinguished Peaks' Values with Their Associated Letters and Percentage of Contribution to the Total Sound Pressure Level of the Wind Turbine*

Letter	High Pass	Peak	Low Pass	% of Total SPL
A	30	80	100	1.12%
B	100	120	160	1.07%
C	160	180	200	0.62%
D	200	260	290	1.80%
E	290	380	440	4.71%
F	470	530	550	2.04%
G	550	570	610	2.51%
H	610	640	650	1.25%
I	650	680	710	1.96%
J	710	750	800	1.56%
K	820	840	860	1.39%

Association to individual point source components. Each distinguished peak's percentage summation was then associated with particular point source contributors depending upon the previous identification of the peak using the decision trees. Weighted percentages were associated to their identified point source contributor when multiple component contributors were detected, providing the described percentage of the individual peak's percentage of the total sound pressure of the wind turbine to each identified component, respectively. The result was the ability to individually associate each point source(s) of contribution percentage (Table 5) to the total sound pressure of the wind turbine. The associated percentages were summed to find the total contribution associated with each identified point source component.

Table 5. *Individual Distinguished Peaks' Values with their Associated Letters and Percentage of Contribution to the Total Sound Pressure Level of the Wind Turbine*

Identified Contributors	Impact Percentage
Aerodynamic	
Inflow Turbulence	2.82%
Blade Impulsive	0.54%
Boundary Layer	3.43%
Trailing Edge	6.20%
Tip Vortex	31.43%
Mechanical	
Generator	18.39%
Rotor Bearings	25.59%
Identified Contributors' Total %	**62.81%**
Unaccounted Contributors' %	37.19%

Any percentage of the total sound pressure that was not contained in the identified peaks was placed in the "Unaccounted Contributors' %" box. This percentage contains the

sound pressure of the unidentified components. They provided minor contributions to the total sound pressure, small enough to be inaudible to the tester during the identification process.

Chapter 5: RESEARCH FINDINGS AND RESULTS OF WITHIN-SUBJECTS' DIAGNOSTIC TOOL ANALYSES

Summary Responses to Research Questions

This study was guided by four research questions. Summary responses to those questions are provided below. Following this section is a more detailed description of the results gleaned from the individual subject wind turbines, upon which the findings of this study were based.

Q1: Does the diagnostic tool described in this paper allow the total sound of a wind turbine to be separated into individual acoustic tracks of specific point source contributors?

Yes, although multiple point source contributors were evident in most acoustic tracks. The diagnostic tool was found to best distinguish narrowband point source contributors. Broadband point source contributors spanned a larger range of frequencies than was encompassed with each band pass filter because they do not present themselves as discrete peaks in the wind turbine's sound signature graph. To accommodate the broadband contributors such as the blade inflow turbulence or the trailing edge vortices, other underlying point sources detected were assigned a percentage of each peak's area of sound pressure. This allowed for a more accurate end result showing each identified source's contribution, rather than simply allocating the entire peak's area of sound pressure to a single point source contributor.

Each track that resulted from the specific band pass filters increased the signal-to-noise ratio for the individual point source that contributed the majority of a peak in relation to all other noises produced by the wind turbine. This allowed the tester to distinguish which point source(s) was contributing the greatest portion of the sound pressure to the individual peak under investigation. However, the fact that the broadband contributors' spectra encompass such a wide range presented a challenge in the acoustic interpretation stage of the diagnostic tool. Mechanical noises produced by the moving parts within the nacelle of the wind turbine were the easiest to identify because they all exist as narrowband spectra, whereas the aerodynamic contributors were all found to be broadband, making them more difficult to identify.

Q2: Does the diagnostic tool described in this paper provide a method to quantify the comparison of individual point source contributor's sound pressure levels to a wind turbine's total acoustic emissions?

Yes, although these results are dependent on the tester's skills in interpreting acoustic associations of the identified point source(s). Overall, it is felt that the diagnostic tool was successfully able to distinguish mechanical producers for quantification but was unable to precisely quantify the aerodynamic producers. The resulting percentages that were presented for the identified point source contributors are believed to be precise in terms of their quantification of the sound pressure contained within each peak band width. The accuracy of the identification is subjective and lends itself to further development in future research.

Q3: Does the greatest sound pressure contributor percentage of the total sound pressure emitted from all tested subject wind turbines tested occur as a result of the blade impulsive noise?

Based on use of the procedures described in Chapter 4, the answer to this question is no. It was originally thought that the greatest percentage of the acoustic emissions would be associated with the blade impulsive noise because this is the sound that most people ascribe to wind turbine noise (as a "whoosh-whoosh" sound). However, this was not observed to be the case for any of the six tested wind turbines. According to the diagnostic tool's analyses, the largest percentage of point source contributors' sound pressure for the small scale turbines was from the blade tip vortex and bearings. The largest percentage of point source contributors' sound pressure for the two largest subjects resulted from the tip vortex and trailing edge.

Further experimentation could qualify some of the decision tree routes, which could alter this interpretation, but based on this analysis of the tested wind turbine subjects, the blade impulsive noise was not found to be the greatest contributor to total sound pressure. See Table 19 for a full description of the point source contributor's percentages for each individual wind turbine subject.

Q4: Do small scale wind turbines of the same rotor diameter emit relatively similar sound signatures (FFT analyses) due to the tendency for a natural frequency of acoustic resonance related to that rotor diameter's dimension?

The two tested small scale wind turbines with the same rotor diameter were the AIR X and the AIR Breeze, both manufactured by Southwest Wind Power. The difference between their sound signatures was examined by comparing the absolute values of the difference for each wind turbine's percentage of its own total sound pressure level. This controlled for differences in wind speed during measurement for each respective wind turbine that resulted in varying total sound pressure levels. The sum of the absolute value

differences between these two turbines was found to be 30.016%. This means that the percentage of each wind turbine's sound pressure level contained within each 10 Hz bin was 30% different from the other, either because one turbine was louder or quieter than the other, or because their sound pressures were contained in different frequencies.

Visually, the two sound signature graphs (Figure 53 and Figure 54), appear to be quite similar in relation to the other tested wind turbine subjects but the sum of the absolute value differences (30.016%) describes a much greater variation than is visible to the tester's qualitative eye.

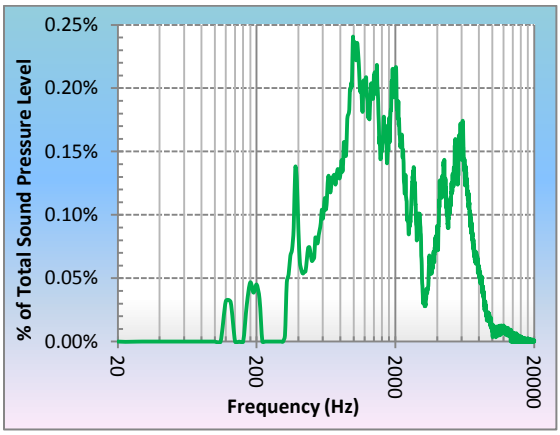

Figure 53. AIR Breeze FFT percentage distribution graph.

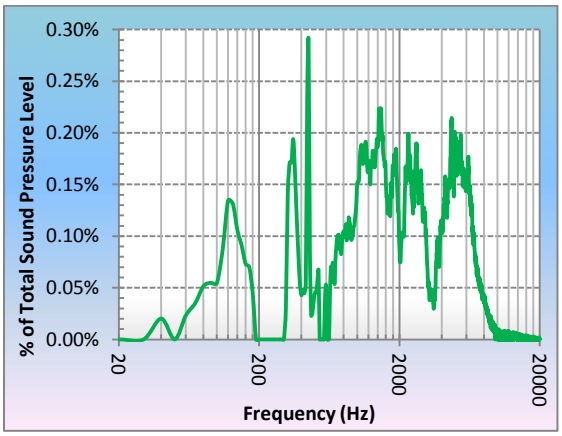

Figure 54. AIR X FFT percentage distribution graph.

It is likely that this FFT quantitative difference results from other variables than the rotor diameter because these turbines have the exact same rotor diameter. Such variables may include the shape of the airfoil design, the difference in particular testing conditions (wind speed, wind direction, atmospheric density), the load put on the generator by each wind turbine's microprocessor, or any number of other variables that result from the complicated nature of the acoustic test and the specific componentry contained within each respective wind turbine. The only way to definitively answer this question would be to set up an experiment that controls for atmospheric variables during testing.

Individual Test Subject Wind Turbine Diagnostic Tool Results

The diagnostic tool was performed on six test subject wind turbines. Pictures of the wind turbines have been provided (Figure 55, Figure 58, Figure 61, Figure 64, Figure 67, and Figure 70). The resulting FFT analyses are provided (Figure 56, Figure 59, Figure 62, Figure 65, Figure 68, and Figure 71). The distinguished peaks graphs used as the acoustic parameters in Audacity are provided (Figure 57, Figure 60, Figure 63, Figure 66, Figure 69, and Figure 72). All decision tree results from each individual peak are provided (Table 7 and Appendix A). Individual peaks' impact percentage on their respective wind turbine are provided (Table 6, Table 9, Table 11, Table 13, Table 15, and Table 17). The resulting estimates of how each point source contributes to the total wind turbine acoustic emissions are provided (Table 8, Table 10, Table 12, Table 12, Table 14, Table 16, and Table 18).

The results shown for each turbine follow the same format. As previously described, first, a graph provides the FFT description of the total wind turbine noise (red line) along with background noise sound pressure (blue line) and the background noise corrected ($Leq_{(A),C}$) wind turbine noise (green line), which is the wind turbine's sound signature. Next, a percentage distribution graph is provided for each turbine, with identified sound pressure peaks marked by red boxes and distinguished by letters. This graph is followed by a table that provides the band-pass filter results for each identified peak, showing quantitatively each peak's contribution to the overall turbine sound. Next, individual tables show the outcome of applying the diagnostic tool's decision tree to each identified peak, with the resulting estimation of that source's contribution to the overall sound signature for the tested turbine. A summary table is provided that shows the total, estimated contributions by point sources that make up the turbine's overall sound signature. Finally, Table 19 compares all of the

results to show how the individual point source percentage of contributions varies between the tested subjects. Results of the analysis described above will be displayed for each tested wind turbine. Further discussion of these findings will be provided at the end of this chapter.

AIR Breeze

Figure 55. Picture of the Air Breeze wind turbine. From "Air Breeze Land" (Sun Electronics, 2012).

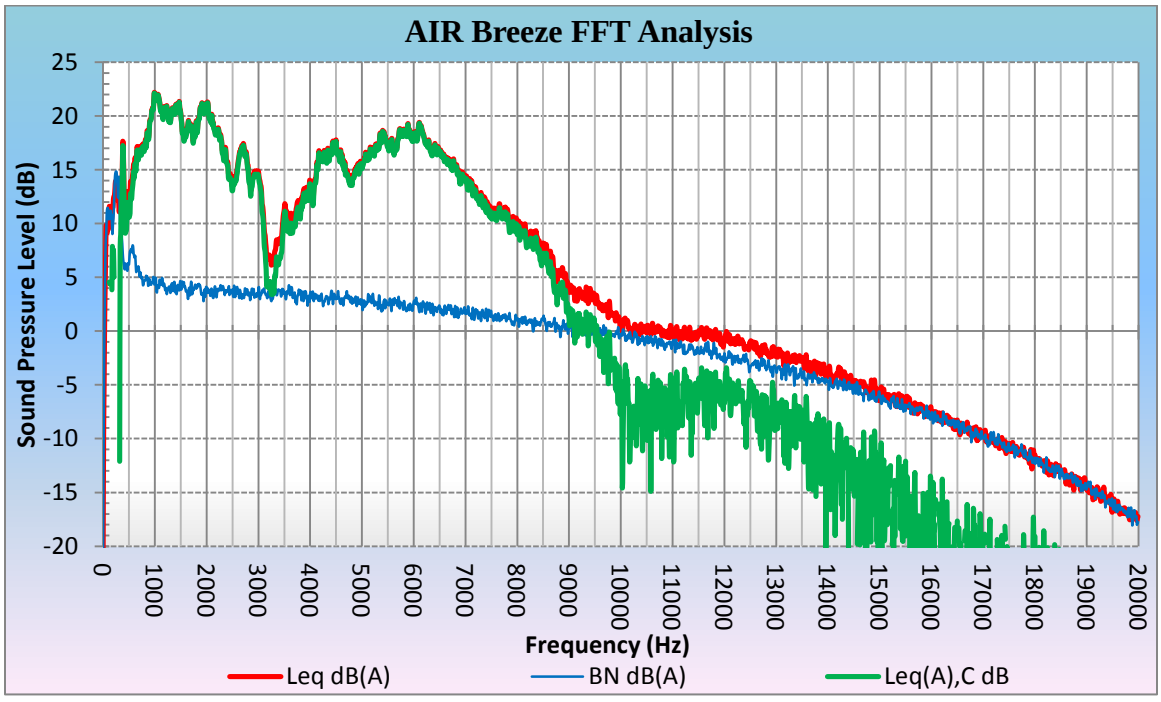

Figure 56. AIR Breeze FFT analysis results graph.

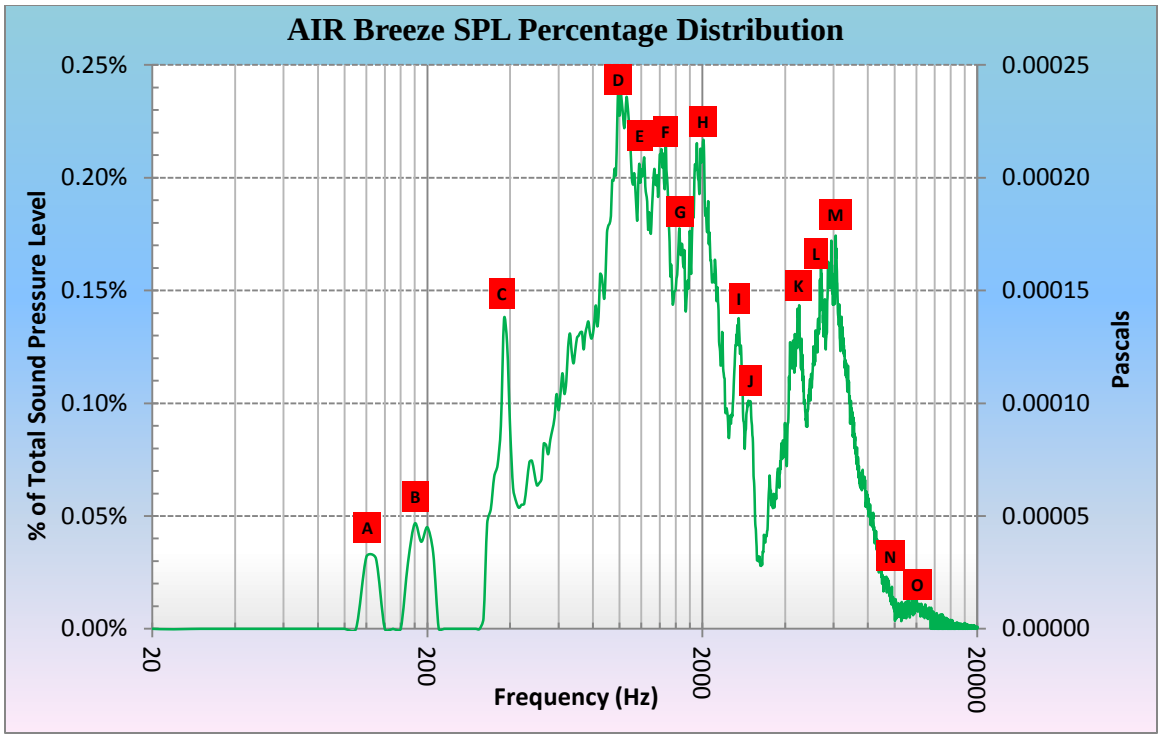

Figure 57. AIR Breeze FFT percentage distribution graph with distinguished peaks' references.

Table 6. *AIR Breeze Distinguished Peaks Used as Band Pass Filter Parameters*

Letter	High-pass	Peak	Low-pass	% of Total SPL
A	110	120	150	0.06%
B	180	190	210	0.13%
C	340	380	420	0.70%
D	940	1010	1160	4.74%
E	1160	1230	1270	2.18%
F	1270	1400	1550	5.41%
G	1550	1650	1730	2.88%
H	1730	1910	2510	12.32%
I	2510	2710	2860	3.88%
J	2860	2920	3250	2.72%
K	3970	4400	4730	8.62%
L	4730	5420	5510	9.48%
M	5510	6110	6320	12.02%
N	8910	9350	9950	1.92%
O	10030	11590	12970	2.63%

Note. This table describes the discrete high-pass, distinguished peak, low-pass filter parameter, and each band pass filter's contributing percentage to the total wind turbine's sound.

Table 7. *Individual Diagnostic Tool Results for the AIR Breeze Wind Turbine, by Peak*

Peak ID			**A**	
High-pass	**Low-pass**	**Frequency Range**	**Amplitude Modulated?**	**Amplitude Affected by Wind Speed?**
110	150	LOW	NO	NO
Point Source(s)			Inflow Turbulence	Blade Impulsive
Weighted Percentages			70%	30%
Total Peak's Percentage of Wind Turbine's SPL			0.06%	

Note. Only this subject's first peak of identifying information has been provided in this section of Chapter 5. See Appendix A for all wind turbine subject individual peak information.

Table 8. *AIR Breeze Total Estimated Point Source Contributions Determined Using the Summed Values of the Individual Band Pass Filtered Tracks*

Identified Contributors	Impact Percentage
Aerodynamic	
Inflow Turbulence	0.58%
Blade Impulsive	7.55%
Boundary Layer	7.91%
Trailing Edge	1.42%
Tip Vortex	20.69%
Mechanical	
Rotor Bearings	30.78%
Identified Contributors' Total %	**68.93%**
Unidentified Contributors' Total %	31.07%

Note. This table shows the total calculated contributing percentages to the wind turbine's acoustic emissions.

AIR X

Figure 58. Picture of the AIR X wind turbine. From "Residential Backyard Wind Generator" (Waste Reducer, 2012) .

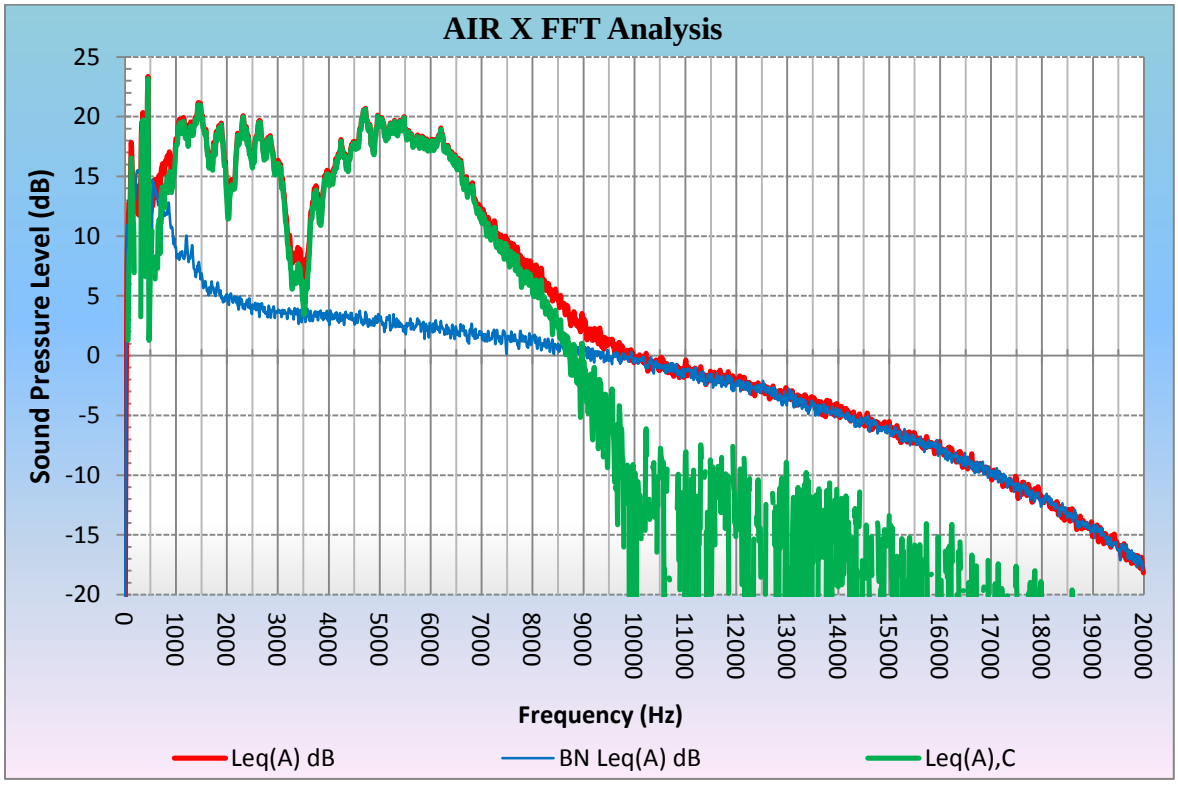

Figure 59. AIR X FFT analysis results graph.

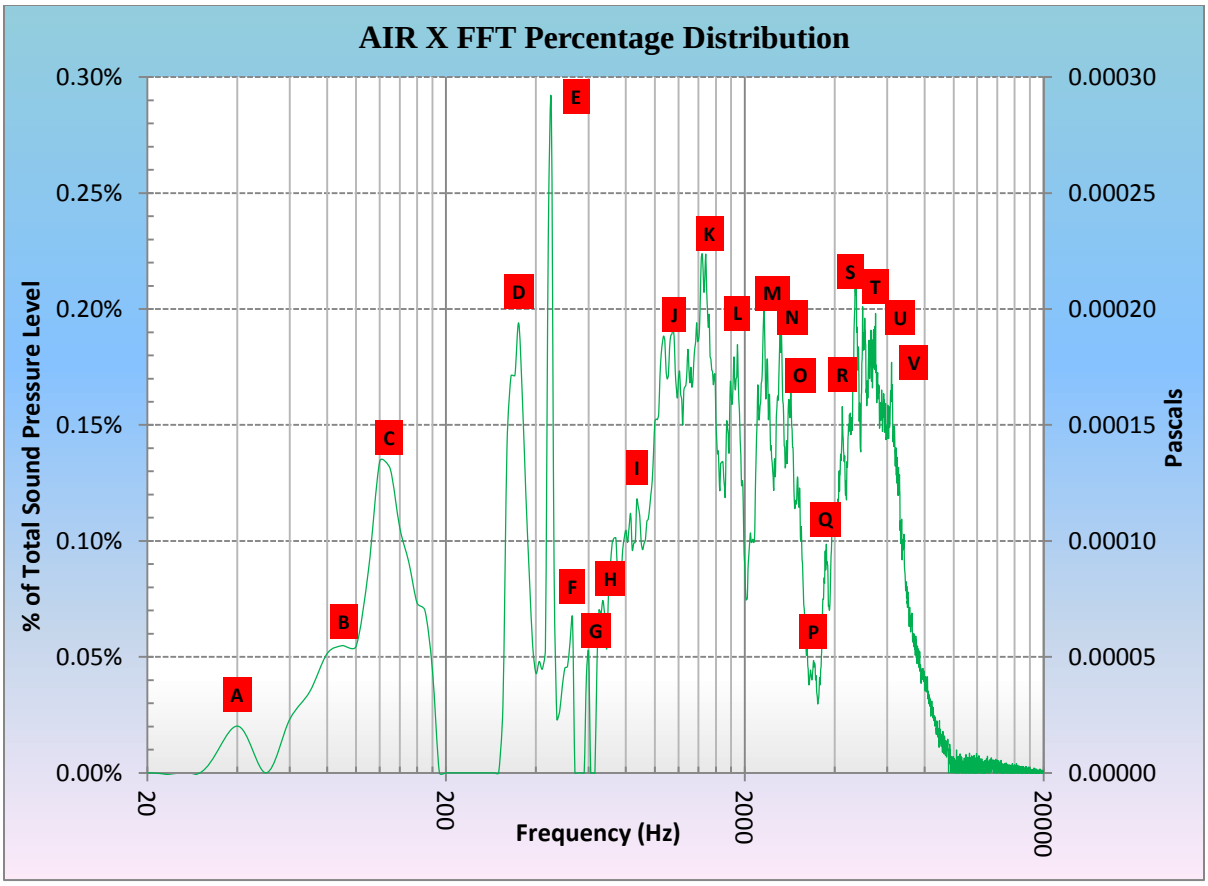

Figure 60. AIR X FFT percentage distribution graph with distinguished peaks' references.

Table 9. *AIR X Distinguished Peaks Used as Band Pass Filter Parameters*

Letter	High-pass	Peak	Low-pass	% of Total SPL
A	30	40	50	0.02%
B	50	90	100	0.16%
C	100	120	200	0.79%
D	290	350	400	1.17%
E	410	450	480	0.78%
F	480	530	560	0.25%
G	560	600	610	0.09%
H	640	670	690	0.33%
I	810	870	860	0.51%
J	1000	1100	1240	4.15%
K	1280	1440	1580	5.70%

Letter	High-pass	Peak	Low-pass	% of Total SPL
L	1700	1890	2010	4.54%
M	2170	2300	2490	5.12%
N	2490	2630	2740	3.91%
O	2740	2850	3260	5.84%
P	3270	3390	3480	0.90%
Q	3500	3720	3810	1.11%
R	3970	4240	4340	4.65%
S	4450	4720	4870	7.23%
T	4870	4960	5120	4.38%
U	5310	5480	5530	3.96%
V	6000	6200	6270	3.11%

Table 10. *AIR X Total Estimated Point Source Contributions Determined Using the Summed Values of the Individual Band Pass Filtered Tracks*

Identified Contributors	Impact Percentage
Aerodynamic	
Inflow Turbulence	0.66%
Blade Impulsive	0.43%
Boundary Layer	0.77%
Trailing Edge	8.03%
Tip Vortex	24.80%
Mechanical	
Rotor Bearings	23.80%
Generator	0.17%
Identified Contributors' Total %	**58.50%**
Unaccounted Contributors' %	41.50%

Sunforce 600

Figure 61. Picture of Sunforce 600 wind turbine. From "Sunforce 600-Watt Wind Turbine with Tower Kit" (Lowe's, 2012).

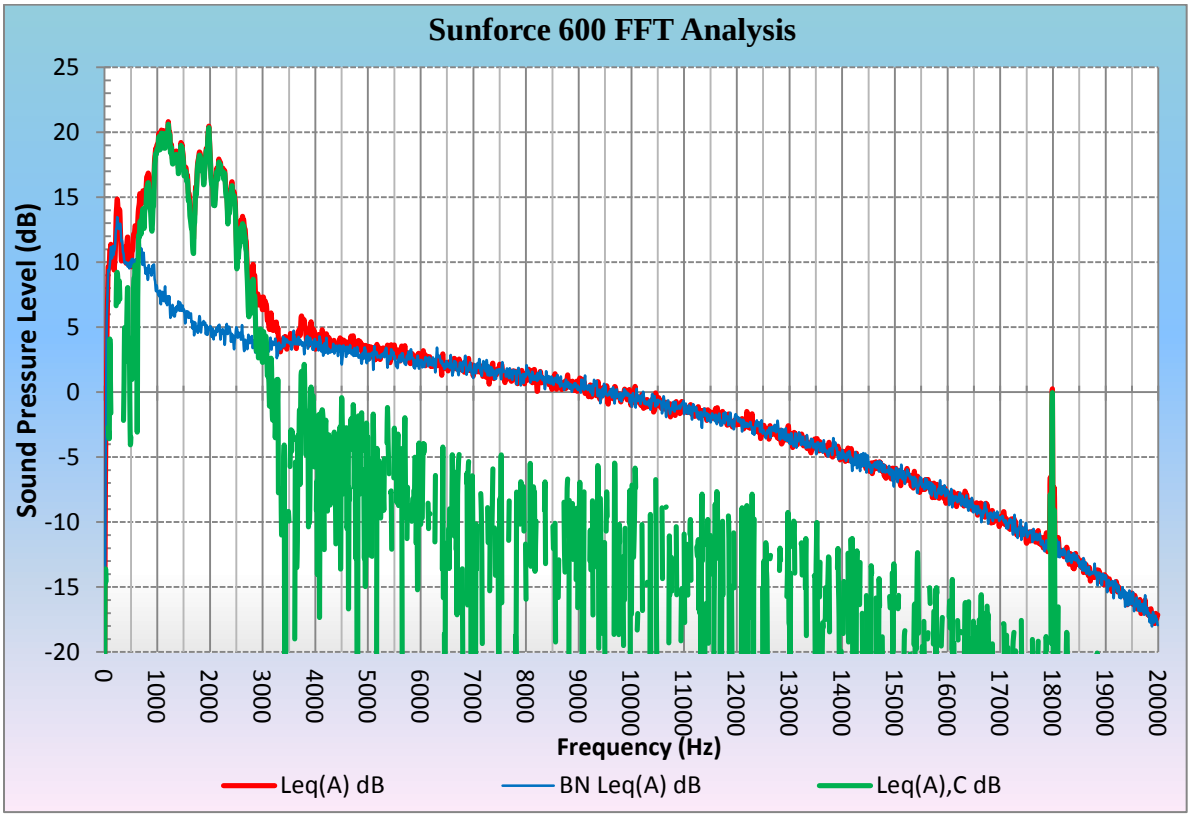

Figure 62. Sunforce 600 FFT analysis results graph.

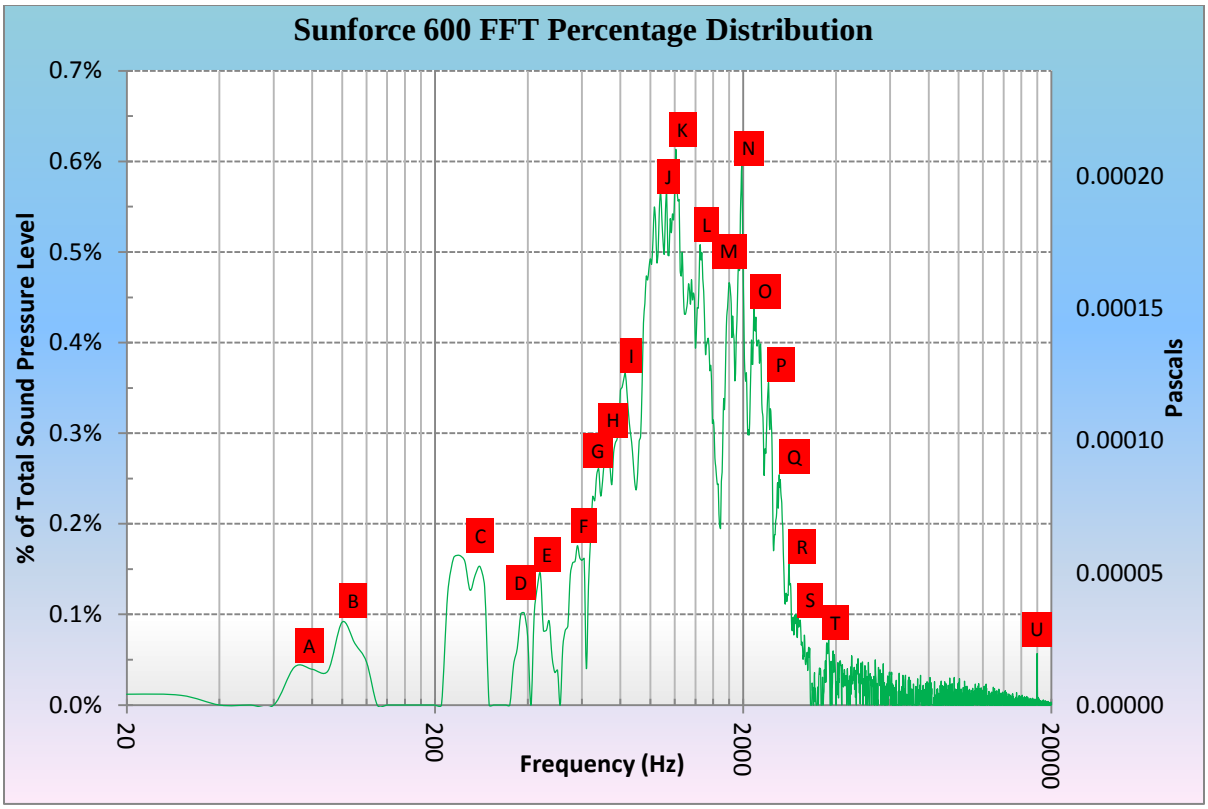

Figure 63. Sunforce 600 FFT percentage distribution graph with distinguished peaks' references.

Table 11. *Sunforce 600 Distinguished Peaks Used as Band Pass Filter Parameters*

Letter	High-pass	Peak	Low-pass	% of Total SPL
A	60	70	90	0.08%
B	90	100	130	0.24%
C	210	240	300	1.16%
D	340	380	410	0.38%
E	410	440	510	0.76%
F	510	580	620	1.35%
G	620	680	690	1.32%
H	690	730	750	1.58%
I	750	830	890	4.36%
J	890	1030	1110	9.69%
K	1110	1210	1290	0.00%

Letter	High-pass	Peak	Low-pass	% of Total SPL
L	1400	1450	1680	10.51%
M	1680	1800	1890	7.77%
N	1890	1980	2070	8.06%
O	2070	2170	2340	9.99%
P	2340	2420	2510	5.08%
Q	2510	2620	2740	4.69%
R	2840	2820	2870	0.39%
S	2870	3010	3140	2.28%
T	3440	3790	4040	1.71%
U	17920	17980	18060	0.23%

Table 12. *Sunforce 600 Total Estimated Point Source Contributions Determined Using the Summed Values of the Individual Band Pass Filtered Tracks*

Identified Contributors	Impact Percentage
Aerodynamic	
Inflow Turbulence	0.67%
Boundary Layer	1.04%
Trailing Edge	32.14%
Tip Vortex	37.56%
Mechanical	
Unknown Electronic Interference	0.23%
Identified Contributors' Total %	**71.65%**
Unaccounted Contributors' %	28.35%

Skystream 3.7

Figure 64. Picture of the Skystream 3.7 wind turbine. From "Skystream 3.7™ Compact Wind Turbine and Wind Energy System" (Solar Direct, 2012).

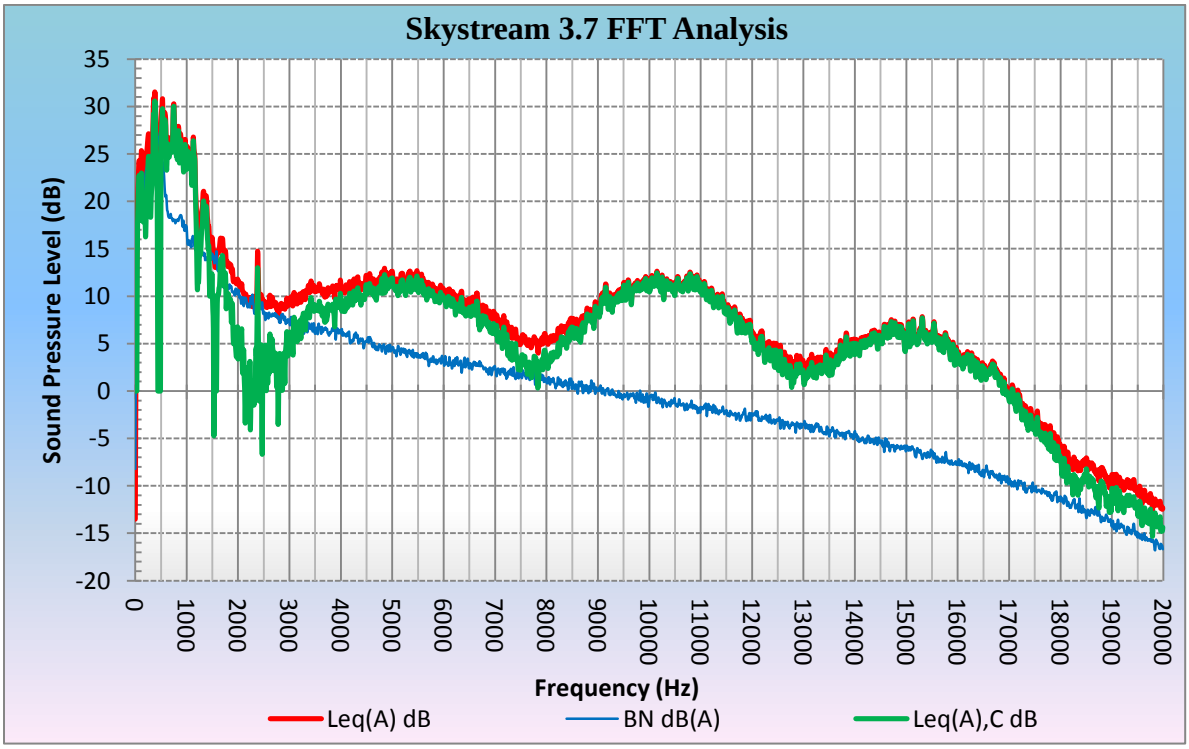

Figure 65. Skystream 3.7 FFT analysis results graph.

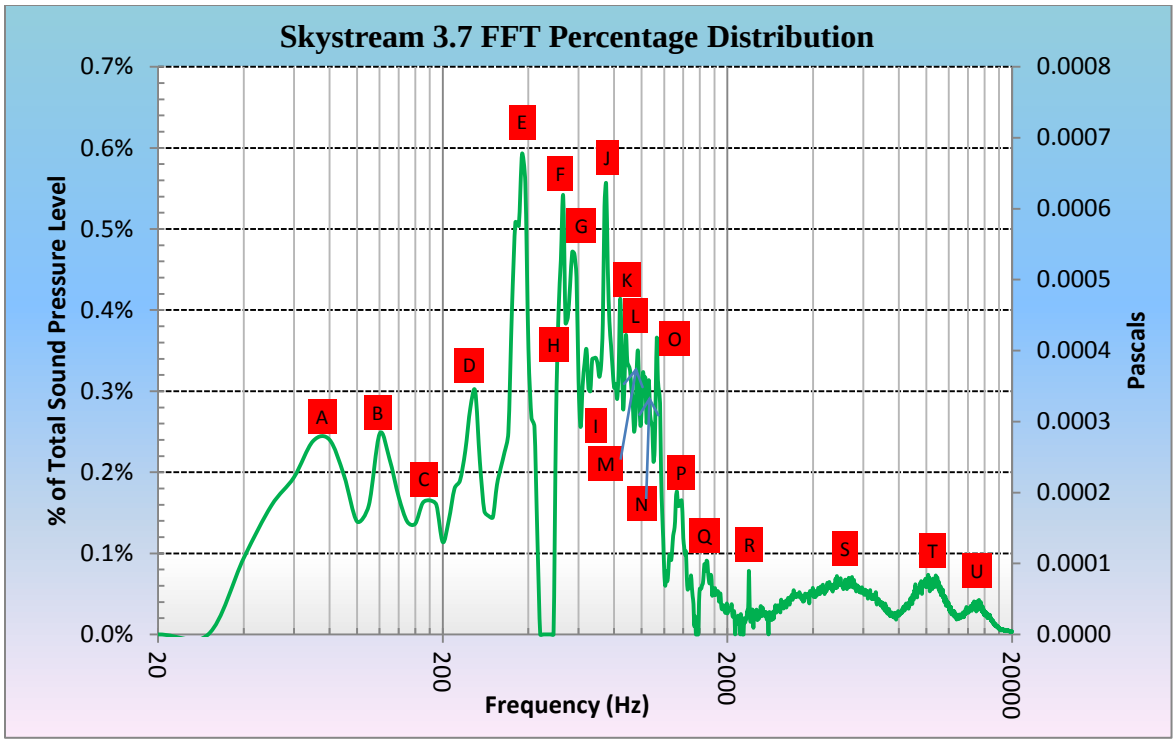

Figure 66. Skystream 3.7 FFT percentage distribution graph with distinguished peaks' references.

Table 13. *Skystream 3.7 Distinguished Peaks Used as Band Pass Filter Parameters*

Letter	High-pass	Peak	Low-pass	% of Total SPL
A	30	80	100	1.12%
B	100	120	160	1.07%
C	160	180	200	0.62%
D	200	260	290	1.80%
E	290	380	440	4.71%
F	470	530	550	2.04%
G	550	570	610	2.51%
H	610	640	650	1.25%
I	650	680	710	1.96%
J	710	750	800	1.56%
K	820	840	860	1.39%

Letter	High-pass	Peak	Low-pass	% of Total SPL
L	860	880	940	2.54%
M	940	970	990	1.48%
N	990	1030	1080	2.62%
O	1100	1130	1210	2.54%
P	1210	1330	1540	3.33%
Q	1540	1700	2190	2.71%
R	2200	2380	2400	0.44%
S	2770	5170	7410	22.56%
T	7410	10510	12380	22.70%
U	12380	15050	17330	7.43%

Table 14. *Skystream 3.7 Total Estimated Point Source Contributions Determined Using the Summed Values of the Individual Band Pass Filtered Tracks*

Identified Contributors	Impact Percentage
Aerodynamic	
Inflow Turbulence	2.82%
Blade Impulsive	0.54%
Boundary Layer	3.43%
Trailing Edge	6.20%
Tip Vortex	31.43%
Mechanical	
Generator	18.39%
Rotor Bearings	25.59%
Identified Contributors' Total %	**62.81%**
Unaccounted Contributors' %	37.19%

Anonymous 50kW

Figure 67. Picture of the Anonymous 50kW wind turbine.

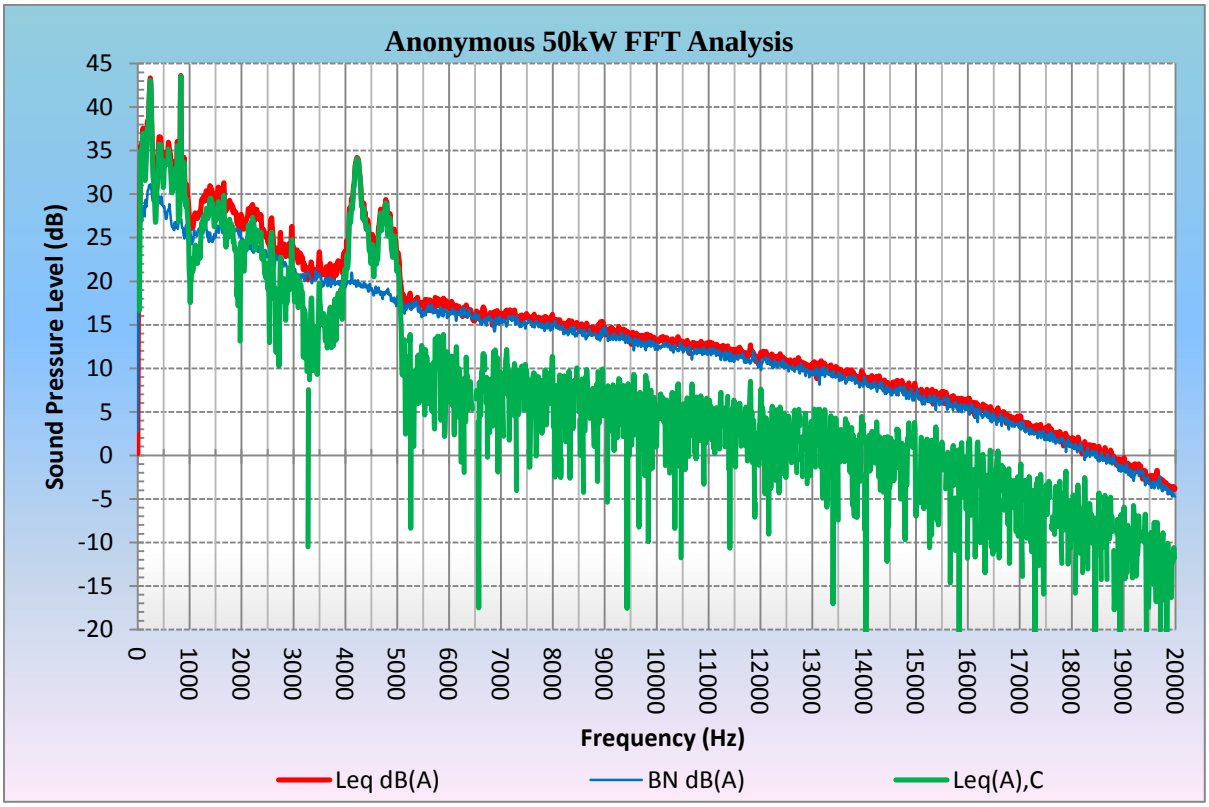

Figure 68. Anonymous 50kW FFT analysis results graph.

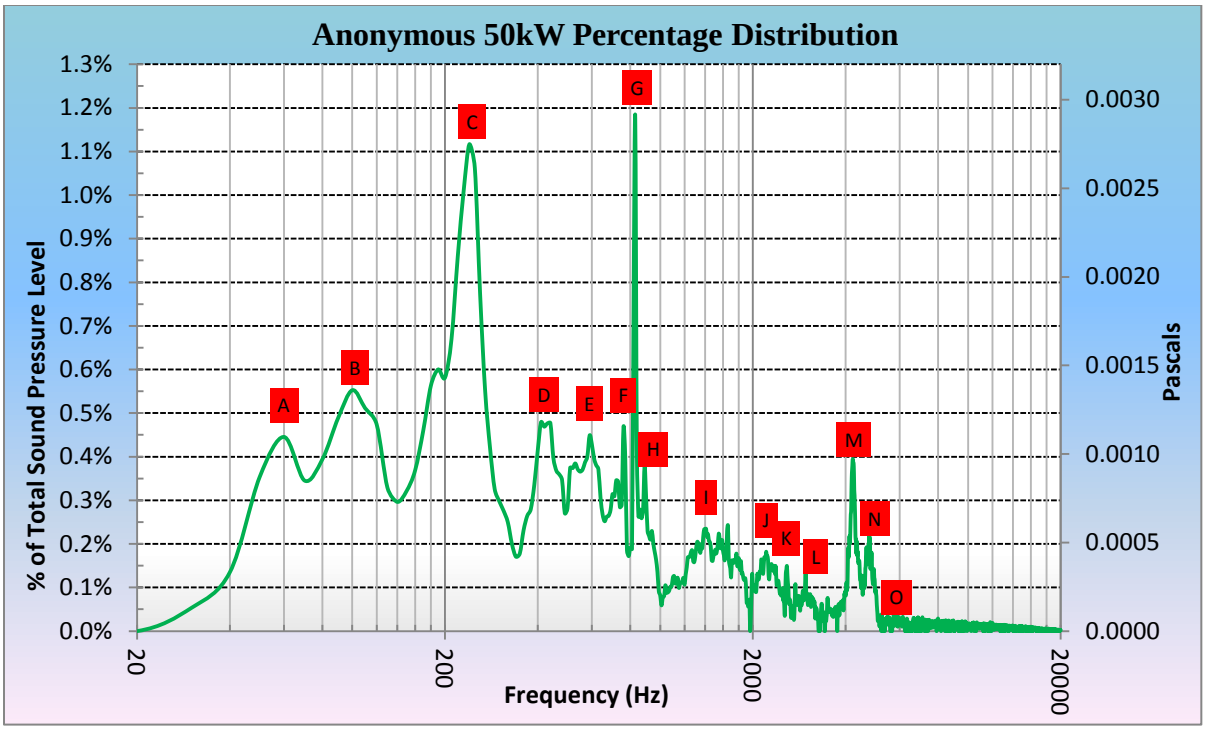

Figure 69. Anonymous 50kW FFT percentage distribution graph with distinguished peaks' references.

Table 15. *Anonymous 50kW Distinguished Peaks Used as Band Pass Filter Parameters*

Letter	High-pass	Peak	Low-pass	% of Total SPL
A	50	60	70	0.80%
B	70	100	140	3.10%
C	140	240	350	11.18%
D	350	420	490	5.07%
E	490	590	670	6.43%
F	670	760	780	3.56%
G	790	830	850	2.92%
H	870	890	1010	2.97%
I	1170	1410	1960	13.03%
J	1960	2210	2540	7.01%
K	2540	2570	2660	3.23%
L	2660	2970	3270	4.00%
M	3990	4220	4620	13.52%
N	4620	4780	5070	6.44%
O	5070	5730	5980	1.99%

Table 16. *Anonymous 50kW Total Estimated Point Source Contributions Determined Using the Summed Values of the Individual Band Pass Filtered Tracks*

Identified Contributors	Impact Percentage
Aerodynamic	
Inflow Turbulence	17.81%
Blade Impulsive	4.83%
Boundary Layer	3.21%
Trailing Edge	5.74%
Tip Vortex	20.88%
Mechanical	
Rotor Bearings	1.49%
Brake	31.27%
Identified Contributors' Total %	**85.23%**
Unaccounted Contributors' %	14.77%

Anonymous 2.3MW

Figure 70. Picture of the Anonymous 2.3MW wind turbine.

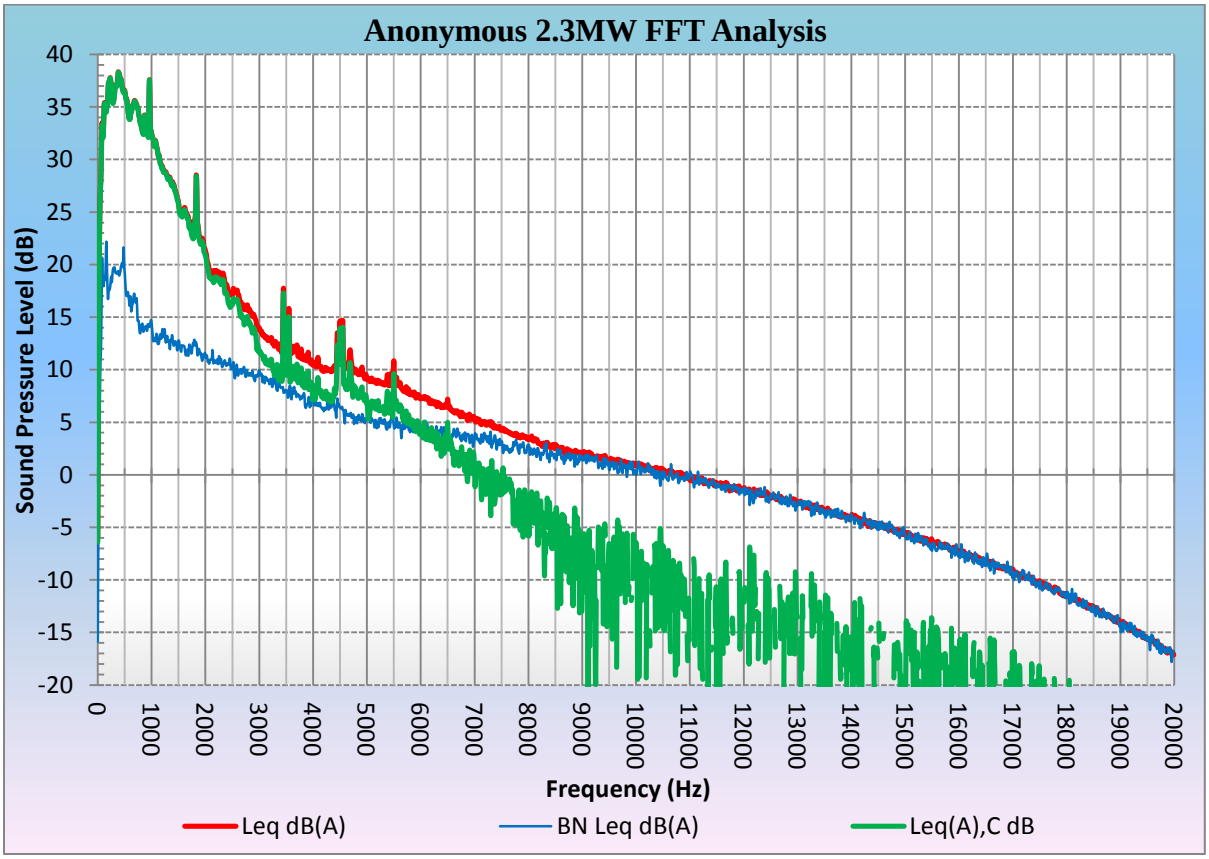

Figure 71. Anonymous 2.3MW FFT analysis results graph.

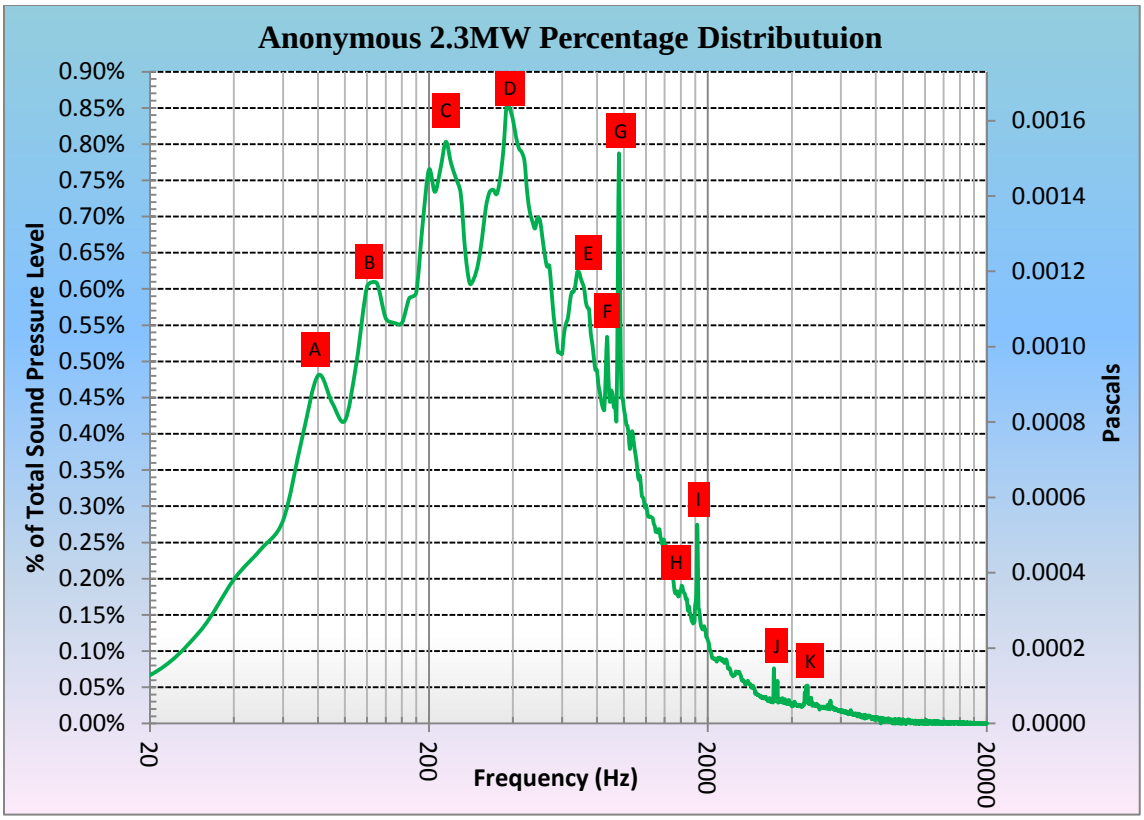

Figure 72. Anonymous 2.3MW FFT percentage distribution graph with distinguished peaks' references.

Table 17. *Anonymous 2.3MW Distinguished Peaks Used as Band Pass Filter Parameters*

Letter	High-pass	Peak	Low-pass	% of Total SPL
A	70	80	100	1.31%
B	100	130	160	3.24%
C	180	230	280	7.26%
D	280	380	580	21.18%
E	580	680	830	13.83%
F	840	870	940	4.59%
G	940	960	1090	6.92%
H	1520	1610	1740	3.85%
I	1740	1830	1880	2.34%
J	3280	3450	3480	0.73%
K	4210	4500	4570	1.09%

Table 18. *Anonymous 2.3MW Total Estimated Point Source Contributions Determined Using the Summed Values of the Individual Band Pass Filtered Tracks*

Identified Contributors	Impact Percentage
Aerodynamic	
Inflow Turbulence	8.91%
Boundary Layer	2.91%
Trailing Edge	21.13%
Tip Vortex	34.06%
Mechanical	
Exhaust Fan	0.07%
Identified Contributors' Total %	**67.08%**
Unaccounted Contributors' %	32.92%

Summary of Findings

All wind turbine subjects' resulting data from the implementation of the diagnostic tool has been combined into a single table for a within-subjects comparison. It can be noticed in Table 19 that for four out of the six tested wind turbines, the tip vortex point source contributor was observed to have the largest impact on the total sound pressure of the wind turbine's acoustic emissions. The smallest wind turbine, the AIR Breeze, was the only subject to contain the largest percentage of its sound pressure resulting from the bearings. The Anonymous 50kW wind turbine contained its greatest percentage of impact resulting from rubbing brakes. This was determined to be a malfunctioning state of operation and was to be fixed after the test had been performed.

Overall, there were more aerodynamic point source noises that were consistently identified for all wind turbine subjects. This may be due to the fact that all of the tested wind

turbines have airfoil shaped blades that produce similar types of noises whereas not all of the wind turbines contained similar mechanical componentry.

Table 19. *Summary Table of Point Source Percentage Contributions to Individual Wind Turbine Sound Pressure Levels*

Point Source Contributors			Wind Turbine					
			AIR Breeze	**AIR X**	**Sunforce 600**	**Skystream 3.7**	**Anonymous 50kW**	**Anonymous 2.3MW**
	Aerodynamic	Blade Impulsive	**7.55%**	**0.43%**	-	**0.54%**	**4.83%**	-
		Boundary Layer	**7.91%**	**0.77%**	**1.04%**	**3.43%**	**3.21%**	**2.91%**
		Inflow Turbulence	**0.58%**	**0.66%**	**0.67%**	**2.82%**	**17.81%**	**8.91%**
		Tip Vortex	**20.69%**	**24.80%**	**37.56%**	**31.43%**	**20.88%**	**34.06%**
		Trailing Edge	**1.42%**	**8.03%**	**32.14%**	**6.20%**	**5.74%**	**21.13%**
	Mechanical	Bearings	**30.78%**	**23.80%**	-	**25.59%**	**1.49%**	-
		Brake	-	-	-		**31.27%**	-
		Generator	-	**0.17%**	-	**18.39%**	-	-
		Exhaust Fan	-	-	-	-	-	**0.07%**
		Unknown Electronic Interference		-	**0.23%**	-	-	-

Note. This table is presented with a color scale that shows the smallest point source contribution percentages in green, medium percentages in yellow, the highest percentages in red, and variations between presented with the appropriate mix of color.

Conclusion Summary

This study's methodology has been shown to provide a solid base to reach the original goal of breaking the total wind turbine's sound down into individual components for analysis, providing tonal analyses that far exceed the information requested by the IEC Standard. The diagnostic tool has provided conclusive evidence regarding the impact of individual point source contributors on the total wind turbine acoustic emissions for each wind turbine test subject. Although the acoustic interpretation that associates particular

percentages of impact to individual point source contributors is subjective in nature, it nevertheless provides credible explanations based on empirical data. There is only a small opportunity for error in the data acquisition and analysis methodologies, rendering results that are believed to be quite close in both quality and quantity to the best information that could be obtained using strictly controlled conditions for testing.

Each wind turbine's results do include a portion of the total sound pressure that remained unidentified because of areas within the sound signature that did not qualify as "distinguished" peaks. The components that contribute to the "unaccounted contributor percentage" have been deemed to pose a low impact to the overall acoustic emissions and do not contain peaks in the sound signature. Without presenting distinguishable peaks, these components are probably producing acoustic emissions that are non-intrusive to the human ear and, therefore, are unlikely to require acoustic mitigation interventions.

Chapter 6: DISCUSSION AND CONCLUSIONS

Implications for the IEC 61400-11 Standard

This study's diagnostic tool was purposefully developed to build upon the IEC Standard. The Standard was designed to accommodate all types of wind turbines on an international scale. The Standard is quite solid in its current format, accounting for an incredible number of variables that a tester may encounter during the on-site testing and likewise during the post-site analysis. Most importantly, the Standard provides a means of quantifying the total noise emitted by a wind turbine and presenting it in a way that allows for comparison of different wind turbines that are tested at any site globally.

Although the Standard provides solid baseline data to characterize the overall sound emitted by a turbine, the required testing parameters are limited in the tonal range that can be reported and thus prevent a more nuanced interpretation of the various factors that influence total turbine noise. Perhaps this was done intentionally to accommodate a vast range of wind turbine designs and technologies while also providing the resulting test information that is not too complicated for the average wind turbine enthusiast or city council member to comprehend. The proposed diagnostic tool is offered as a way to complement the existing IEC Standard by providing an advanced characterization of a wind turbine's sound signature. This information could be invaluable in the further evolution of wind turbine technology and toward its greater acceptance in a broader range of settings.

The use of advanced acoustic software may produce a more in-depth characterization of a wind turbine's acoustic emissions, but it also requires that more specialized knowledge be obtained by the tester than is already expected by the IEC Standard. Furthermore, the proposed diagnostic tool requires a great deal more time to apply than the IEC Standard does in its current state. This time, inevitably, relates to an increased cost, not only economically, but also in terms of the man-hours that must be devoted to the intricacies contained within the diagnostic tool's methodology. Thus, barring future changes in the IEC Standard itself and further refinement of the proposed diagnostic tool, the strategies described via this study may remain specialized "add-ons" adopted by manufacturers interested in continuing improvements in turbine design. At the very least, it is hoped that this study will provide a deeper understanding of the factors that can contribute to wind turbine noise, regardless of whether or not a more sophisticated characterization is undertaken.

Implications for the Wind Energy Industry

This diagnostic tool could have a large impact on the wind energy industry. Noise pollution is a large concern for the development of any newly created energy producing plant. Through the use of this diagnostic tool, the research and design groups involved in wind turbine technologies can assess the current state of their wind turbine's acoustic emissions and more efficiently progress towards a quieter wind turbine, minimizing the particular point source contributors that are most intrusive to the human ear. If this tool is accepted by wind turbine manufacturers, the goal of quieter wind turbines may be achieved more readily than would otherwise be the case.

Currently, turbine manufacturers must adhere to the testing parameters outlined in the IEC Standard. A tool that provides them with strategies to incrementally reduce contributors

to the overall sound could provide invaluable assistance to reducing the overall acoustic emissions of their wind turbine. However, if the diagnostic tool is used to identify a particular contributor for acoustic mitigation, it may induce an increase of acoustic emissions from a different contributor. For example, if the blade tip noise is reduced by designing a more bluntly shaped tip, the trailing edge noise may increase as a result. The desirable outcome would be to decrease the total wind turbine's sound pressure level, perhaps through finding a compromise among individual point source contributor designs that makes the total sound less obtrusive to the human ear. It is not realistic to aim to completely remove all acoustic emissions because of the inherent nature of noise produced by the necessary moving parts of a wind turbine.

The renewable energy industry has been quite hesitant with each step in its development, making sure the choices made are the best possible ones from economic, environmental, and technological perspectives. The choices we make as a society include the judgments of those who speak both for and against acceptance of renewable energy technologies into our society, as well as what we believe will provide the best future for all living things. Tools that can positively impact the choices we make today could have a lasting effect on future civilizations.

Possible Applications of this Diagnostic Tool

The number of possibilities for use of this diagnostic tool is broad. As its methods and results are discussed with more individuals in the wind energy industry, more applications are realized. Some of the possible applications that have been identified include research and design, maintenance monitoring, and site installation planning.

Research and Design

For research and design in particular, the described diagnostic tool provides information that a manufacturer would not obtain through IEC Standard testing alone or through other forms of previously developed engineering formulae. The Standard may certify a wind turbine for manufacturing but it is not designed to provide specific descriptive details needed by engineers in the designing process. The amount of information resulting from this diagnostic tool is far beyond what will be found in a typical IEC Standard report. The degree of acoustic mining that is achieved through use of the diagnostic tool's methodology reveals possible parameters that would have been overlooked otherwise. It not only provides the isolation and identification of specific narrowband tones that are most noticeable to the human ear, it also quantifies those tones to an high degree of precision. This quantification may be the best information for design engineers to alert them of the most important point sources to focus on mitigating for an overall reduction of the wind turbine acoustic emissions.

Maintenance Monitoring

Through discussions held at a wind energy conference, it was brought to my attention that this tool could be used to routinely monitor a wind turbine's performance. Although it is not a direct result of the IEC Standard for data acquisition, if a microphone continuously measured a wind turbine's acoustic emissions, small changes in operation and acoustic output could be identified much earlier than the human ear would detect, thus potentially signaling needed maintenance or repair.

As a result of the microphone's sensitivity level, which is far beyond a human ear's ability, it would have the capacity to detect the slightest of acoustic variations produced by

the wind turbine. This early detection could notify the wind turbine's managers, letting them know which component is out of a particular acceptance range. Not only would it keep the wind turbine in a pristine working condition, it would alert the site manager with enough advance notification to expect a particular maintenance so that he or she could have plenty of time to schedule the necessary personnel and equipment to accomplish the repair. This would save time and, indirectly, money, which is a valuable asset for many electrical power plants and businesses alike.

Site Installation Planning

When planning the installation of a wind turbine, local governments often require that the turbine will remain under a particular sound pressure level (see Table 1). However, it is difficult for someone to imagine what a wind turbine will sound like or how loud it will be if they have never actually visited one in real life. A dB sound pressure level value may simply be a written number for some, unable to portray the physical feeling they may experience when the proposed turbine is actually installed.

The diagnostic tool provides actual acoustic recordings that can be listened to in order to help determine whether or not a turbine's acoustic emissions are acceptable. As demonstrated in this study, it's possible to describe acoustic emissions quantitatively and through narrative descriptions, but to truly get a sense for a noise, it is best understood by a hearing human ear.

Evolution has provided us with an incredibly intricate set of senses to understand the reality around us, one of which is hearing. As was described earlier in this paper (Figure 10), the human ear may seem like a foreign planet to some, involving a system of microscopic organs (Figure 11) that translate a physical presence of energy into a mental interpretation we

call sound. Our sense of hearing is our best asset when it comes to interpreting acoustic energies with a huge range of frequencies and relative pressures.

These real-life applications are but just a few of the possibilities that may result from use of the described diagnostic tool in this study. New uses are continuously arising, and with increased use of this tool the importance of noise detection and mitigation may also increase.

Future Research

This diagnostic tool presents many possibilities for future research. It has provided a suggested path for the investigation of a wind turbine's acoustic emissions, although there are clearly opportunities for refinement of the methodology. The room for improvement presents itself in a variety of ways, some of which would include the ability to better analyze broadband point source contributors and an increase in the specificity of the acoustic identification decision trees. Furthermore, through the use of controlled experiments individual components of the tool can be further validated. An experimental design would have entailed the use of controlled variables, possibly in a laboratory setting where the environmental conditions during testing do not affect recording. If individual point source contributors were targeted in an experimental format, these specific measurements could be acoustically or mathematically subtracted from the wind turbine's total acoustic emission recording, providing more precise identifications for analysis.

As previously discussed, aerodynamic noise identification was observed to be the most difficult step of the diagnostic tool. Many of the associations of particular acoustic characteristics were made based upon assumptions that could be better qualified through advanced research on individual component contributors. The broadband spectra were unable to be fully captured by individual band pass filters without including the narrowband

contributors occurring within the same particular band width. This provides an area for improvement in the acoustic processing methodology that may include an alteration to the specific steps described in the diagnostic tool.

The acoustic identification decision trees were developed through experience using the diagnostic tool in this study. More test subjects with an increased variety of componentry could be processed using this protocol to determine whether or not the chosen paths still prove to be applicable and reliable. The literature review provides suggestions for particular components' acoustic criteria, but it would be interesting to verify these claims with further research on existing wind turbine designs. As wind turbine diagnostic tools progress they will enhance our ability to develop this emerging renewable energy technology.

Final Remarks

This study builds upon the existing IEC 61400-11 Standard for measuring the noise emissions from wind turbines by marrying the measured data acquired through application of this standard with acoustical software applications that allow in-depth analysis of that acoustic data. The goal of the study was to create a methodology for identifying point source contributors to a turbine's overall noise level, thus providing a basis for potential mitigation of sound levels through modification of individual turbine components. A novel diagnostic tool was proposed that incorporates use of band-pass filtering and analysis of sound pressure levels at peak frequencies. The resulting data were then analyzed using decision trees developed to help associate peak sound levels with individual components.

This analysis was implicitly affected by the exploration of the science of acoustics presented in Chapter 2, which motivated a more in-depth examination of the noise emitted by wind turbines with the goal of attaining a better understanding of the factors that contribute

to this noise. The conclusions that can be drawn from this research have many implications for the IEC 61400-11 Standard as well as for the wind turbine manufacturing industry. It is the hope of this writer that the two disjointed disciplines of acoustics and wind energy may be brought a step closer through the novel approach developed in this study.

It is inevitable that wind turbine technology will progress and gain greater acceptance, whether it be sooner or later. Society's default preference for maintaining the status quo will eventually switch to recognizing wind energy as a clean, affordable form of electrical production for our ever-growing global energy needs. The sustainable choice of wind energy could alter the fate of this planet if it is embraced, although it could take some time and further technological development before this becomes a reality.

REFERENCES

Alberts, D. J. (2006). *Primer for Addressing Wind Turbine Noise.* Lawrence Technological University.

Canadian Centre for Occupational Health and Safety Administration. (2004, May 17). *Noise - Measurement of Workplace Noise*. Retrieved 2012, from CCOHS: Canada's National Centre for Occupational Health and Safety Information: http://www.ccohs.ca/oshanswers/phys_agents/noise_measurement.html

Clerc, L. (2011). *Understanding the Ear*. (Clerc Center) Retrieved from Gallaudet University: http://www.gallaudet.edu/Clerc_Center/Information_and_Resources/Info_to_Go/Hearing_Loss_Information/Understanding_the_Ear.html

Connexa Energy. (2012). *Bergey 1kW Battery Charging Wind Turbine*. Retrieved from Connexa Energy, LLC: http://connexaenergy.com/Default.aspx?tabid=931&CategoryID=146&List=0&SortField=ProductName%2CProductName&Level=1&ProductID=510

Epsilon Associates, Inc. (2006). *Sound Level Impact Assessment Report: Minuteman Savoy Wind Project.* Maynard, Massachusetts. Retrieved from http://www.minutemanwind.com/pdf/Savoy%20Noise%20Final%20Report.pdf

ETSU Working Group on Wind Turbine Noise. (1996). *The Assessment & Rating of Noise from Wind Farms: ETSU-R-97.* Department of Trade and Industry. Retrieved from http://www.hayesmckenzie.co.uk/downloads/ETSU%20Full%20copy%20(Searchable).pdf

Fastl, H., & Zwicker, E. (2007). *Psycho-Acoustics: Facts and Models* (3rd ed.). (T. S. Huang, M. R. Schroeder, & T. Kohonen, Eds.) Berlin, Germany: Springer.

Hansen, M. O. (2008). *Aerodynamics of Wind Turbines* (2nd ed.). Sterling, VA: Earthscan.

Hessler, G. F., & Hessler, D. M. (2006, November). Baseline Environmental Sound Levels for Wind Turbine Projects. *Sound and Vibration, 40*(11), pp. 10-13. Retrieved from http://www.sandv.com/downloads/0611hess.pdf

Hubbard, H. H., & Shepherd, K. P. (1994). Wind Turbine Acoustics. In T. A. Engineers, & D. A. Spera (Ed.), *Wind Turbine Technology: Fundamental Concepts of Wind Turbine Engineering* (pp. 323-370). New York: ASME.

International Electrotechnical Commission. (2002, May). *International Electrotechnical Commission 61672-1 ed.1.0: Electroacoustics – Sound Level Meters – Part 1: Specifications.* Retrieved from International Electrotechnical Commission Webstore.

International Electrotechnical Commission. (2006, November). *IEC 61400-11 ed. 2.1: Wind turbine generator systems - Part 11: Acoustic noise measurement techniques.* Retrieved from International Electrotechnical Commission Webstore: http://www.asugards.net/dbpics/uploads/iec61400-11%7Bed2.1%7Den.pdf

LM Wind Power. (2012). *Aerodynamics*. Retrieved from Blades - LM Wind Power: http://www.lmwindpower.com/Blades/Products/Performance/Aerodynamics.aspx

Lowe's. (2012). *Shop Sunforce 600-Watt Wind Turbine with Tower Kit at Lowes.com*. Retrieved from Lowe's Home Improvement: Appliances, Tools, Hardware, Paint, Flooring: http://www.lowes.com/pd_322515-11338-45644_0__?productId=3353362

Lynette, R., & Gipe, P. (1994). Commercial Wind Turbine Systems and Applications. In T. A. Engineers, & D. A. Spera (Ed.), *Wind Turbine Technology: Fundamental Concepts of Wind Turbine Engineering* (pp. 139-214). Sterling, VA: ASME.

Migliore, P., van Dam, J., & Huskey, A. (2004). *Acoustic Tests of Small Wind Turbines.* National Wind Technology Center. Golden, CO: National Renewable Energy Laboratory.

Nave, C. R. (2012a). *Inverse Square Law, Sound*. (Georgia State University) Retrieved from HyperPhysics: http://hyperphysics.phy-astr.gsu.edu/hbase/acoustic/invsqs.html

Nave, C. R. (2012b). *Sound and Hearing: Longitudinal Waves*. (Georgia State University) Retrieved from HyperPhysics: http://hyperphysics.phy-astr.gsu.edu/hbase/hframe.html

Nave, C. R. (2012c). *Sound and Hearing: Sensitivity of Human Ear*. (Georgia State University) Retrieved from HyperPhysics: http://hyperphysics.phy-astr.gsu.edu/hbase/sound/earsens.html#c1

Nave, C. R. (2012d). *Sound and Hearing: Sound Waves in Air*. (Georgia State University) Retrieved from HyperPhysics: http://hyperphysics.phy-astr.gsu.edu/hbase/hframe.html

Nave, C. R. (2012e). *Sound and Hearing: Transverse Waves*. (Georgia State University) Retrieved from HyperPhysics: http://hyperphysics.phy-astr.gsu.edu/hbase/hframe.html

Noise Pollution Clearinghouse. (2012). *Comparison of Various Standards for Safe Noise-Exposure*. Retrieved from Noise Pollution Clearinghouse, quieting noise pollution: http://www.nonoise.org/hearing/exposure/standardschart.htm

Northern Power Systems. (2012). *Gearless Direct Drive: Northern Power Systems*. Retrieved from Welcome: Northern Power Systems: http://www.northernpower.com/technology/direct-drive.php

Occupational Safety & Health Administration. (2012). *Appendix I:A-3. Sound Propagation*. (United States Department of Labor) Retrieved from Occupational Safety & Health Administration: http://www.osha.gov/dts/osta/otm/noise/health_effects/soundpropagation.html

Pichert, D., & Katsikopoulos, K. V. (2008). Green defaults: Information presentation and pro-environmental behaviour. *Journal of Environmental Psychology*, 63-73.

Prospathopoulos, J. M., & Voutsinas, S. G. (2005, May). Noise Propagation Issues in Wind Energy Applications. *Journal of Solar Energy Engineering, 127*(2), pp. 234-241. doi:10.1115/1.1862257

Ramen, G. (2010). Advances in Measuring Noise from Wind Turbines. *Noise and Vibration Worldwide, 9*(3), 11-20.

Rogers, A. L., Manwell, J. F., & Wright, S. (2006). *Wind Turbine Acoustic Noise.* University of Massachusetts at Amherst, Department of Mechanical and Industrial Engineering. Amherst, MA 01003: Renewable Energy Research Laboratory. Retrieved from http://www.ceere.org/rerl/publications/whitepapers/Wind_Turbine_Acoustic_Noise_Rev2006.pdf

Solar Direct. (2012). *Wind Power - Skystream 3.7 General Information*. Retrieved from Solar Direct: http://www.solardirect.com/wind-power/skystream/st-general-info.html

Stankovic, S., Campbell, N., & Harries, A. (2009). *Urban Wind Energy.* Sterling, VA: Earthscan.

Sun Electronics. (2012). *Air Breeze Land*. Retrieved from Solar Panels, PV Systems and Inverters Distributor: http://www.sunelec.com/air-breeze-land-p-205.html

Waste Reducer. (2012). *Residential Backyard Wind Generator*. Retrieved from Waste Reducer: http://www.wastereducer.com/

Wenger, J. (2006, June 27). *Protein Tied to Usher Syndrome May Be Hearing's 'Missing Link'*. Retrieved from National Institute on Deafness and Other Communication (NIDCD): http://www.nidcd.nih.gov/news/releases/06/Pages/06_27_06.aspx

APPENDICES

Appendix A: Individual Subject Decision Tree Peak Results

AIR Breeze

Peak ID			A	
High-pass	**Low-pass**	**Frequency Range**	**Amplitude Modulated?**	**Amplitude Affected by Wind Speed?**
110	150	LOW	NO	NO
Point Source(s)			Inflow Turbulence	Blade Impulsive
Weighted Percentages			70%	30%
Total Peak's Percentage of Wind Turbine's SPL			0.06%	

Peak ID			B	
High-pass	**Low-pass**	**Frequency Range**	**Amplitude Modulated?**	**Amplitude Affected by Wind Speed?**
180	210	LOW	YES	NO
Point Source(s)			Blade Impulsive	Inflow Turbulence
Weighted Percentages			60%	40%
Total Peak's Percentage of Wind Turbine's SPL			0.13%	

Peak ID			C	
High-pass	**Low-pass**	**Frequency Range**	**Amplitude Modulated?**	**Amplitude Affected by Wind Speed?**
340	420	MEDIUM	YES	NO
Point Source(s)			Inflow Turbulence	Blade Impulsive
Weighted Percentages			70%	30%
Total Peak's Percentage of Wind Turbine's SPL			0.70%	

Peak ID			D	
High-pass	**Low-pass**	**Frequency Range**	**Amplitude Modulated?**	**Amplitude Affected by Wind Speed?**
940	1160	MEDIUM	NO	YES
Point Source(s)			Boundary Layer	Trailing Edge
Weighted Percentages			70%	30%
Total Peak's Percentage of Wind Turbine's SPL			4.74%	

Peak ID			E	
High-pass	**Low-pass**	**Frequency Range**	**Amplitude Modulated?**	**Amplitude Affected by Wind Speed?**
1160	1270	MEDIUM	NO	YES
Point Source(s)			Boundary Layer	Tip Vortex
Weighted Percentages			60%	40%
Total Peak's Percentage of Wind Turbine's SPL			2.18%	

Peak ID			F	
High-pass	**Low-pass**	**Frequency Range**	**Amplitude Modulated?**	**Amplitude Affected by Wind Speed?**
1270	1550	MEDIUM	NO	YES
Point Source(s)		Boundary Layer	Tip Vortex	Blade Impulsive
Weighted Percentages		50%	30%	20%
Total Peak's Percentage of Wind Turbine's SPL			5.41%	

Peak ID			G	
High-pass	**Low-pass**	**Frequency Range**	**Amplitude Modulated?**	**Amplitude Affected by Wind Speed?**
1550	1730	MEDIUM	NO	YES
Point Source(s)		Tip Vortex	Boundary Layer	Bearings
Weighted Percentages		60	20%	20%
Total Peak's Percentage of Wind Turbine's SPL			2.88%	

Peak ID			H	
High-pass	**Low-pass**	**Frequency Range**	**Amplitude Modulated?**	**Amplitude Affected by Wind Speed?**
1730	2510	MEDIUM	YES	YES
Point Source(s)		Blade Impulsive	Tip Vortex	Bearings
Weighted Percentages		50	20%	30%
Total Peak's Percentage of Wind Turbine's SPL			12.32%	

Peak ID			I	
High-pass	**Low-pass**	**Frequency Range**	**Amplitude Modulated?**	**Amplitude Affected by Wind Speed?**
2510	2860	MEDIUM	NO	YES
Point Source(s)			Tip Vortex	Bearings
Weighted Percentages			60%	40%
Total Peak's Percentage of Wind Turbine's SPL			3.88%	

Peak ID			J	
High-pass	**Low-pass**	**Frequency Range**	**Amplitude Modulated?**	**Amplitude Affected by Wind Speed?**
2860	3250	MEDIUM	YES	NO
Point Source(s)			Bearings	Tip Vortex
Weighted Percentages			50%	50%
Total Peak's Percentage of Wind Turbine's SPL			2.72%	

Peak ID			K	
High-pass	**Low-pass**	**Frequency Range**	**Amplitude Modulated?**	**Amplitude Affected by Wind Speed?**
3970	4730	MEDIUM	YES	NO
Point Source(s)			Bearings	Tip Vortex
Weighted Percentages			60%	40%
Total Peak's Percentage of Wind Turbine's SPL			8.62%	

Peak ID			L	
High-pass	**Low-pass**	**Frequency Range**	**Amplitude Modulated?**	**Amplitude Affected by Wind Speed?**
4730	5510	MEDIUM	YES	NO
Point Source(s)			Bearings	Tip Vortex
Weighted Percentages			70%	30%
Total Peak's Percentage of Wind Turbine's SPL			9.48%	

Peak ID			M	
High-pass	**Low-pass**	**Frequency Range**	**Amplitude Modulated?**	**Amplitude Affected by Wind Speed?**
5510	6320	HIGH	YES	NO
Point Source(s)			Bearings	Tip Vortex
Weighted Percentages			70%	30%
Total Peak's Percentage of Wind Turbine's SPL			12.02%	

Peak ID			N	
High-pass	**Low-pass**	**Frequency Range**	**Amplitude Modulated?**	**Amplitude Affected by Wind Speed?**
8910	9950	HIGH	YES	NO
Point Source(s)			Bearings	Tip Vortex
Weighted Percentages			80%	20%
Total Peak's Percentage of Wind Turbine's SPL			1.92%	

Peak ID			O	
High-pass	**Low-pass**	**Frequency Range**	**Amplitude Modulated?**	**Amplitude Affected by Wind Speed?**
10030	12970	HIGH	YES	NO
Point Source(s)			Bearings	Tip Vortex
Weighted Percentages			70%	30%
Total Peak's Percentage of Wind Turbine's SPL			2.63%	

AIR X

Peak ID			A	
High-pass	**Low-pass**	**Frequency Range**	**Amplitude Modulated?**	**Amplitude Affected by Wind Speed?**
30	50	LOW	YES	YES
Point Source(s)			Blade Impulsive	Inflow Turbulence
Weighted Percentages			60%	40%
Total Peak's Percentage of Wind Turbine's SPL			0.02%	

Peak ID			B	
High-pass	**Low-pass**	**Frequency Range**	**Amplitude Modulated?**	**Amplitude Affected by Wind Speed?**
50	100	LOW	NO	YES
Point Source(s)			Inflow Turbulence	Blade Impulsive
Weighted Percentages			60%	40%
Total Peak's Percentage of Wind Turbine's SPL			0.16%	

Peak ID			C	
High-pass	**Low-pass**	**Frequency Range**	**Amplitude Modulated?**	**Amplitude Affected by Wind Speed?**
100	200	LOW	NO	YES
Point Source(s)			Inflow Turbulence	Trailing Edge
Weighted Percentages			70%	30%
Total Peak's Percentage of Wind Turbine's SPL			0.79%	

Peak ID			D	
High-pass	**Low-pass**	**Frequency Range**	**Amplitude Modulated?**	**Amplitude Affected by Wind Speed?**
290	400	MEDIUM	NO	YES
Point Source(s)			Trailing Edge	Blade Impulsive
Weighted Percentages			70%	30%
Total Peak's Percentage of Wind Turbine's SPL			1.17%	

Peak ID			E	
High-pass	**Low-pass**	**Frequency Range**	**Amplitude Modulated?**	**Amplitude Affected by Wind Speed?**
410	480	MEDIUM	NO	YES
Point Source(s)			Boundary Layer	Trailing Edge
Weighted Percentages			80%	20%
Total Peak's Percentage of Wind Turbine's SPL			0.78%	

Peak ID			F	
High-pass	**Low-pass**	**Frequency Range**	**Amplitude Modulated?**	**Amplitude Affected by Wind Speed?**
480	560	MEDIUM	NO	YES
Point Source(s)		Boundary Layer	Trailing Edge	Tip Vortex
Weighted Percentages		60%	30%	10%
Total Peak's Percentage of Wind Turbine's SPL			0.25%	

Peak ID			G	
High-pass	**Low-pass**	**Frequency Range**	**Amplitude Modulated?**	**Amplitude Affected by Wind Speed?**
560	610	MEDIUM	NO	YES
Point Source(s)		Trailing Edge	Tip Vortex	Generator
Weighted Percentages		50%	30%	20%
Total Peak's Percentage of Wind Turbine's SPL			0.09%	

Peak ID			H	
High-pass	**Low-pass**	**Frequency Range**	**Amplitude Modulated?**	**Amplitude Affected by Wind Speed?**
640	690	MEDIUM	NO	YES
Point Source(s)		Tip Vortex	Trailing Edge	Generator
Weighted Percentages		50%	20%	30%
Total Peak's Percentage of Wind Turbine's SPL			0.33%	

Peak ID			I	
High-pass	**Low-pass**	**Frequency Range**	**Amplitude Modulated?**	**Amplitude Affected by Wind Speed?**
810	860	MEDIUM	NO	YES
Point Source(s)		Trailing Edge	Tip Vortex	Generator
Weighted Percentages		60%	20%	10%
Total Peak's Percentage of Wind Turbine's SPL			0.51%	

Peak ID			J	
High-pass	**Low-pass**	**Frequency Range**	**Amplitude Modulated?**	**Amplitude Affected by Wind Speed?**
1000	1240	MEDIUM	NO	YES
Point Source(s)			Trailing Edge	Tip Vortex
Weighted Percentages			70%	30%
Total Peak's Percentage of Wind Turbine's SPL			4.15%	

Peak ID			K	
High-pass	**Low-pass**	**Frequency Range**	**Amplitude Modulated?**	**Amplitude Affected by Wind Speed?**
1280	1580	MEDIUM	NO	YES
Point Source(s)			Trailing Edge	Tip Vortex
Weighted Percentages			60%	40%
Total Peak's Percentage of Wind Turbine's SPL			5.70%	

Peak ID			L	
High-pass	**Low-pass**	**Frequency Range**	**Amplitude Modulated?**	**Amplitude Affected by Wind Speed?**
1700	2010	MEDIUM	NO	YES
Point Source(s)			Tip Vortex	Rotor Bearings
Weighted Percentages			90%	10%
Total Peak's Percentage of Wind Turbine's SPL			4.54%	

Peak ID			M	
High-pass	**Low-pass**	**Frequency Range**	**Amplitude Modulated?**	**Amplitude Affected by Wind Speed?**
2170	2490	MEDIUM	NO	YES
Point Source(s)			Tip Vortex	Rotor Bearings
Weighted Percentages			80%	20%
Total Peak's Percentage of Wind Turbine's SPL			5.12%	

Peak ID			N	
High-pass	**Low-pass**	**Frequency Range**	**Amplitude Modulated?**	**Amplitude Affected by Wind Speed?**
2490	2740	MEDIUM	NO	YES
Point Source(s)			Tip Vortex	Rotor Bearings
Weighted Percentages			70%	30%
Total Peak's Percentage of Wind Turbine's SPL			3.91%	

Peak ID			O	
High-pass	**Low-pass**	**Frequency Range**	**Amplitude Modulated?**	**Amplitude Affected by Wind Speed?**
2740	3260	MEDIUM	NO	YES
Point Source(s)			Tip Vortex	Rotor Bearings
Weighted Percentages			60%	40%
Total Peak's Percentage of Wind Turbine's SPL			5.84%	

Peak ID			P	
High-pass	**Low-pass**	**Frequency Range**	**Amplitude Modulated?**	**Amplitude Affected by Wind Speed?**
3270	3480	MEDIUM	NO	YES
Point Source(s)			Tip Vortex	Rotor Bearings
Weighted Percentages			60%	40%
Total Peak's Percentage of Wind Turbine's SPL			0.90%	

Peak ID			Q	
High-pass	**Low-pass**	**Frequency Range**	**Amplitude Modulated?**	**Amplitude Affected by Wind Speed?**
3500	3810	MEDIUM	YES	NO
Point Source(s)			Rotor Bearings	Tip Vortex
Weighted Percentages			60%	40%
Total Peak's Percentage of Wind Turbine's SPL			1.11%	

Peak ID			R	
High-pass	**Low-pass**	**Frequency Range**	**Amplitude Modulated?**	**Amplitude Affected by Wind Speed?**
3970	4340	MEDIUM	YES	NO
Point Source(s)			Rotor Bearings	Tip Vortex
Weighted Percentages			70%	30%
Total Peak's Percentage of Wind Turbine's SPL			4.65%	

Peak ID			S	
High-pass	**Low-pass**	**Frequency Range**	**Amplitude Modulated?**	**Amplitude Affected by Wind Speed?**
4450	4870	MEDIUM	YES	NO
Point Source(s)			Rotor Bearings	Tip Vortex
Weighted Percentages			70%	30%
Total Peak's Percentage of Wind Turbine's SPL			7.23%	

Peak ID			T	
High-pass	**Low-pass**	**Frequency Range**	**Amplitude Modulated?**	**Amplitude Affected by Wind Speed?**
4870	5120	MEDIUM	YES	NO
Point Source(s)			Rotor Bearings	Tip Vortex
Weighted Percentages			80%	20%
Total Peak's Percentage of Wind Turbine's SPL			4.38%	

Peak ID			U	
High-pass	**Low-pass**	**Frequency Range**	**Amplitude Modulated?**	**Amplitude Affected by Wind Speed?**
5310	5330	MEDIUM	YES	NO
Point Source(s)			Rotor Bearings	Tip Vortex
Weighted Percentages			80%	20%
Total Peak's Percentage of Wind Turbine's SPL			3.96%	

Peak ID			V	
High-pass	**Low-pass**	**Frequency Range**	**Amplitude Modulated?**	**Amplitude Affected by Wind Speed?**
6000	6270	HIGH	YES	NO
Point Source(s)			Rotor Bearings	Tip Vortex
Weighted Percentages			90%	10%
Total Peak's Percentage of Wind Turbine's SPL			3.11%	

Sunforce 600

Peak ID			A	
High-pass	**Low-pass**	**Frequency Range**	**Amplitude Modulated?**	**Amplitude Affected by Wind Speed?**
60	90	LOW	NO	YES
Point Source(s)				Inflow Turbulence
Weighted Percentages				100%
Total Peak's Percentage of Wind Turbine's SPL			0.08%	

Peak ID			B	
High-pass	**Low-pass**	**Frequency Range**	**Amplitude Modulated?**	**Amplitude Affected by Wind Speed?**
90	130	LOW	NO	YES
Point Source(s)				Inflow Turbulence
Weighted Percentages				100%
Total Peak's Percentage of Wind Turbine's SPL			0.24%	

Peak ID			C	
High-pass	**Low-pass**	**Frequency Range**	**Amplitude Modulated?**	**Amplitude Affected by Wind Speed?**
210	300	MEDIUM	NO	YES
Point Source(s)			Boundary Layer	Inflow Turbulence
Weighted Percentages			70%	30%
Total Peak's Percentage of Wind Turbine's SPL			1.16%	

Peak ID			D	
High-pass	**Low-pass**	**Frequency Range**	**Amplitude Modulated?**	**Amplitude Affected by Wind Speed?**
340	410	MEDIUM		
Point Source(s)			Boundary Layer	Trailing Edge
Weighted Percentages			60%	40%
Total Peak's Percentage of Wind Turbine's SPL			0.38%	

Peak ID			E	
High-pass	**Low-pass**	**Frequency Range**	**Amplitude Modulated?**	**Amplitude Affected by Wind Speed?**
410	510	MEDIUM	NO	YES
Point Source(s)			Trailing Edge	Tip Vortex
Weighted Percentages			80%	20%
Total Peak's Percentage of Wind Turbine's SPL			0.76%	

Peak ID			F	
High-pass	**Low-pass**	**Frequency Range**	**Amplitude Modulated?**	**Amplitude Affected by Wind Speed?**
510	620	MEDIUM	NO	YES
Point Source(s)			Trailing Edge	Tip Vortex
Weighted Percentages			80%	20%
Total Peak's Percentage of Wind Turbine's SPL			1.35%	

Peak ID			G	
High-pass	**Low-pass**	**Frequency Range**	**Amplitude Modulated?**	**Amplitude Affected by Wind Speed?**
620	690	MEDIUM	NO	YES
Point Source(s)			Trailing Edge	Tip Vortex
Weighted Percentages			70%	30%
Total Peak's Percentage of Wind Turbine's SPL			1.32%	

Peak ID			H	
High-pass	**Low-pass**	**Frequency Range**	**Amplitude Modulated?**	**Amplitude Affected by Wind Speed?**
690	750	MEDIUM	NO	YES
Point Source(s)			Trailing Edge	Tip Vortex
Weighted Percentages			60%	40%
Total Peak's Percentage of Wind Turbine's SPL			1.58%	

Peak ID			I	
High-pass	**Low-pass**	**Frequency Range**	**Amplitude Modulated?**	**Amplitude Affected by Wind Speed?**
750	890	MEDIUM	NO	YES
Point Source(s)			Trailing Edge	Tip Vortex
Weighted Percentages			60%	40%
Total Peak's Percentage of Wind Turbine's SPL			4.36%	

Peak ID			J	
High-pass	**Low-pass**	**Frequency Range**	**Amplitude Modulated?**	**Amplitude Affected by Wind Speed?**
890	1110	MEDIUM	NO	YES
Point Source(s)			Trailing Edge	Tip Vortex
Weighted Percentages			60%	40%
Total Peak's Percentage of Wind Turbine's SPL			9.69%	

Peak ID			K	
High-pass	**Low-pass**	**Frequency Range**	**Amplitude Modulated?**	**Amplitude Affected by Wind Speed?**
1110	1290	MEDIUM	NO	YES
Point Source(s)			Trailing Edge	Tip Vortex
Weighted Percentages			70%	30%
Total Peak's Percentage of Wind Turbine's SPL			0.00%	

Peak ID			L	
High-pass	**Low-pass**	**Frequency Range**	**Amplitude Modulated?**	**Amplitude Affected by Wind Speed?**
1400	1680	MEDIUM	NO	YES
Point Source(s)			Trailing Edge	Tip Vortex
Weighted Percentages			60%	40%
Total Peak's Percentage of Wind Turbine's SPL			10.51%	

Peak ID			M	
High-pass	**Low-pass**	**Frequency Range**	**Amplitude Modulated?**	**Amplitude Affected by Wind Speed?**
1680	1890	MEDIUM	NO	YES
Point Source(s)			Trailing Edge	Tip Vortex
Weighted Percentages			60%	40%
Total Peak's Percentage of Wind Turbine's SPL			7.77%	

Peak ID			N	
High-pass	**Low-pass**	**Frequency Range**	**Amplitude Modulated?**	**Amplitude Affected by Wind Speed?**
1890	2070	MEDIUM	NO	YES
Point Source(s)			Trailing Edge	Tip Vortex
Weighted Percentages			50%	50%
Total Peak's Percentage of Wind Turbine's SPL			8.06%	

Peak ID			O	
High-pass	**Low-pass**	**Frequency Range**	**Amplitude Modulated?**	**Amplitude Affected by Wind Speed?**
2070	2340	MEDIUM	NO	YES
Point Source(s)			Tip Vortex	Trailing Edge
Weighted Percentages			70%	30%
Total Peak's Percentage of Wind Turbine's SPL			9.99%	

Peak ID			P	
High-pass	**Low-pass**	**Frequency Range**	**Amplitude Modulated?**	**Amplitude Affected by Wind Speed?**
2340	2510	MEDIUM	NO	YES
Point Source(s)			Tip Vortex	Trailing Edge
Weighted Percentages			80%	20%
Total Peak's Percentage of Wind Turbine's SPL			5.08%	

Peak ID			Q	
High-pass	**Low-pass**	**Frequency Range**	**Amplitude Modulated?**	**Amplitude Affected by Wind Speed?**
2510	2740	MEDIUM	NO	YES
Point Source(s)			Tip Vortex	Trailing Edge
Weighted Percentages			80%	20%
Total Peak's Percentage of Wind Turbine's SPL			4.69%	

Peak ID			R	
High-pass	**Low-pass**	**Frequency Range**	**Amplitude Modulated?**	**Amplitude Affected by Wind Speed?**
2840	2870	MEDIUM	NO	YES
Point Source(s)			Tip Vortex	Trailing Edge
Weighted Percentages			90%	10%
Total Peak's Percentage of Wind Turbine's SPL			0.39%	

Peak ID			S	
High-pass	**Low-pass**	**Frequency Range**	**Amplitude Modulated?**	**Amplitude Affected by Wind Speed?**
2870	3140	MEDIUM	NO	YES
Point Source(s)				Tip Vortex
Weighted Percentages				100%
Total Peak's Percentage of Wind Turbine's SPL			2.28%	

Peak ID			T	
High-pass	**Low-pass**	**Frequency Range**	**Amplitude Modulated?**	**Amplitude Affected by Wind Speed?**
3440	4040	MEDIUM	YES	NO
Point Source(s)				Tip Vortex
Weighted Percentages				100%
Total Peak's Percentage of Wind Turbine's SPL			1.71%	

Peak ID			U	
High-pass	**Low-pass**	**Frequency Range**	**Amplitude Modulated?**	**Amplitude Affected by Wind Speed?**
17920	18060	HIGH		
Point Source(s)			Unknown Electronic Interference	
Weighted Percentages				100%
Total Peak's Percentage of Wind Turbine's SPL			0.23%	

Skystream 3.7

Peak ID			A	
High-pass	**Low-pass**	**Frequency Range**	**Amplitude Modulated?**	**Amplitude Affected by Wind Speed?**
30	100	LOW	NO	YES
Point Source(s)				Inflow Turbulence
Weighted Percentages				100%
Total Peak's Percentage of Wind Turbine's SPL			1.12%	

Peak ID			B	
High-pass	**Low-pass**	**Frequency Range**	**Amplitude Modulated?**	**Amplitude Affected by Wind Speed?**
100	160	LOW	NO	YES
Point Source(s)				Inflow Turbulence
Weighted Percentages				100%
Total Peak's Percentage of Wind Turbine's SPL			1.07%	

Peak ID			C	
High-pass	**Low-pass**	**Frequency Range**	**Amplitude Modulated?**	**Amplitude Affected by Wind Speed?**
160	200	LOW	NO	YES
Point Source(s)				Inflow Turbulence
Weighted Percentages				100%
Total Peak's Percentage of Wind Turbine's SPL			0.62%	

Peak ID			D	
High-pass	**Low-pass**	**Frequency Range**	**Amplitude Modulated?**	**Amplitude Affected by Wind Speed?**
200	290	MEDIUM	NO	YES
Point Source(s)		Boundary Layer	Blade Impulsive	Generator
Weighted Percentages		60	30%	10%
Total Peak's Percentage of Wind Turbine's SPL			1.80%	

Peak ID			E	
High-pass	**Low-pass**	**Frequency Range**	**Amplitude Modulated?**	**Amplitude Affected by Wind Speed?**
290	440	MEDIUM	NO	YES
Point Source(s)		Boundary Layer	Trailing Edge	Generator
Weighted Percentages		50%	30%	20%
Total Peak's Percentage of Wind Turbine's SPL			4.71%	

Peak ID			F	
High-pass	**Low-pass**	**Frequency Range**	**Amplitude Modulated?**	**Amplitude Affected by Wind Speed?**
470	550	MEDIUM	NO	YES
Point Source(s)			Generator	Trailing Edge
Weighted Percentages			60%	40%
Total Peak's Percentage of Wind Turbine's SPL			2.04%	

Peak ID			G	
High-pass	**Low-pass**	**Frequency Range**	**Amplitude Modulated?**	**Amplitude Affected by Wind Speed?**
550	610	MEDIUM	NO	YES
Point Source(s)			Generator	Trailing Edge
Weighted Percentages			70%	30%
Total Peak's Percentage of Wind Turbine's SPL			2.51%	

Peak ID			H	
High-pass	**Low-pass**	**Frequency Range**	**Amplitude Modulated?**	**Amplitude Affected by Wind Speed?**
610	650	MEDIUM	NO	YES
Point Source(s)			Trailing Edge	Generator
Weighted Percentages			60%	40%
Total Peak's Percentage of Wind Turbine's SPL			1.25%	

Peak ID			I	
High-pass	**Low-pass**	**Frequency Range**	**Amplitude Modulated?**	**Amplitude Affected by Wind Speed?**
650	710	MEDIUM	NO	YES
Point Source(s)			Tip Vortex	Generator
Weighted Percentages			60%	40%
Total Peak's Percentage of Wind Turbine's SPL			1.96%	

Peak ID			J	
High-pass	**Low-pass**	**Frequency Range**	**Amplitude Modulated?**	**Amplitude Affected by Wind Speed?**
710	800	MEDIUM	NO	YES
Point Source(s)			Trailing Edge	Generator
Weighted Percentages			60%	40%
Total Peak's Percentage of Wind Turbine's SPL			1.56%	

Peak ID			K	
High-pass	**Low-pass**	**Frequency Range**	**Amplitude Modulated?**	**Amplitude Affected by Wind Speed?**
820	860	MEDIUM	NO	YES
Point Source(s)			Tip Vortex	Generator
Weighted Percentages			70%	30%
Total Peak's Percentage of Wind Turbine's SPL			1.39%	

Peak ID			L	
High-pass	**Low-pass**	**Frequency Range**	**Amplitude Modulated?**	**Amplitude Affected by Wind Speed?**
860	940	MEDIUM	NO	YES
Point Source(s)			Generator	Tip Vortex
Weighted Percentages			60%	40%
Total Peak's Percentage of Wind Turbine's SPL			2.54%	

Peak ID			M	
High-pass	**Low-pass**	**Frequency Range**	**Amplitude Modulated?**	**Amplitude Affected by Wind Speed?**
940	990	MEDIUM	NO	YES
Point Source(s)			Generator	Trailing Edge
Weighted Percentages			50%	50%
Total Peak's Percentage of Wind Turbine's SPL			1.48%	

Peak ID			N	
High-pass	**Low-pass**	**Frequency Range**	**Amplitude Modulated?**	**Amplitude Affected by Wind Speed?**
990	1080	MEDIUM	NO	YES
Point Source(s)			Generator	Trailing Edge
Weighted Percentages			70%	30%
Total Peak's Percentage of Wind Turbine's SPL			2.62%	

Peak ID			O	
High-pass	**Low-pass**	**Frequency Range**	**Amplitude Modulated?**	**Amplitude Affected by Wind Speed?**
1100	1210	MEDIUM	NO	YES
Point Source(s)			Generator	Tip Vortex
Weighted Percentages			80%	20%
Total Peak's Percentage of Wind Turbine's SPL			2.54%	

Peak ID			P	
High-pass	**Low-pass**	**Frequency Range**	**Amplitude Modulated?**	**Amplitude Affected by Wind Speed?**
1210	1540	MEDIUM	NO	YES
Point Source(s)			Generator	Tip Vortex
Weighted Percentages			80%	20%
Total Peak's Percentage of Wind Turbine's SPL			3.33%	

Peak ID			Q	
High-pass	**Low-pass**	**Frequency Range**	**Amplitude Modulated?**	**Amplitude Affected by Wind Speed?**
1540	2190	MEDIUM	NO	YES
Point Source(s)			Tip Vortex	Generator
Weighted Percentages			70%	30%
Total Peak's Percentage of Wind Turbine's SPL			2.71%	

Peak ID			R	
High-pass	**Low-pass**	**Frequency Range**	**Amplitude Modulated?**	**Amplitude Affected by Wind Speed?**
2200	2400	MEDIUM	NO	YES
Point Source(s)			Tip Vortex	Generator
Weighted Percentages			80%	20%
Total Peak's Percentage of Wind Turbine's SPL			0.44%	

Peak ID			S	
High-pass	**Low-pass**	**Frequency Range**	**Amplitude Modulated?**	**Amplitude Affected by Wind Speed?**
2770	7410	MEDIUM	NO	YES
Point Source(s)			Tip Vortex	Generator
Weighted Percentages			90%	10%
Total Peak's Percentage of Wind Turbine's SPL			22.56%	

Peak ID			T	
High-pass	**Low-pass**	**Frequency Range**	**Amplitude Modulated?**	**Amplitude Affected by Wind Speed?**
7410	12380	HIGH	YES	NO
Point Source(s)			Rotor Bearings	Tip Vortex
Weighted Percentages			80%	20%
Total Peak's Percentage of Wind Turbine's SPL			22.70%	

Peak ID			U	
High-pass	**Low-pass**	**Frequency Range**	**Amplitude Modulated?**	**Amplitude Affected by Wind Speed?**
12380	15050	HIGH	YES	NO
Point Source(s)				Rotor Bearings
Weighted Percentages				100%
Total Peak's Percentage of Wind Turbine's SPL			7.43%	

Anonymous 50kW

Peak ID			A	
High-pass	**Low-pass**	**Frequency Range**	**Amplitude Modulated?**	**Amplitude Affected by Wind Speed?**
50	70	LOW	YES	YES
Point Source(s)			Blade Impulsive	Inflow Turbulence
Weighted Percentages			60%	40%
Total Peak's Percentage of Wind Turbine's SPL			0.80%	

Peak ID			B	
High-pass	**Low-pass**	**Frequency Range**	**Amplitude Modulated?**	**Amplitude Affected by Wind Speed?**
70	140	LOW	YES	YES
Point Source(s)			Blade Impulsive	Inflow Turbulence
Weighted Percentages			60%	40%
Total Peak's Percentage of Wind Turbine's SPL			3.10%	

Peak ID			C	
High-pass	**Low-pass**	**Frequency Range**	**Amplitude Modulated?**	**Amplitude Affected by Wind Speed?**
140	350	MEDIUM	NO	YES
Point Source(s)				Inflow Turbulence
Weighted Percentages				100%
Total Peak's Percentage of Wind Turbine's SPL			11.18%	

Peak ID			D	
High-pass	**Low-pass**	**Frequency Range**	**Amplitude Modulated?**	**Amplitude Affected by Wind Speed?**
350	490	MEDIUM	NO	YES
Point Source(s)				Inflow Turbulence
Weighted Percentages				100%
Total Peak's Percentage of Wind Turbine's SPL			5.07%	

Peak ID			E	
High-pass	**Low-pass**	**Frequency Range**	**Amplitude Modulated?**	**Amplitude Affected by Wind Speed?**
490	670	MEDIUM	NO	YES
Point Source(s)			Boundary Layer	Trailing Edge
Weighted Percentages			50%	50%
Total Peak's Percentage of Wind Turbine's SPL			6.43%	

Peak ID			F	
High-pass	**Low-pass**	**Frequency Range**	**Amplitude Modulated?**	**Amplitude Affected by Wind Speed?**
670	780	MEDIUM	YES	YES
Point Source(s)			Blade Impulsive	Trailing Edge
Weighted Percentages			70%	30%
Total Peak's Percentage of Wind Turbine's SPL			3.56%	

Peak ID			G	
High-pass	**Low-pass**	**Frequency Range**	**Amplitude Modulated?**	**Amplitude Affected by Wind Speed?**
790	850	MEDIUM	NO	YES
Point Source(s)			Trailing Edge	Tip Vortex
Weighted Percentages			50%	50%
Total Peak's Percentage of Wind Turbine's SPL			2.92%	

Peak ID			H	
High-pass	**Low-pass**	**Frequency Range**	**Amplitude Modulated?**	**Amplitude Affected by Wind Speed?**
870	1010	MEDIUM	YES	NO
Point Source(s)			Brake	Tip Vortex
Weighted Percentages			80%	20%
Total Peak's Percentage of Wind Turbine's SPL			2.97%	

Peak ID			I	
High-pass	**Low-pass**	**Frequency Range**	**Amplitude Modulated?**	**Amplitude Affected by Wind Speed?**
1170	1960	MEDIUM	NO	YES
Point Source(s)			Tip Vortex	Brake
Weighted Percentages			80%	20%
Total Peak's Percentage of Wind Turbine's SPL			13.03%	

Peak ID			J	
High-pass	**Low-pass**	**Frequency Range**	**Amplitude Modulated?**	**Amplitude Affected by Wind Speed?**
1960	2540	MEDIUM	NO	YES
Point Source(s)			Tip Vortex	Brake
Weighted Percentages			80%	20%
Total Peak's Percentage of Wind Turbine's SPL			7.01%	

Peak ID			K	
High-pass	**Low-pass**	**Frequency Range**	**Amplitude Modulated?**	**Amplitude Affected by Wind Speed?**
2540	2660	MEDIUM	YES	NO
Point Source(s)			Brake	Tip Vortex
Weighted Percentages			80%	20%
Total Peak's Percentage of Wind Turbine's SPL			3.23%	

Peak ID			L	
High-pass	**Low-pass**	**Frequency Range**	**Amplitude Modulated?**	**Amplitude Affected by Wind Speed?**
2660	3270	MEDIUM	YES	NO
Point Source(s)			Brake	Tip Vortex
Weighted Percentages			80%	20%
Total Peak's Percentage of Wind Turbine's SPL			4.00%	

Peak ID			M	
High-pass	**Low-pass**	**Frequency Range**	**Amplitude Modulated?**	**Amplitude Affected by Wind Speed?**
3990	4620	MEDIUM	YES	NO
Point Source(s)			Brake	Tip Vortex
Weighted Percentages			90%	10%
Total Peak's Percentage of Wind Turbine's SPL			13.52%	

Peak ID			N	
High-pass	**Low-pass**	**Frequency Range**	**Amplitude Modulated?**	**Amplitude Affected by Wind Speed?**
4620	5070	MEDIUM	YES	NO
Point Source(s)			Brake	Bearings
Weighted Percentages			80%	20%
Total Peak's Percentage of Wind Turbine's SPL			6.44%	

Peak ID			O	
High-pass	**Low-pass**	**Frequency Range**	**Amplitude Modulated?**	**Amplitude Affected by Wind Speed?**
5070	5980	MEDIUM	YES	NO
Point Source(s)			Brake	Bearings
Weighted Percentages			90%	10%
Total Peak's Percentage of Wind Turbine's SPL			1.99%	

Anonymous 2.3MW

Peak ID			A	
High-pass	**Low-pass**	**Frequency Range**	**Amplitude Modulated?**	**Amplitude Affected by Wind Speed?**
70	100	LOW	NO	YES
Point Source(s)				Inflow Turbulence
Weighted Percentages				100%
Total Peak's Percentage of Wind Turbine's SPL			1.31%	

Peak ID			B	
High-pass	**Low-pass**	**Frequency Range**	**Amplitude Modulated?**	**Amplitude Affected by Wind Speed?**
100	160	LOW	NO	YES
Point Source(s)				Inflow Turbulence
Weighted Percentages				100%
Total Peak's Percentage of Wind Turbine's SPL			3.24%	

Peak ID			C	
High-pass	**Low-pass**	**Frequency Range**	**Amplitude Modulated?**	**Amplitude Affected by Wind Speed?**
180	280	MEDIUM	NO	YES
Point Source(s)			Inflow Turbulence	Boundary Layer
Weighted Percentages			60%	40%
Total Peak's Percentage of Wind Turbine's SPL			7.26%	

Peak ID			D	
High-pass	**Low-pass**	**Frequency Range**	**Amplitude Modulated?**	**Amplitude Affected by Wind Speed?**
280	580	MEDIUM	NO	YES
Point Source(s)			Trailing Edge	Tip Vortex
Weighted Percentages			70%	30%
Total Peak's Percentage of Wind Turbine's SPL			21.18%	

Peak ID			E	
High-pass	**Low-pass**	**Frequency Range**	**Amplitude Modulated?**	**Amplitude Affected by Wind Speed?**
580	830	MEDIUM	NO	YES
Point Source(s)			Tip Vortex	Trailing Edge
Weighted Percentages			70%	30%
Total Peak's Percentage of Wind Turbine's SPL			13.83%	

Peak ID			F	
High-pass	**Low-pass**	**Frequency Range**	**Amplitude Modulated?**	**Amplitude Affected by Wind Speed?**
840	940	MEDIUM	NO	YES
Point Source(s)			Tip Vortex	Trailing Edge
Weighted Percentages			70%	30%
Total Peak's Percentage of Wind Turbine's SPL			4.59%	

Peak ID			G	
High-pass	**Low-pass**	**Frequency Range**	**Amplitude Modulated?**	**Amplitude Affected by Wind Speed?**
940	1090	MEDIUM	NO	YES
Point Source(s)				Tip Vortex
Weighted Percentages				100%
Total Peak's Percentage of Wind Turbine's SPL			6.92%	

Peak ID			H	
High-pass	**Low-pass**	**Frequency Range**	**Amplitude Modulated?**	**Amplitude Affected by Wind Speed?**
1520	1740	MEDIUM	NO	YES
Point Source(s)			Tip Vortex	Trailing Edge
Weighted Percentages			80%	20%
Total Peak's Percentage of Wind Turbine's SPL			3.85%	

Peak ID			I	
High-pass	**Low-pass**	**Frequency Range**	**Amplitude Modulated?**	**Amplitude Affected by Wind Speed?**
1740	1880	MEDIUM	NO	YES
Point Source(s)				Tip Vortex
Weighted Percentages				100%
Total Peak's Percentage of Wind Turbine's SPL			2.34%	

Peak ID			J	
High-pass	**Low-pass**	**Frequency Range**	**Amplitude Modulated?**	**Amplitude Affected by Wind Speed?**
3280	3480	MEDIUM	NO	YES
Point Source(s)			Tip Vortex	Exhaust Fan
Weighted Percentages			90%	10%
Total Peak's Percentage of Wind Turbine's SPL			0.73%	

Peak ID			K	
High-pass	**Low-pass**	**Frequency Range**	**Amplitude Modulated?**	**Amplitude Affected by Wind Speed?**
4210	4570	MEDIUM	NO	YES
Point Source(s)				Tip Vortex
Weighted Percentages				100%
Total Peak's Percentage of Wind Turbine's SPL			1.09%	

Appendix B: Instrumentation NIST Calibration Certificates

Scantek, Inc.
CALIBRATION LABORATORY

ISO 17025: 2005, ANSI/NCSL Z540:1994 Part 1
ACCREDITED by NVLAP (an ILAC and APLAC signatory)

NVLAP®
NVLAP Lab Code: 200625-0

Calibration Certificate No.24012

Instrument:	**Sound Level Meter**	*Date Calibrated:*	**6/3/2011** *Cal Due:*
Model:	**noiseLab3-NI-9233**	*Status:*	**Received** / **Sent**
Manufacturer:	**Delta**	*In tolerance:*	X / X
Serial number:	**14136F2**	*Out of tolerance:*	
Tested with:	**Microphone MP201 s/n 461270** **Preamplifier MA231 s/n 470777**	*See comments:*	X
Type (class):	**1**	*Contains non-accredited tests:*	__Yes _X_ No
		Calibration service:	__ Basic _X_ Standard
Customer:	**Appalachian State University** **Dr. Dennis Scanlin** **Katherine Harper Hall**	*Address:*	**397 Rivers Street** **Boone, NC 28607**
Tel/Fax:	**919-644-7025 (Brian Baker - QPS)**		

Tested in accordance with the following procedures and standards:
Calibration of Sound Level Meters, Scantek Inc., 06/07/2005
SLM & Dosimeters – Acoustical Tests, Scantek Inc., 06/15/2005

Instrumentation used for calibration: Nor-1504 Norsonic Test System:

Instrument - Manufacturer	Description	S/N	Cal. Date	Traceability evidence Cal. Lab / Accreditation	Cal. Due
483B-Norsonic	SME Cal Unit	25747	Jan 4, 2011	Scantek, Inc./ NVLAP	Jan 4, 2012
DS-360-SRS	Function Generator	61646	Nov 13, 2009	ACR Env. / A2LA	Nov 13, 2011
34401A-Agilent Technologies	Digital Multimeter	MY41022043	Nov 17, 2010	ACR Env. / A2LA	Nov 17, 2011
DPI 141-Druck	Pressure Indicator	790/00-04	Dec 13, 2010	ACR Env. / A2LA	Dec 13, 2012
HM30-Thommen	Meteo Station	1040170/39633	Jun 26, 2010	ACR Env. / A2LA	Dec 26, 2011
PC Program 1019 Norsonic	Calibration software	v.5.0	Validated July 2009	-	-
1251-Norsonic	Calibrator	30878	Dec 7, 2010	Scantek, Inc./ NVLAP	Dec 7, 2011

Instrumentation and test results are traceable to SI (International System of Units) through standards maintained by NIST (USA) and NPL (UK).

Environmental conditions:

Temperature (°C)	Barometric Pressure (kPa)	Relative Humidity (%)
24.1 °C	100.895 kPa	36.8 %RH

Calibrated by	Valentin Buzduga	**Checked by**	Mariana Buzduga
Signature		Signature	
Date	6/09/2011	Date	6/9/2011

Document stored as: Z:\Calibration Lab\SLM 2011\DeltaNoiseLab3-9233_14136F2_M1.doc

Scantek, Inc.
CALIBRATION LABORATORY

ISO 17025: 2005, ANSI/NCSL Z540:1994 Part 1
ACCREDITED by NVLAP (an ILAC and APLAC signatory)

NVLAP®
NVLAP Lab Code: 200625-0

Calibration Certificate No.24013

Instrument: **Microphone**
Model: **MP201**
Manufacturer: **BSWA**
Serial number: **461270**

Date Calibrated: **6/1/2011** *Cal Due:*

Status:	Received	Sent
In tolerance:	X	X
Out of tolerance:		
See comments:		

Contains non-accredited tests: __Yes _X_ No

Customer: **Appalachian State University**
Dr. Dennis Scanlin
Katherine Harper Hall

Address: **397 Rivers Street**
Boone, NC 28607

Tel/Fax: **919-644-7025 (Brian Baker - QPS)**

Tested in accordance with the following procedures and standards:
Procedure for Calibration of Measurement Microphones, Scantek Inc., 06/15/2005

Instrumentation used for calibration: N-1504 Norsonic Test System:

Instrument - Manufacturer	Description	S/N	Cal. Date	Traceability evidence	Cal. Due
				Cal. Lab / Accreditation	
483B-Norsonic	SME Cal Unit	25747	Jan 4, 2011	Scantek, Inc./ NVLAP	Jan 4, 2012
DS-360-SRS	Function Generator	61646	Nov 13, 2009	ACR Env. / A2LA	Nov 13, 2011
34401A-Agilent Technologies	Digital Multimeter	MY41022043	Nov 17, 2010	ACR Env. / A2LA	Nov 17, 2011
DPI 141-Druck	Pressure Indicator	790/00-04	Dec 13, 2010	ACR Env. / A2LA	Dec 13, 2012
HM30-Thommen	Meteo Station	1040170/3963 3	Jun 26, 2010	ACR Env./ A2LA	Dec 26, 2011
PC Program 1017 Norsonic	Calibration software	v.5.0	Validated July 2009	-	-
1253-Norsonic	Calibrator	28326	Dec 6, 2010	Scantek, Inc./ NVLAP	Dec 6, 2011
1203-Norsonic	Preamplifier	14059	Jan 5, 2011	Scantek, Inc./ NVLAP	Jan 5, 2012
4180-Brüel&Kjær	Microphone	2246115	Dec 14, 2009	NPL (UK) / UKAS	Dec 14, 2011

Instrumentation and test results are traceable to SI - BIPM through standards maintained by NPL (UK) and NIST (USA)

Calibrated by	Valentin Buzduga	Checked by	Mariana Buzduga
Signature		Signature	
Date	6/01/2011	Date	6/9/2011

Scantek, Inc.
CALIBRATION LABORATORY

ISO 17025: 2005, ANSI/NCSL Z540:1994 Part 1
ACCREDITED by NVLAP (an ILAC and APLAC signatory)

NVLAP®
NVLAP Lab Code: 200625-0

Calibration Certificate No.24014

Instrument:	**Acoustical Calibrator**	*Date Calibrated:* **6/2/2011**	*Cal Due:*		
Model:	**CA111**	*Status:*	**Received**	**Sent**
Manufacturer:	**BSWA**	*In tolerance:*	**X**	**X**
Serial number:	**470124**	*Out of tolerance:*		
Class (IEC 60942):	**1**	*See comments:*	**X**	
Barometer type:		*Contains non-accredited tests:*	**__Yes _X_ No**	
Barometer s/n:				

Customer: **Appalachian State University**
Dr. Dennis Scanlin
Katherine Harper Hall

Address: **397 Rivers Street**
Boone, NC 28607

Tel/Fax: **919-644-7025 (Brian Baker - QPS)**

Tested in accordance with the following procedures and standards:
Calibration of Acoustical Calibrators, Scantek Inc., 06/06/2005

Instrumentation used for calibration: Nor-1504 Norsonic Test System:

Instrument - Manufacturer	Description	S/N	Cal. Date	Traceability evidence Cal. Lab / Accreditation	Cal. Due
483B-Norsonic	SME Cal Unit	25747	Jan 4, 2011	Scantek, Inc./ NVLAP	Jan 4, 2012
DS-360-SRS	Function Generator	61646	Nov 13, 2009	ACR Env. / A2LA	Nov 13, 2011
34401A-Agilent Technologies	Digital Multimeter	MY41022043	Nov 17, 2010	ACR Env. / A2LA	Nov 17, 2011
DPI 141-Druck	Pressure Indicator	790/00-04	Dec 13, 2010	ACR Env. / A2LA	Dec 13, 2012
8903A-HP	Audio Analyzer	2514A05691	Dec 1, 2010	ACR Env./ A2LA	Dec 1, 2013
HM30-Thommen	Meteo Station	1040170/39633	Jun 26, 2010	ACR Env./ A2LA	Dec 26, 2011
PC Program 1018 Norsonic	Calibration software	v.5.0	Validated July 2009	-	
1253-Norsonic	Calibrator	28326	Dec 6, 2010	Scantek, Inc./ NVLAP	Dec 6, 2011
1203-Norsonic	Preamplifier	14059	Jan 5, 2011	Scantek, Inc./ NVLAP	Jan 5, 2012
4180-Brüel&Kjær	Microphone	2246115	Dec 14, 2009	NPL (UK) / UKAS	Dec 14, 2011

Instrumentation and test results are traceable to SI (International System of Units) through standards maintained by NIST (USA) and NPL (UK)

Calibrated by	Valentin Buzduga	Checked by	Mariana Buzduga
Signature		Signature	
Date	6/02/2011	Date	6/9/2011

Svend Ole Hansen ApS
SCT. JØRGENS ALLÉ 7 · DK-1615 KØBENHAVN V · DENMARK
TEL: (+45) 33 25 38 38 · FAX: (+45) 33 25 38 39 · WWW.SOHANSEN.DK

WIND ENGINEERING FLUID DYNAMICS

CERTIFICATE FOR CALIBRATION OF CUP ANEMOMETER

Certificate number: 09.02.4413 **Date of issue:** August 17, 2009

Type: Thies 4.3351.00.000 **Serial number:** 0709076

Manufacturer: ADOLF THIES GmbH & Co.KG, Hauptstrasse 76, 37083 Göttingen, Germany

Client: Sky Power Int'l LLC, 250 Sawdust Road, 29657-8521 Liberty SC, USA

Anemometer received: August 4, 2009 **Anemometer calibrated:** August 15, 2009

Calibrated by: mh **Calibration procedure:** IEC 61400-12-1, MEASNET

Certificate prepared by: jsa **Approved by:** Calibration engineer, soh Svend Ole Hansen

Calibration equation obtained: v [m/s] = 0.04608 · f [Hz] + 0.21060

Standard uncertainty, slope: 0.00144 **Standard uncertainty, offset:** 0.07116

Covariance: -0.0000009 (m/s)²/Hz **Coefficient of correlation:** $\rho = 0.999989$

Absolute maximum deviation: -0.037 m/s at 14.928 m/s

Barometric pressure: 1011.6 hPa **Relative humidity:** 24.4%

Succession	Velocity pressure, q. [Pa]	Temperature in wind tunnel [°C]	Temperature in control room [°C]	Wind velocity, v. [m/s]	Frequency, f. [Hz]	Deviation, d. [m/s]	Uncertainty u_c (k=2) [m/s]
2	9.25	34.4	27.6	4.029	83.0578	-0.008	0.030
4	14.09	34.3	27.6	4.971	103.7233	-0.019	0.034
6	20.31	34.2	27.6	5.967	125.0156	-0.004	0.039
8	27.53	34.1	27.6	6.946	146.1466	0.002	0.045
10	36.07	34.0	27.6	7.949	167.7608	0.009	0.051
12	45.58	33.9	27.6	8.936	188.9812	0.018	0.057
13-last	56.78	33.9	27.6	9.973	211.9338	-0.003	0.063
11	68.17	34.0	27.6	10.928	232.3098	0.013	0.069
9	81.20	34.0	27.6	11.928	253.6160	0.032	0.075
7	95.14	34.1	27.6	12.913	275.5274	0.008	0.082
5	110.37	34.2	27.6	13.910	297.8301	-0.023	0.088
3	127.06	34.3	27.6	14.928	320.2301	-0.037	0.095
1-first	144.52	34.6	27.6	15.928	340.8941	0.011	0.101

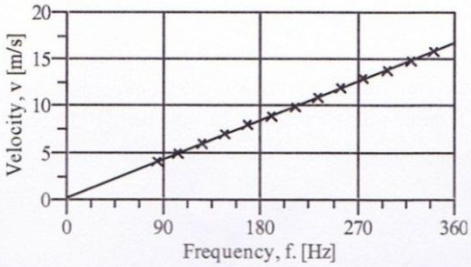

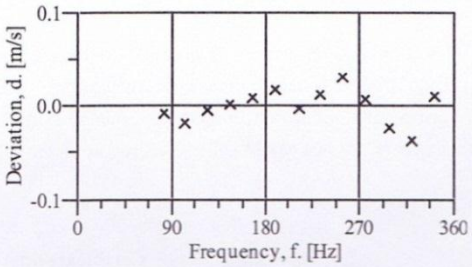

ilac-MRA DANAK CAL Reg.nr. 452 Accreditation to ISO 17025 measnet

EQUIPMENT USED

Serial number	Description
-	Boundary layer wind tunnel.
1255	Control cup anemometer.
-	Mounting tube, D = 35 mm
t3	PT100 temperature sensor, wind tunnel.
t4	PT100 temperature sensor, control room.
950610	PPC500 Furness pressure manometer
Z0420014	HMW71U Humidity transmitter
U4220037	PTB100AVaisala analogue barometer.
P11	Pitot tube
001551	Computer Board. 16 bit A/D data acquisition board.
-	PC dedicated to data acquisition.

Traceable calibrations of the equipment are carried out by external accredited institutions: Furness (PPC500) and Saab Metech. A real-time analysis module within the data acquisition software detects pulse frequency.

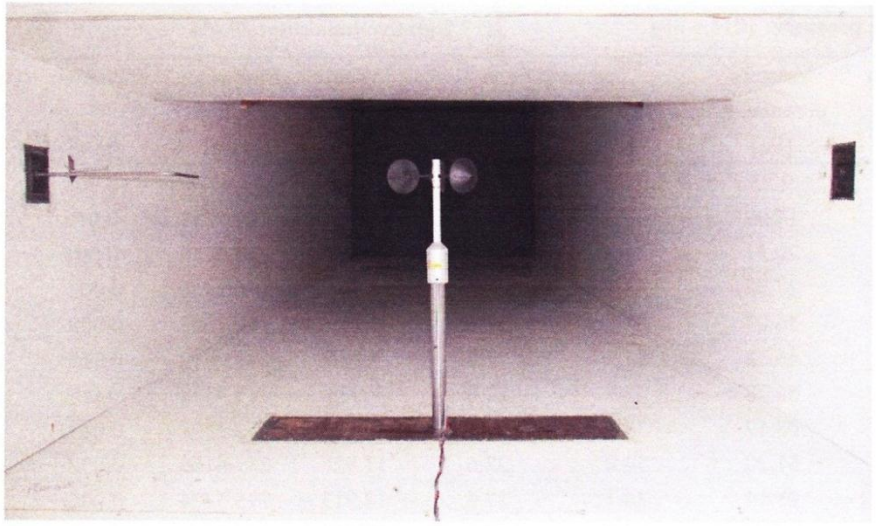

Photo of a cup anemometer in the wind tunnel. The shown anemometer is of the same type as the calibrated one.

UNCERTAINTIES

The documented uncertainty is the total combined uncertainty at 95% confidence level (k=2) in accordance with EA-4/02. The uncertainty at 10 m/s comply with the requirements in the MEASNET procedure that prescribes an absolute uncertainty less than 0.1 m/s at a mean wind velocity of 10 m/s, that is 1%. See Document 97.00.004 "MEASNET-Test report on the calibration campaign" for further details.

Certificate number: 09.02.4413

Appendix C: Decibel to Pascal Conversion Chart

$$Pascal = (2 \times 10^{-5}) \times 10^{Decibel/20}$$

$$Decibel\ (Sound\ Pressure\ Level) = 20 \log_{10} {}^{Pascal}/_{20\mu Pa}$$

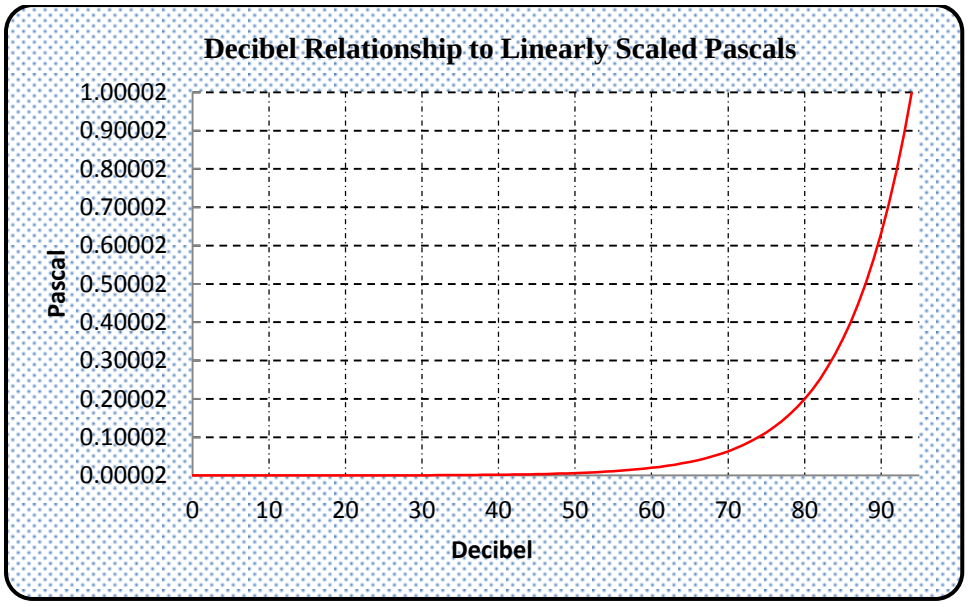

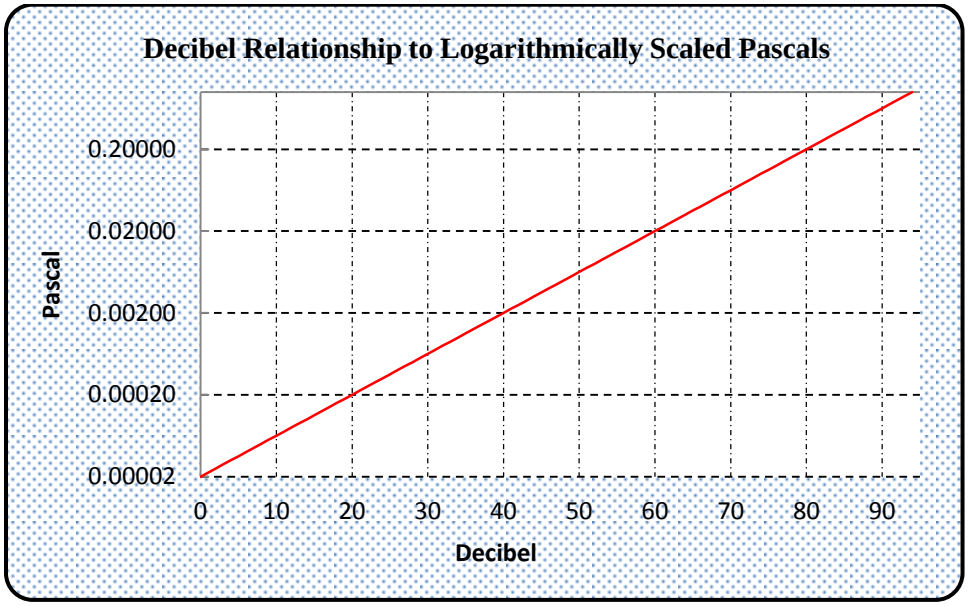

Decibel	Pascal
-94	0.0000000004
-93	0.0000000004
-92	0.0000000005
-91	0.0000000006
-90	0.0000000006
-89	0.0000000007
-88	0.0000000008
-87	0.0000000009
-86	0.0000000010
-85	0.0000000011
-84	0.0000000013
-83	0.0000000014
-82	0.0000000016
-81	0.0000000018
-80	0.0000000020
-79	0.0000000022
-78	0.0000000025
-77	0.0000000028
-76	0.0000000032
-75	0.0000000036
-74	0.0000000040
-73	0.0000000045
-72	0.0000000050
-71	0.0000000056
-70	0.0000000063
-69	0.0000000071
-68	0.0000000080
-67	0.0000000089
-66	0.0000000100
-65	0.0000000112
-64	0.0000000126
-63	0.0000000142
-62	0.0000000159
-61	0.0000000178
-60	0.0000000200
-59	0.0000000224
-58	0.0000000252

Decibel	Pascal
0	0.0000200000
1	0.0000224404
2	0.0000251785
3	0.0000282508
4	0.0000316979
5	0.0000355656
6	0.0000399052
7	0.0000447744
8	0.0000502377
9	0.0000563677
10	0.0000632456
11	0.0000709627
12	0.0000796214
13	0.0000893367
14	0.0001002374
15	0.0001124683
16	0.0001261915
17	0.0001415892
18	0.0001588656
19	0.0001782502
20	0.0002000000
21	0.0002244037
22	0.0002517851
23	0.0002825075
24	0.0003169786
25	0.0003556559
26	0.0003990525
27	0.0004477442
28	0.0005023773
29	0.0005636766
30	0.0006324555
31	0.0007096268
32	0.0007962143
33	0.0008933672
34	0.0010023745
35	0.0011246827
36	0.0012619147

Decibel	Pascal
-57	0.0000000283
-56	0.0000000317
-55	0.0000000356
-54	0.0000000399
-53	0.0000000448
-52	0.0000000502
-51	0.0000000564
-50	0.0000000632
-49	0.0000000710
-48	0.0000000796
-47	0.0000000893
-46	0.0000001002
-45	0.0000001125
-44	0.0000001262
-43	0.0000001416
-42	0.0000001589
-41	0.0000001783
-40	0.0000002000
-39	0.0000002244
-38	0.0000002518
-37	0.0000002825
-36	0.0000003170
-35	0.0000003557
-34	0.0000003991
-33	0.0000004477
-32	0.0000005024
-31	0.0000005637
-30	0.0000006325
-29	0.0000007096
-28	0.0000007962
-27	0.0000008934
-26	0.0000010024
-25	0.0000011247
-24	0.0000012619
-23	0.0000014159
-22	0.0000015887
-21	0.0000017825
-20	0.0000020000

Decibel	Pascal
37	0.0014158916
38	0.0015886565
39	0.0017825019
40	0.0020000000
41	0.0022440369
42	0.0025178508
43	0.0028250751
44	0.0031697864
45	0.0035565588
46	0.0039905246
47	0.0044774423
48	0.0050237729
49	0.0056367659
50	0.0063245553
51	0.0070962678
52	0.0079621434
53	0.0089336718
54	0.0100237447
55	0.0112468265
56	0.0126191469
57	0.0141589157
58	0.0158865647
59	0.0178250188
60	0.0200000000
61	0.0224403691
62	0.0251785082
63	0.0282507509
64	0.0316978638
65	0.0355655882
66	0.0399052463
67	0.0447744228
68	0.0502377286
69	0.0563676586
70	0.0632455532
71	0.0709626778
72	0.0796214341
73	0.0893367184
74	0.1002374467

Decibel	Pascal
-19	0.0000022440
-18	0.0000025179
-17	0.0000028251
-16	0.0000031698
-15	0.0000035566
-14	0.0000039905
-13	0.0000044774
-12	0.0000050238
-11	0.0000056368
-10	0.0000063246
-9	0.0000070963
-8	0.0000079621
-7	0.0000089337
-6	0.0000100237
-5	0.0000112468
-4	0.0000126191
-3	0.0000141589
-2	0.0000158866
-1	0.0000178250

Decibel	Pascal
75	0.1124682650
76	0.1261914689
77	0.1415891569
78	0.1588656469
79	0.1782501876
80	0.2000000000
81	0.2244036909
82	0.2517850824
83	0.2825075089
84	0.3169786385
85	0.3556558820
86	0.3990524630
87	0.4477442277
88	0.5023772863
89	0.5636765863
90	0.6324555320
91	0.7096267785
92	0.7962143411
93	0.8933671843
94	1.0023744673

VITA

Jon Christopher Kirchner was born in 1986. He was raised in Lexington, Virginia where his father taught him architectural and woodworking skills at a young age. Mr. Kirchner combined these skills with his mother's artistic skills to build a unique set of creative building skills. He found affection for the study of acoustics and continued to investigate this incredible phenomenon through his life interests in art, music, and technology. Mr. Kirchner graduated from Rockbridge County High School in 2004 and progressed to acquire his Bachelor of Arts degree in Studio Art with a minor in Astronomy from the University of Virginia where he graduated in 2008. His understanding of how the universe works and his acute attention to his surroundings spurred him to seek a Master of Science degree in Technology from Appalachian State University in Boone, North Carolina to study renewable energy technologies and from where he will graduate in May 2012.

Throughout his education, his curriculum has revolved around how we perceive space, time and all of the subtle parameters that compose that continuum. This knowledge surfaces through Mr. Kirchner's form of creative thought processes that use his diverse range of knowledge to find inventive and novel solutions to discovered problems in ever shifting ways. Mr. Kirchner is a member of the Phi Kappa Phi Honors Society as a result of his ranking in the top 5% of his entire graduate school class. His mailing address is 505 Pickett Street, Lexington, Virginia, 24450. His parents and mentors are Mr. Fred Kirchner and Mrs. Jean Kirchner.